

A.P. Dimri · Amulya Chevuturi

Western Disturbances - An Indian Meteorological Perspective

 Springer

Western Disturbances - An Indian Meteorological Perspective

A.P. Dimri • Amulya Chevuturi

Western Disturbances - An Indian Meteorological Perspective

 Springer

A.P. Dimri
School of Environmental Sciences
Jawaharlal Nehru University
New Delhi, India

Amulya Chevuturi
School of Environmental Sciences
Jawaharlal Nehru University
New Delhi, India

ISBN 978-3-319-26735-7 ISBN 978-3-319-26737-1 (eBook)
DOI 10.1007/978-3-319-26737-1

Library of Congress Control Number: 2016930300

© Springer International Publishing Switzerland 2016

This work is subject to copyright. All rights are reserved by the Publisher, whether the whole or part of the material is concerned, specifically the rights of translation, reprinting, reuse of illustrations, recitation, broadcasting, reproduction on microfilms or in any other physical way, and transmission or information storage and retrieval, electronic adaptation, computer software, or by similar or dissimilar methodology now known or hereafter developed.

The use of general descriptive names, registered names, trademarks, service marks, etc. in this publication does not imply, even in the absence of a specific statement, that such names are exempt from the relevant protective laws and regulations and therefore free for general use.

The publisher, the authors and the editors are safe to assume that the advice and information in this book are believed to be true and accurate at the date of publication. Neither the publisher nor the authors or the editors give a warranty, express or implied, with respect to the material contained herein or for any errors or omissions that may have been made.

Printed on acid-free paper

This Springer imprint is published by SpringerNature
The registered company is Springer International Publishing AG Switzerland.

Foreword

The Indian subcontinent experiences mainly four seasons. Among them, the Southwest monsoon season (June to September) is the most important season as it contributes 70–90 % of the annual rainfall over the country. However, the northern parts of the country and neighboring Pakistan also experience a wet season during the winter, due to the passage of western disturbances, winter weather systems moving eastwards across the region. This season is very important as it plays a major role in the winter crop (Rabi) production and hydrology over the region. This region has a complex topography due to the Himalayas. The weather systems moving across this region interact with this complex topography and lead to more complexity to the dynamics and predictability of weather systems. The synoptic features and dynamics of these weather systems were not explored in the past due to lack of adequate observations and modeling efforts. Over the years, our understanding of these winter weather systems has improved substantially due to improvement of observational networks over the region and systematic modeling efforts. Better understanding of these systems has also helped to improve weather prediction skills over the region, which is reflected in the operational weather forecasts issued by the India Meteorological Department.

In concert with these developments, this book *Western Disturbances, An Indian Meteorological Perspective* by Prof A.P. Dimri and Dr. Chevuturi will prove to bridge an indispensable knowledge gap for earth scientists at all stages of their careers, from undergraduate students to the professionals. Western disturbances in the context of Indian meteorology are an important weather phenomenon which in the current context of climate change has gained importance due to its influence on the Himalayan snow cover, glaciers, northern Indian river feed, agriculture, etc. This book will provide readers with a broad perspective on development and interpretation of physical, dynamical, and thermodynamical processes associated with winter weather systems over the Indian subcontinent. The description accompanied by numerous illustrations sufficiently provides concise deliberations for established researchers and also policy makers. The book provides most adequate composite integration of available references right from the last decade to the latest.

In the first chapter of the book, updated understanding on structure and evolution of western disturbances is provided. This chapter provides more comprehension than many other treatments on the subject. With the advent of computational facilities, observational reanalysis, and numerical methods, constructing the natural environment became much easier. Simulations of the atmospheric flows/interactions are better understood and explained with such efforts. Chapter 2 dwells into those details and synthesizes efforts carried on this direction with the latest positioning. In the recent decade it is observed that midlatitude westerlies have strengthened their interactions with other seasonal weather systems. Chapter 3 deliberates on factors leading to such interaction and their effect. It is one of the important aspects in the context of recent global changes. In Chap. 4, discussion on western disturbances embedded within large-scale westerlies is provided. In the context of global change, this is one of the most important aspects providing understanding of large-scale flows affecting the life cycle of weather systems. In the fifth chapter, the western disturbances and their impacts and climate change issues are discussed. Prof. Dimri and Dr. Chevuturi have provided here an excellent summary on the Indian winter weather systems at different spatial and temporal scales. I believe this book will be an excellent reference for students, professionals, and policy makers on the winter weather systems over India.

Indian Institute of Tropical Meteorology
Pune, India

M. Rajeevan

Preface

Meteorology, climatology, and atmospheric sciences have been extensively studied over India. But sometimes, a unified compilation of such an extensive knowledge resource base is lacking, which may result in gaps in the information flow. With India having a vast and heterogeneous geography, it is imperative to have detailed understanding of its intricacies. This book comprehensively reviews a weather phenomenon impacting the Indian subcontinent. Western disturbances (WDs), the wintertime precipitating events, are the focus of this book. This book can be used as a reference by students, professors, and other research scholars to achieve a detailed understanding on the subject. Other than its importance in terms of a meteorological phenomenon, WDs as precipitating events have significant consequences on the ecology and the socioeconomy of the region. Overall this book answers the questions of what/when/why/how about the WDs. This book defines WDs and details the physical and dynamical understanding of their structure and migration. It also includes the causes and impacts with detailed illustrations and various case studies for a clear understanding of the subject.

The book's visualization and conception came about during our research tenure that focused on the Himalayan climate. Wintertime precipitation over the Himalayas and northern India is a very interesting topic and has not been comprehensively researched. So many research questions on the topic are still unanswered. Further, most of the research is available in older formats that are not easily accessible. Without a review or a textbook understanding of the topic, intensive research on the topic is challenging. Thus, we came to believe that such a book would be a requirement in this field of research, especially from the point of view of young researchers. All of these reasons compelled us as researchers to write this book. During the course of writing, we grew as authors and researchers. Despite our previous experience on the topic, while doing the researching behind this book, our knowledge grew as new information was uncovered. It was a uniquely interesting learning experience for us.

We would like to express gratitude for the scholastic support of the various experts whose peer-reviewed papers and other research work has been used and referred to in this book. Acknowledgment is indeed due to the different sources of

observational datasets that have been properly cited within the book. We would also like to thank our editor at Springer Petra van Steenbergen and our publisher Springer for making this book possible. We convey our appreciation for the reviewers for their suggestions and comments that helped us in improving the book. Last but not the least, we would also like to thank our colleagues, friends, and family who supported us in our endeavor and helped us during our journey.

New Delhi, India

A.P. Dimri
Amulya Chevuturi

Contents

1 Western Disturbances – Structure	1
1.1 Introduction	3
1.2 Origin and Migration of Western Disturbances.....	5
1.3 Western Disturbances at a Synoptic Scale.....	10
1.4 Structure of Western Disturbances	14
1.5 Western Disturbances and Linkages with Large-Scale Forcing	19
References.....	21
2 Western Disturbances – Dynamics and Thermodynamics	27
2.1 Dynamics of Western Disturbances.....	29
2.2 Modelling Studies Related to Western Disturbances.....	32
2.3 Interplay With Himalayan Orography and Land-use – Land-Cover Interactions	45
References.....	55
3 Western Disturbances – Indian Seasons	61
3.1 Winter	63
3.2 Pre-Monsoon	65
3.3 Monsoon.....	67
3.4 Post-Monsoon.....	77
References.....	79
4 Western Disturbances – Indian Winter Monsoon	83
4.1 Introduction	84
4.2 Interannual Variability of the Indian Winter Monsoon.....	86

4.3 Sub-seasonal Oscillation Associated with the Indian Winter Monsoon	92
4.3.1 Wet and Dry Winters over the WH and Its Associated Circulation.....	93
4.3.2 Large-Scale Global and Local Forcings.....	99
4.4 Intraseasonal Oscillation Associated with the Indian Winter Monsoon	101
References.....	109
5 Western Disturbances – Impacts and Climate Change	113
5.1 Winter Precipitation and Its Impacts	113
5.2 Severe Weather	116
5.3 Western Disturbances in the Changing Climate	120
5.4 Western Disturbances and Future Research	124
References.....	125
Index.....	129

List of Figures

Fig. 1.1	Map of Indian Subcontinent.....	2
Fig. 1.2	Meteosat satellite image (Channel 2) for a WD travelling towards India. Satellite images of (a–j) are from 06 January 2009 to 15 January 2009 each at 0000 UTC. <i>Red circle</i> marks the migrating WD.....	8
Fig. 1.3	An asymmetric upper-air trough with closer packing in the rear	11
Fig. 1.4	500h Pa geopotential ($\times 10^{-2}$ m; <i>shaded</i>) and wind (m/s; <i>arrow</i>) for 05 February 2002 to 09 February 2002 with WRF model simulation (Dimri and Chevuturi 2014).....	16
Fig. 1.5	Vertical distribution of geopotential height anomaly averaged over latitude (25°N–40°N) for WD in February 2002.....	17
Fig. 1.6	Same as Fig. 1.5 but averaged over longitude (65°E–85°E).....	18
Fig. 1.7	Conceptual model of WDs (<i>MI</i> : Moisture incursion, <i>PRECIP</i> : Precipitation, <i>SL</i> : Surface low, <i>STWJ</i> : Sub-tropical westerly jet, <i>TA</i> : Westward tilted axis in vertical, <i>WD</i> : Upper air western disturbance).....	20
Fig. 2.1	(a) Schematic representation of cascading Himalayan mountain ranges (Pir Panjal- Great Himalaya-Zaskar-Ladhak-Karakoram) and western-central–eastern Himalayan region (b) Topographic ($\times 10^3$ m) overview of the Himalayas.....	28
Fig. 2.2	Reanalysis of sea level pressure at 0000 UTC on (a) 19 Jan 1997 and (b) corresponding 24 h forecast of sea level pressure in 08 difference model experiments	37

Fig. 2.3	500 hPa Geopotential height (m) after 48 h model forecast valid at 0000 UTC on 23 Jan 1999 over flat (a , b and c) and normal topography (d , e and f) with different model horizontal resolutions	39
Fig. 2.4	Precipitation (cm/24 h) after 48 h model forecast valid at 0000 UTC on 23 Jan 1999 over flat (a , b and c) and normal topography (d , e and f) with different model horizontal resolutions	40
Fig. 2.5	500 hPa wind (m/s; <i>arrow</i>); geopotential height (m; <i>red contour</i>) and wind speed above 22 m/s (<i>grey shed</i>) in (a) model, (b) MERRA and (c) NCEP-NNRPII on 07 Feb 2002 0000 UTC	41
Fig. 2.6	Spatial distribution of model simulated maximum (a) CAPE (J/kg) and (b) CIN (J/kg) on 07 Feb 2002 0000 UTC.....	42
Fig. 2.7	Longitude-pressure cross section (at the line across peak precipitation spatial distribution of the storm) at 1700 UTC 17 Jan 2013 for geopotential height anomaly (<i>shaded</i>) and perturbation geopotential height (m; <i>contour</i>)	43
Fig. 2.8	Time-pressure cross section (area averaged over the grid around NCR) for CAPE (J/kg; <i>shaded</i>), temperature ($^{\circ}\text{C}$; <i>black contours</i>) and specific humidity (g/kg; <i>blue contours</i>)	44
Fig. 2.9	Vertical cross section of vorticity ($\times 10^5 \text{ s}^{-1}$, <i>shaded</i>), model precipitation (cm/day; <i>green line</i>) and observed precipitation (cm/day; <i>purple line</i>) along 33°N for the WD case studied.....	48
Fig. 2.10	Lon-pressure cross section vertical distribution at 34°N latitude of model simulated meridional wind (ms^{-1}) (continuous <i>black contour</i>) and air specific humidity ($\times 10^{-3}$) (broken <i>red contour</i>) at 0000 UTC during active WD (a) 21 Jan 1999 (b) 22 Jan 1999 (c) 23 Jan 1999 (<i>Left hand side</i> vertical axis corresponds to the pressure distribution and <i>right hand side</i> vertical axis corresponds to the topography $\times 10^2 \text{ m}$)	50
Fig. 2.11	Twenty-four hour cumulative precipitation on 22 December 2006 in (a) observational data (APHRODITE) and (b) the corresponding REMO simulated field, and geopotential height (m; <i>shade</i>) and vector wind (m/s; <i>arrow</i>) in the REMO simulation at (c) 850 hPa on 20 December 2006, (d) 500 hPa on 20 December 2006, and (e) 500 hPa on 20 December 2006.....	51

Fig. 2.12 Lon-pressure cross section vertical distribution at 34°N latitude of model simulated geopotential height (m; *continuous black contour*) and air specific humidity ($\times 10^{-3}$; *shaded*) at 0000 UTC during active WD (a) 20 Dec 2006 (b) 21 Dec 2006 (c) 22 Dec 2006 (*Left hand side* vertical axis corresponds to the pressure distribution and right hand side vertical axis corresponds to the topography $\times 10^2$ m) 53

Fig. 2.13 Lon–pressure distribution of vorticity ($\times 10^{-5}/s$; *shade*), relative humidity (%; *broken contour*), and topography ($\times 10^3$ m; shaded bar) on (a) 19 December 2006, (b) 20 December 2006, (c) 21 December 2006, (d) 22 December 2006, (e) 23 December 2006, and (f) 24 December 2006 at 35°N Lat in the REMO simulation 54

Fig. 3.1 Kalpana satellite images for (a) 15 June 2013 (0600 UTC), (b) 16 June 2013 (0600 UTC) and (c) 17 June 2013 (0600 UTC). (d–f) is same as (a–b) but with INSAT-3A with thermal infrared band 71

Fig. 3.2 Geopotential height anomaly (*shaded*) and perturbation geopotential height ($\times 10^2$ m/s; *contour*) over the axis normal to the formation of TCS for different time periods 73

Fig. 3.3 Conceptual model of the PEM towards Himalayas 75

Fig. 4.1 (a) Topography ($\times 10^{-3}$ m; *shaded*) and ratio of 0.05° grids for stations (%; *contour*) over the western Himalayas. The area of $30^\circ N, 72^\circ E$ to $37^\circ N, 82^\circ E$ is considered in the present chapter; (b) winter season precipitation climatology (mm/DJF) based on APHRODITE precipitation observed data reanalysis 85

Fig. 4.2 (a) The monthly (Dec, Jan, and Feb) and seasonal (DJF) precipitation (mm/d) anomaly in APHRODITE observational reanalysis and (b) difference in 3-month (Dec, Jan, and Feb) average wet- and dry-year composites precipitation (*shaded*) and region with 99 % confidence level (within *contour*) 87

Fig. 4.3 Difference between 03 (DJF) month average wet and dry composites of wind (m/s; *contour*; winds above 99 % significant level are *plotted*) and geopotential height (m; *shaded*; region within contour corresponds to 99 % significant level) at (a) 200 hPa (b) 500 hPa and (c) 850 hPa 88

Fig. 4.4 Seasonal anomalous velocity potential ($\times 10^{-6}$ m²/s; *contour*) with corresponding anomalous divergent wind (m/s; *arrow*) at $\sigma=0.1682$ and anomalous outgoing longwave radiation (W/m²; *shade*) for (a) wet and (b) dry year composites and seasonal anomalous stream function ($\times 10^{-6}$ m²/s; *contour*) with corresponding anomalous rotational wind (m/s; *arrow*) at $\sigma=0.1682$ and anomalous outgoing longwave radiation (W/m²; *shade*) for (c) wet and (d) dry year composites..... 90

Fig. 4.5 Correlation between 28 years (1980–2007) area averaged winter precipitation $-D(-1)JF(0) -$ (mm/d) with sea surface temperature (°C) during (a) D(-2)JF(-1) (b) MAM(-1) (c) JJA(-1) (d) SON(-1) and (e) D(-1)JF(0). (Figures in bracket correspond to sea surface temperature with previous and corresponding seasons). Region within *contour* corresponds to 99 % significant level..... 91

Fig. 4.6 Correlation between seasonal (DJF) and monthly (Dec, Jan, and Feb) interannual precipitation variability based on APHRODITE..... 92

Fig. 4.7 Cumulative average monthly anomalous precipitation (mm/month) during wet composites of (a) Dec, (b) Jan, and (c) Feb and for dry composites of (d) Dec, (e) Jan, and (f) Feb. Masking with 10 mm/month was employed..... 94

Fig. 4.8 Monthly difference in (wet–dry) anomaly for 200 hPa geopotential height (hPa, *contour*) and wind vector (ms⁻¹, *arrow*) for (a) Dec, (b) Jan, and (c) Feb. The hatched region corresponds to ≥ 95 %. Similarly, only winds with 95 % significance and above are shown..... 95

Fig. 4.9 Same as Fig. 4.8, but for outgoing longwave radiation (W/m²; *shaded*)..... 97

Fig. 4.10 Longitude–pressure vertical cross section at 30°N of the anomalous meridional moisture flux (kg/m/s) during wet ((a), (b), and (c)) and dry ((d), (e), and (f)) composites of Dec, Jan, and Feb, respectively 98

Fig. 4.11 Area-averaged (30°N 72°E to 37°N 82°E) vertical cross-sectional distribution of anomalous air temperature (°C) in (a) wet and (b) dry composites for Dec (*black line*), Jan (*red line*), and Feb (*green line*) and area-averaged (30°N 72°E to 37°N 82°E) anomalous 2-m surface-air temperature (*black line*; °C) and anomalous precipitation (mm/d) during (c) wet and (d) dry year composites of Dec, Jan, and Feb..... 100

- Fig. 4.12 (a) Based on 28 years (Dec 1979, Jan, Feb 1980 to Dec 2006, Jan, Feb 2007) of data, time-series of WHDP climatology (bar; *left axis*), pentad precipitation climatology (*black line with open circles; left axis*), and 7–25-day filtered precipitation anomaly (*red line with open circles; right axis*). The line of 95 % significance is also shown and the period above this corresponds to climatological active phases. (b) The 28-winter (DJF) ensemble spectrum of the WHDP time series from 15 Nov. to 15 Mar. (120 days). A *red* noise spectrum (*dashed curve*) and its 95 % level of significance (*solid curve*) are also shown. (c) Interannual variation in the WHDP spectrum from 1980–2007. The thick *black* solid line shows the 95 % level of significance 102
- Fig. 4.13 Composite of vertical integrated moisture flux (vector; 40 kg/m/s) and divergence (shaded; $\times 1e^5/s$) based on 7–25-day filtered values of specific humidity and wind anomalous fields from day –8 to day +8 based on WHDP. Day 0 corresponds to the active peak of 7–25-day WHDP variation. Values above 95 % statistically significant are plotted with *shade* 103
- Fig. 4.14 Composite of 7–25-day filtered 500 hPa streamfunction ($\times 1e-6 m^2/s$) and wind (m/s) anomalies from day –8 to day +8 based on WHDP. Day 0 corresponds to the active peak of 7–25-day WHDP variation. The contour interval for streamfunction is $5 \times 1e-6 m^2/s$, and the 95 % statistically significant streamfunction is shaded. The strength of the wind vector is 15 m/s, and the 95 % statistically significant wind is plotted with *red* color 105
- Fig. 4.15 Composite of 7–25-day filtered OLR (W/m^2 ; *shade*), 500 hPa streamfunction ($\times 1e-6 m^2/s$), and wind (m/s) anomalies from day –8 to day +8 based on WHDP. Day 0 corresponds to the active peak of 7–25-day WHDP variation. The contour interval for streamfunction is $4 \times 1e-6 m^2/s$. The strength of the wind vector is 5 m/s 106
- Fig. 4.16 Time-longitude cross-sectional distribution at 35°N of composites for 7–25-day filtered OLR (W/m^2 ; *shade*), 500 hPa height (hPa; *contour*), 500 hPa wind (m/s; *arrow*), and precipitation (mm/d; *red curve; upper axis*) anomalies from day –8 to day +8 based on WHDP. Day 0 corresponds to the active peak of 7–25-day WHDP variation. The *yellow* curve corresponds to anomalous precipitation (mm/d; *yellow curve; upper axis*) from day –8 to day +8 based on WHDP and (b) Schematic representation of physical mechanism associated with enhanced IWM during ENSO phases 107

List of Table

Table 2.1	Summary of the WD studies using modelling efforts	33
-----------	---	----

Chapter 1

Western Disturbances – Structure

Abstract The Indian subcontinent is characterized by its large spatial expanse along with heterogeneity and the variability of land use and land cover. These characteristics of India cause an extraordinary variety of climatic regimes over the various parts of the country. Western disturbances (WDs) are one of the many varied types of weather systems affecting Indian climate. The WD phenomenon causes precipitation over the Indian region mostly during the winter period and mostly over the northern part. WDs are a type of extra-tropical cyclone, which have mid-latitude frontal characteristics, that migrate eastward embedded in the subtropical westerly jet stream. But WDs are not just a typical extra-tropical cyclone, but they also have unique characteristics and dynamics. This chapter provides a detailed introduction to the topic and discusses the origin, migration, large-scale flow linkages and structure of WDs.

The Indian subcontinent is characterized by topographic heterogeneity and land use and land cover variability from north to south and west to east. Indian geography varies from the expanse of the *Himalayas*, through the *Gangetic Plains* in the north, the *Thar Desert* in the west, the *Peninsular Plateau* and to the *Coastal Ghats* in south (Survey of India Maps; Fig. 1.1). With these diverse topographical features and a large spatial expanse, India also shows an extraordinary variety of climatic regimes over different parts of the country (Gadgil and Joshi 1983). Based on Koppen-Geiger climatic classification (based on station data for precipitation and temperature), India has been divided into these regions and conditions: the northernmost Himalayas as *highlands with temperate* like conditions; *humid subtropical* conditions in the rest of the Himalayas and Gangetic Plains; *arid* conditions in the Thar region; the Indian peninsular region having *tropical wet and dry* climate; and the Coastal Ghats and Indian islands having *tropical wet* conditions, with a few parts of the peninsula and central India showing a *semi arid* climate (Peel et al. 2007). The Indian climate is known to be strongly influenced by the Himalayan Mountains and the Thar Desert (Reddy 2008).

The India Meteorological Department (IMD) has classified four broad climatic sub regions in India for long range forecasting, viz.: (i) *North and North East India*, (ii) *North West India*, (iii) *Central India* and (iv) *South Peninsula*. Further these sub-regions are classified into 36 different sub-divisions for short and medium range forecasting (www.imd.gov.in). In addition, the annual climatic cycle over India is

divided into four seasons as per the IMD classification: (i) *pre-monsoon (March-April-May)*, (ii) *monsoon (June-July-August-September)*, (iii) *post-monsoon (October-December)* and (iv) *winter (January-February)* (Attri and Tyagi 2010; Hingane et al. 1985; Parthasarathy et al. 1994; Rao and Ramamurti 1968). Deviations, termed as extremes or anomalies (Dash et al. 2009; Goswami et al. 2006; Karl and Easterling 1999), are observed in the weather conditions from these year to year climatic trends. The extreme weather conditions are usually categorized due to meteorological factors and their subsequent impacts (Easterling et al. 2000). With reference to the seasons, various types of extreme events can be observed and which can be categorized as: (i) *cold waves, fog, snow storms and associated avalanches*; (ii) *heat waves and severe storms like thunderstorms hailstorms and dust storms*; (iii) *heavy rains and associated landslides and flashfloods*; and (iv) *tropical cyclones and droughts* (De et al. 2005).



Fig. 1.1 Map of Indian Subcontinent (Source: http://www.travelindia-guide.com/maps/topographical_map.php; http://www.travelindia-guide.com/maps/political_map.php)



Fig. 1.1 (continued)

1.1 Introduction

WDs are a weather phenomenon which causes precipitation over the Indian region. The precipitation caused by the WDs contributes significantly to the northern Indian winter (December-January-February) monsoon (IWM) (Dimri 2013a, b) and thus has major consequences throughout the region. The importance of the

hydrological cycle, with precipitation as its main components, is immeasurable. Precipitation along with temperature is one of the most significant factors determining the ecology of a region and thus, in turn, influences societal structure and the economy of the said region. The climatic zones of a region are defined on the basis of the amount and type of precipitation received, thus defining arctic regions, temperate regions, tropical regions, etc. (Peel et al. 2007). Based on these regional variations in precipitation, the vegetation of a region is defined and its ecological demarcation such as desert, tropical forest, tundra vegetation, etc. Precipitation is also crucial for replenishing the fresh water resources on the land surface in the form of rivers, lakes or even glaciers. From an economic standpoint, even if environmental services rendered by precipitation are not considered, it still plays a significant role. For sustaining the food requirements of the growing population, agriculture is indispensable and in a country like India precipitation is a major source of irrigation. Other secondary services, which can be traced back to precipitation, are power generation and associated developmental projects and industrial and domestic use of water. There is an inverse relationship between Eurasian snow cover (and albedo) and the strength of the following Indian summer monsoon (ISM) (Vernekar et al. 1995; Dash et al. 2004, 2005; Mangain et al. 2010). A recent weakening of the El-Nino Southern Oscillation (ENSO)-ISM relationship (Kucharski et al. 2007) suggests an increased role of the ‘internal’ interannual variability of the ISM which has not yet been detected in the context of wintertime Himalayan snow cover (KrishnaKumar et al. 1999, 2006; Saha et al. 2011). Snowfall in the central Himalayas occurs during southward excursions of the subtropical westerly jet (SWJ) (Schiemann et al. 2009) associated with terrain-locked low pressure systems (WDs) at the notch formed by the Himalayas and the Hindu Kush Mountains (Lang and Barros 2004). The mass balance of glaciers in the northwestern Himalayas is very much dependent upon winter precipitation (Bolch et al. 2012). The wintertime snow-cover build up is necessary for Himalayan glaciers forming the snow-fed rivers and winter (rabi) crop growth (Rangachary and Bandyopadhyay 1987; Benn and Owen 1998; Roy 2009; Thayyen and Gergan 2010).

So on one hand it can be said that precipitation of water is the source of life; but on the other hand it may be the cause of hazards to life and property in extreme conditions. The flood-like conditions in a continuous precipitation time period and draught conditions during the dry years are foremost examples of how precipitation negatively impacts lives. Anomalies in the mean climatic trends, defined as the severe weather events, or in the scope of this study, severe precipitating events, are also another illustration of harm caused by precipitation. Extreme precipitating events are of various kinds like cloudbursts, continuous torrential rains, severe snow storms or even thunderstorms and hailstorms. Such events in themselves are disastrous, but can further cause severe damage due to their secondary impacts. These resulting impacts include events like flashfloods, glacial lakes outburst floods, landslides, avalanches. These events usually lead to significant cases of harm to human life and may also have health impacts in certain instances. Negative impacts on resources are realized in the form of crop damage, transport disruption and damage to property ultimately impacting people, infrastructure and economy. Natural haz-

ards including landslides, avalanches, and floods that can be directly attributed to these winter storms and the associated precipitation are well documented (Rangachary and Bandyopadhyay 1987; Ganju and Dimri 2004; Das et al. 2006; Srinivasan et al. 2005; Thayyen et al. 2012). WDs are also associated with the formation of fog conditions over northern India during winters (De et al. 2005). Additionally, in the context of the precipitation forming mechanism in conjunction with the complex topography, very little was published until Smith's (1979) classic review on 'The influence of the mountains on the atmosphere' and the more recent paper by Houze Jr's (2012) 'Orographic effects of precipitating clouds'. Because WDs impact a region without an extensive observational network, this made the studies of WDs even more elusive.

From the preceding discussion, it is clear that a fundamental understanding of the dynamics of WDs is therefore essential not only to short-term and seasonal hydrometeorological forecasting but also to the assessment of regional climate change and its impacts. The objective of this book is to provide an overview of the state of knowledge of WDs in the context of prior and current research.

1.2 Origin and Migration of Western Disturbances

WDs are in part extra-tropical cyclones originating as mid-latitude frontal systems and migrating eastward embedded in the subtropical westerly jet stream (SWJ) (Mull and Desai 1947). As per Alexander and Srinivasan (1974) *'The mean jet stream over the Indian sub-continent (in winter) lies near Lat. 27°N at a height of about 12 km (200 mb). The mean wind speed at the core is about 100 kts. There is a slight shift in the axis of the jet (by about 2–3 degrees of latitude) southwards as the season advances and towards end of winter or early spring, the jet stream reaches the southernmost position'*. Typical extra-tropical cyclones develop due to the imbalance between colder polar and warmer equatorial air masses. This imbalance is significant over the mid-latitudes and thus, these extra-tropical cyclones are also called mid-latitude fronts. The temperature gradient between polar and equatorial regions is most pronounced during the winters and thus these storms are more intense during the winters (AIR Worldwide 2012). Sub-tropical Westerly Jet (SWJ) is a jet stream that is contained in the mid-latitudes in the upper layers of the troposphere which develops around the Himalayan and Tibetan high ground (Alexander and Srinivasan 1974). According to Singh (1971a, 1980) there is a primary SWJ around 31°N at 200 hPa level. Further, there is a discrete jet present south of the primary jet termed as a secondary SWJ which is located around 23°N. WDs are eastward moving wave disturbances since these are embedded in the primary SWJ and move along the flow of the air within the jet stream. Deep troughs of the wave disturbances may be associated with the secondary SWJ. Detailed discussion on the jet stream and the WD is given later in this section. The disturbances start out as frontal systems and develop characteristics of a depression and extra-tropical cyclones, which, along with the surface low developed over western India, are defined as WDs (Dimri and Chevuturi 2014). They mainly originate in the

Mediterranean or West Atlantic region and travel across Iran, Iraq, Afghanistan, Pakistan and India (Rao and Srinivasan 1969). The disturbances discussed in their work are in the form of waves within the SWJ. These wave disturbances develop as extra-tropical cyclones over the Mediterranean Sea. The WDs as discussed are usually eastward moving systems from the Mediterranean Sea to India, but in some cases these might also have a convoluted path as they travel towards India. The WD of 28–31 December 1960 moved south east from Mediterranean region towards the Arabian Sea, gained moisture and suddenly turned towards India by moving in a north-easterly direction (Rao and Srinivasan 1969). Thus, the track of the WD systems may vary based on their migration and may intensify as these pass over a large moisture source.

First we will be discussing the origin and formation of these WDs in their early stages. A Ukaranian high intensifies and starts extending southwards towards the Iran region. This causes the intrusion of cold air from a polar front towards a region of comparatively warmer and moist air (Datta and Gupta 1967). These conditions are favorable for the development of frontogenesis. Associated with this frontogenesis, there is cyclogenesis taking place in the upper layers of the atmosphere over the Mediterranean region. Winds preceding the trough increase in intensity causing the divergence favorable for the cyclogenesis. The cold air intrusion develops a steep temperature gradient promoting frontogenesis. Likewise, an increase in the relative vorticity due to shifting of air mass from higher to lower latitudes favors cyclogenesis. The cyclogenesis further enhances the Mediterranean lows which exhibit an eastward movement. With the frontogenesis and cyclogenesis, the depression that is developed becomes a occluded front and the cold front trails the depression being formed (Mull and Desai 1947) and tracing the origin of the WDs. Riehl (1962) classified them as ‘weak’ extra-tropical disturbances originating in the Mediterranean traveling with the narrow but intense jet stream flowing around the southern rim of the Indian Himalayas. Palmen and Newton (1969) reported that frontal cyclones as upper air troughs have a life cycle which can decay into various forms. Initialization of an upper-air trough formation is associated with the front, forming on its western side. An intense upstream ridge forms a deep trough downstream without the additional advantage of cold-air incursion to intensify the front (Singh et al. 1981). In Palmen and Newton (1969), as the frontal surface moves towards the eastern side of the trough from the western side, the trough slowly decays.

Further characterization of WDs by Datta and Gupta (1967) indicated that they move at a speed of 8–10° longitude/day (e.g., 10–12 m/s), except during the formation and dissipation stages when the movement is comparatively slow. Whereas, Subbaramayya and Raju (1982) showed that the WD systems had an eastward propagating rate of 5–10° longitude per day and Rao and Srinivasan (1969) reported a propagation rate of 5° longitude per day. According to various studies, different life cycle durations have been suggested for the WDs. Dutta and Gupta (1967) reported a life cycle of WD as of 3–4 days, Rao and Srinivasan (1969) analysed a period of 2–4 days for induced low systems, and Rao and Rao (1971) showed a 8–10 day quasi-periodicity that they assigned to WD. But according to the Subbaramayya and

Raju (1982) study, there two systems of WDs with different periodicity exist. The long-period system had a periodicity of 10.0–12.5 days, the short-period system had a periodicity for 4.5–5.5 days and they concluded that the short-period systems are caused by WDs. Similar findings were reported by Chattopadhyay (1970), who studied three different periodicities during the winter period: shorter periodicities of 2.5–3.5 days, medium periodicity of 4.0–5.3 days and larger periodicity of 8.0–9.6 days. For all of these, the medium periodicities were deemed to be caused by the WDs. During the migration of the primary WD originating at the Mediterranean region, some secondary low pressure systems may become associated with the primary WD low. When the depression of the WD becomes occluded, the cold front trails behind the depression and sometimes secondaries form at the bend of the trailing front. Other times the secondaries form at the angle of the residual warm sector of the occluded depression (Mull and Desai 1947). These secondaries form due to distribution of mountains or seas in the surrounding regions (Malurkar 1947). Secondaries develop at coastal regions west of the River Nile, south of Egypt, Sudan, the Red Sea, the Gulf of Aden, the Oman Peninsula and the Arabian Sea and sometimes at the head of Bay of Bengal. A rapid occurrence of successive depressions causes a stable trough over the Persian Gulf with no secondary development possible. But secondaries may develop due to intrusion of air from cold Siberian anti-cyclones in the rear of the depression (Mull and Desai 1947). The secondary extra-tropical depression usually develops around the Persian Gulf or the Black Sea. Secondaries give rise to disturbed weather over the region and migrate eastward to north-eastward. These secondaries usually intensify the occluded parent depression. The secondary depressions, being shallow systems did not extend above 700 hPa, could not be tracked in the synoptic charts, and thus posed a challenge for forecasters (Agnihotri and Singh 1982). These secondaries of the extra-tropical systems were generated over the eastern Mediterranean system and migrated eastward to north-eastward and have a weak organization at the surface. The secondaries migrate at the rate of 10° longitude per day from the Middle-East to India and generally take 2 days to arrive over India. The primary WD is termed – the main WD, and the secondaries are termed – the induced WD.

In layman terms, WDs are atmospheric disturbances that originate west of India, in the Mediterranean region, and travel towards India where they cause precipitation. Figure 1.2 shows satellite images of a WD travelling towards India. In the figure it can be noted clearly that a disturbance is generated over the Mediterranean region on the 7 February 2009, while there is no disturbance on 6 February 2009. This disturbance travels eastward in the subsequent days, reaches northern India around 13 February 2009 and remains active until 14 February 2009, after which it dissipates. WDs result in the overcast skies associated with precipitation, but they lose frontal characteristics during their travel towards India and may develop into a depression, due to the lowering of temperature and pressure gradients (Rao and Rao 1971; Srinivasan 1971). The moisture in these storms usually originates over the Mediterranean Sea and the Atlantic Ocean. As they migrate eastward, these wave disturbances also pick up moisture from the Caspian and Arabian Seas as per their migratory pattern. WDs may intensify due to moisture incursion from the Arabian

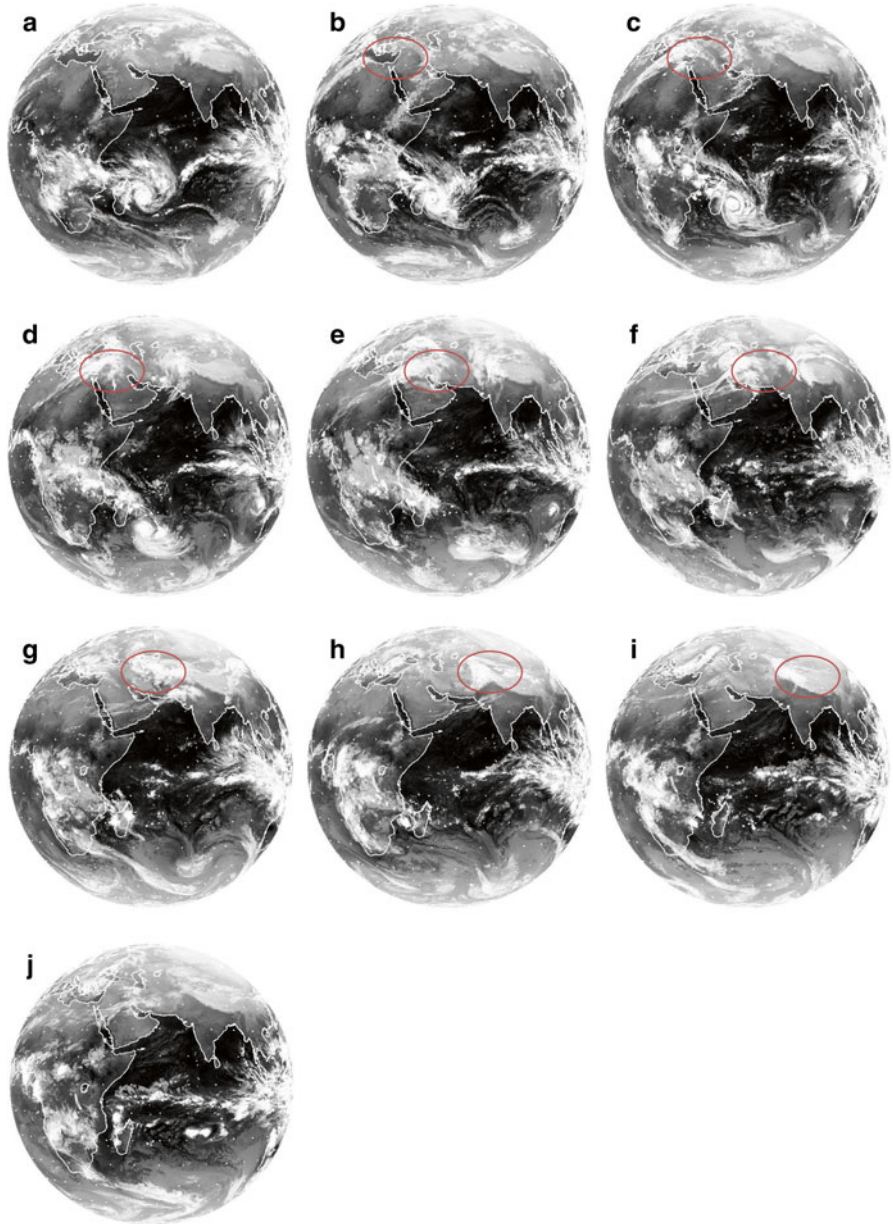


Fig. 1.2 Meteosat satellite image (Channel 2) for a WD travelling towards India. Satellite images of (a–j) are from 06 January 2009 to 15 January 2009 each at 0000 UTC. *Red circle* marks the migrating WD

Sea and from the Bay of Bengal, when over India, and are also influenced by the topography of the region (Singh et al. 1981). From the figure, it is evident that WDs intensify during the migration towards India from the accumulated moisture.

As mentioned in the above paragraph, the WDs are embedded in the SWJ. The presence and behaviour of the jet stream over the central Asia is important for a number of reasons. Its associated processes are interesting and challenging to study. In particular, upper-level flow over the Tibetan plateau responds to the Asian continent's physical and thermodynamical interactions (Academica Sinica 1957; Webster et al. 1998; Yanai et al. 1992; Wu and Liu 2003; Duan and Wu 2005). The increased availability of upper-air soundings from the 1950s to the 1970s enabled studies of jet stream dynamics leading to improved understanding (Chaudhury 1950; Murray 1953; Mohri 1953; 1958; Riehl et al. 1954; Bannon 1954; Endlich and McLean 1957; Defant and Taba 1957, 1958; Newton and Persson 1962; Serebreny et al. 1962). In the context of Indian weather, Ramaswamy (1956) elucidated the role of the SWJ in the pre-monsoon large-scale convection which lead to advances in thunderstorm predictability. In a subsequent study, Ramaswamy (1962) demonstrated the interaction of the tropical easterly jet (TEJ) and SWJ in defining gaps and active conditions during the ISM. However, the role of the jets in controlling winter weather was poorly understood until radiosonde observations revealed the quasi-permanent SWJ over the Indian subcontinent from October to May (Koteswaram et al. 1953; Koteswaram and Parathasarathy 1954). Knowledge of the day-to-day positioning of the jet streams proved invaluable for prognostic evaluation of Indian weather (Koteswaram 1957a, b). According to Singh (1971a, b), there is a SWJ located at 31°N which form major westerlies for the migratory WDs movement. There is also a secondary and less defined SWJ at 23–25°N which becomes distinct in the presence of WDs with deep troughs. There is also a Polar Front Jet at 43°N at 240 hPa which is located north of India (Singh 1971b). In winter, the Polar Front Jet located at 43°N can merge with the SWJ (Singh 1971b). The confluence forces the SWJ to rise, thus allowing the southward migration of cold and dry polar air from the north. The temperature gradient intensifies and builds SWJ with an elongated wind structure which can extend throughout the troposphere. An analysis of temperature at three tropospheric pressure levels reveals two dynamic zones over western and central India at 25°N and one over northwest India at 33°N (Singh 1980). The southern zone corresponds to the meeting of a tropical air mass and a mid-latitude air mass which coincides with the axes of WDs (Dimri and Chevuturi 2014). The southern zone is related to the evolution of an upper tropospheric temperature structure over the Middle East and synoptic predictability of the behavior of the jet stream over India. It has thus long been recognized that the seasonal meridional translation/progression of the SWJ is a good index for the determination of the natural synoptic scale weather/seasonal patterns (Bugayev et al. 1957; Academica Sinica 1957; Chanysheva et al. 1995). Schiemann et al. (2009) has characterized a SWJ over the Tibetan Plateau region which has a pronounced seasonal cycle. The WDs form as wave troughs in the westerlies at the 500 hPa level. These waves have variations in their intensity and amplitude during their eastward migration. There is also a possibility of merging of the waves to form deeper troughs as time

progresses (Ramaswamy 1966). Due to the upper level trough, cyclogenesis is observed at sea level and synchronized with the movement of the trough. During winter (December-April), during which WDs are pronounced over the northern India, this remains located at the southern edge of the Tibetan Plateau. Also, its intensity in terms of its monthly mean horizontal wind speed is strongest in winter and decreases in spring. It is important to mention, as Nigam and Lindzen (1989) has already shown, the modest variation in the latitudinal positioning of the jet over the Himalayas modulates the amount of stationary wave flux reaching from mid- and high latitudes. There are studies using the modern day reanalysis data which establish the relationship between the jet intensity and baroclinic wave activity over Northern Atlantic (Nakamura 1992) and the relationship between seasonal cycle of jet with meridional temperature gradient in the upper troposphere (Kuang and Zhang 2005). The baroclinic activity associated with WDs will be discussed in detail in the next chapter.

1.3 Western Disturbances at a Synoptic Scale

WDs develop instability in the atmosphere as they migrate over the Indian region. Specifically, the interaction of the WDs with the northwestern Himalayas orography (Ramaswamy 1956) causes their intensification and the subsequent precipitation. The WDs cause this instability due to the baroclinicity developing in the atmosphere. Baroclinicity develops a strong temperature gradient in the upper troposphere (Singh and Agnihotri 1977), which enhances the instability conditions. The first long-term weather forecasts, using the link between the nature of snowfall and accumulation patterns in the Himalayas and rainfall in the rest of India, were conducted after the establishment of the India Meteorological Department in 1875 (Blanford 1884). The problem of long-range forecasting (LRF) of ISM rainfall has been one of the major tasks of Indian meteorologists for more than a century (Blanford 1884; Walker 1924; Montgomery 1940). Flohn (1968), for the first time, provided an explanation of the role of the high Tibetan region in the role of wind within a limited set of observations. Over the western mountains and valleys, the largest portion of rainfall is produced by the traveling disturbances during the winter. *‘This is an unique type of climate rarely adequately treated in textbooks of climatology’*. To look into the winter weather, Venkiteshwaran (1939) relied on a simple sounding balloon at Agra (near New Delhi, India) to measure a synoptic weather system during the winter of 1931, referring to it as a ‘Winter Disturbance’. An analysis of the relative positions of the tropical and extratropical depressions provided the first systematic analysis to help predict wet and dry disturbances and providing the terminology ‘Western Disturbance’ for the first time in the published literature (Malurkar 1947). The origin and structure of western depressions over northwest India was first described and classified as ‘weak’ extratropical disturbances traveling with the narrow but intense jet stream flowing around the southern rim of the Indian Himalayas (Mull and Desai 1947; Riehl 1962). This jet stream has already be discussed as the SWJ over

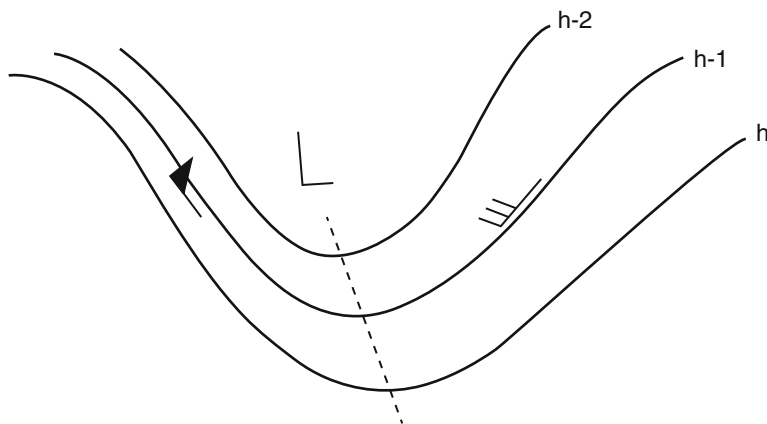


Fig. 1.3 An asymmetric upper-air trough with closer packing in the rear (Source: Pisharoty and Desai 1956)

northern India. Extra-tropical storms are a global, rather than a localized, phenomena with moisture usually carried in the upper atmosphere and they behave locally as frontal systems. Primarily, interaction of air masses with different characteristics leads to formation of discontinuity surfaces called frontal systems. The atmosphere above India has a high probability of formation of fronts during winter season (Ramaswamy 1966). These fronts get disorganized and migrate along with the WDs and cause the associated changes in the atmosphere.

Winter WDs are very similar to the Bjerknes cyclones of the Pacific and Atlantic with an asymmetric upper-air trough with closer packing at the back of the formation (Fig. 1.3) (Pisharoty and Desai 1956). This is caused by the counter patterns of strong winds west of the trough and weak winds east of the trough in the upper levels of atmosphere. This pattern generates cyclonic vorticity in the trough line, and subsidence associated with this vorticity increases low-level cyclonic circulation downwards. In the following chapters, a detailed description on the northwesterly tilt of 'so-called' closer packing associated with WDs from the surface to the upper atmosphere is elucidated. For a synoptic analysis of a WDs life cycle Rao and Rao (1971) reported on a generalized case of a WD. This can be considered an approximation of the synoptic situation of WD but not as representative synoptic situation. The WD started out as an eastward moving sea-level low over Afghanistan. On the subsequent day, this low had become well marked and now was lying over Pakistan and the western Indian region. On the next day, it was located over western India and had completely developed into a depression. After that, it weakened into a trough of low pressure and moved further east-north-eastward, and on the subsequent day it became more feeble and moved past West Bengal and Assam region and dissipated. As described by the Rao and Rao (1971) study, the WDs intensify or the trough deepens as they arrive over the northern Indian region. According to Pisharoty and Desai (1956), the addition of warm and moist air from the Arabian Sea and Bay of Bengal cause the increase in instability of the system and increased intensity.

Pisharoty and Desai (1956) explained that the heavy rainfall over the eastern Himalayan region was a result of the interaction of WDs with a break in the summer monsoon trough. Examining 10 years (1945–1955) of precipitation records over the Indian subcontinent, Mooley (1957) systematically classified synoptic situations across the Himalayan region. In contrast to Pisharoty and Desai (1956), Mooley suggested that WDs differ from extratropical depressions in that they generally do not always have well-marked cold or warm fronts either at the surface or upper levels, and concluded that orographic convergence plays a leading role in the production of locally heavy rain (Dimri and Niyogi 2012). This explanation added clarification to the presence of extratropical cyclones in the mid-latitude westerlies. In showing that WDs are preceded by warm and moist air from southern latitudes and succeeded by cold and dry air from northern latitudes, Mooley (1957) provided the first evidence linking the occasional presence of WDs during summertime with intensification of the ISM. Interlocking/merging of WD lows with the intertropical convergence zone (ITCZ) associated with the ISM invigorates the monsoon flow. Although this study examined various facets of WD structure, interactions with Himalayan topography and ISM, among others, it did not provide a full description of the underlying dynamics. This was achieved by Singh (1963) with an in-depth study of a WD on 28–31 December 1960, including vertical structure, evolution and decay, and associated jet stream movement. Singh's study showed that the vertical structure of WDs exhibits two synoptic components: an upper-level trough and a lower-level cyclonic circulation. The upper level trough is mainly associated with the SWJ which is 'in tune' with the traveling extratropical cyclone and existence of lower-level cyclonic circulation becomes embedded with this upper-level trough. This combination is defined as WD which is 'a subtle difference' than the explicit extratropical cyclone (Riehl 1962). And this hypothesis is proven with modeling efforts by Dimri and Chevuturi (2014). Further, Ramaswamy (1966) analysed WDs, based on the principle of conservation of vorticity and dynamical consequences, and changed the ongoing practice of forecasters relying on delineation of frontal systems at the synoptic scale. Chakravarti (1968a, b) advanced two important insights: first he stipulated the governing role of the Indian Himalayas in WD dynamics, and second, he noted that WDs leading to precipitation are initially generated and travel in upperatmospheric flow patterns. As an increasing number of ground and upper-air observations became available, the India Meteorological Department (IMD) published its first manual to guide forecast analysis at the synoptic scale (Rao and Srinivasan 1969). Singh and Kumar (1977) established that a well-organized upper tropospheric frontal layer in westerlies over a pre-existing surface low is essential for WD development. The upper-level front propagates eastward in association with an upper-air trough, and the growth of the upstream ridge is one of the key mechanisms to create a deep trough downstream (Singh et al. 1981).

Some wave-like disturbances also are known to impact China and the Eastern China Sea during the winter months and sometimes during the summer periods also. As the SWJ shifts northwards, there is also an impact over the China region during the summer period. During the winter period, the wave-like disturbances that we describe as WDs impact China with a periodicity of 4–5 days (Nitta et al. 1973) in February and even a 6–7 day period (Yoshizaki 1974) in January. Similarly, Hara

et al. (2004) studied the WDs causing avalanches in the southern Tibetan Plateau. They reported that a meso-alpha-scale quasi-stationary extratropical cyclone appeared along the Himalayan and Tibetan region, which is triggered as a trough west of the region. These waves propagated as tropospheric Rossby waves and coastal Kelvin waves or coastally trapped waves. The orography caused the blocking of the trough and slowed down the eastward movement of the system. Though this study pointed out that the vertical structure of the cyclone is barotropic, we will show from extensive review and research that it is not so. The WDs are caused due to baroclinic instabilities and will be described in detail in the next chapter. Also, since the focus of the book is the Indian region, we will not be going into much detail about other regions.

On a climatological basis, approximately four to six intensive WDs occur annually during the winter months from November to March (Mohanty et al. 1998), but there are higher precipitation days corresponding to the average life cycle of 2–3 days of WDs over the Western Himalayas (WH). In the WD shown in Fig. 1.2, it is noted that the lifecycle of the WD over the WH is 2 days. But the life cycles and periodicity of the WDs may vary according to the intensity and movement of the WDs. This has been discussed in the above section in much detail. Further, the WDs might have a longer life span if multiple WDs are moving in continuous succession (Rao and Srinivasan 1969). Further, not all WDs may cause precipitation, a characteristic which is dependent upon the moisture that is infused during the migration and the instability conditions. Mohanty et al. (1998) suggested approximately four to six intensive WDs in the winter season, whereas Chattopadhyay (1970) had reported the occurrence on an average of five WDs per month. According to Dimri (2006), Indian winters are impacted by six to seven WDs per month, of which two or three WDs can cause severe weather conditions.

For the last aspect of the synoptic study of WD, we will be discussing the clouds associated with this precipitating system. The winter season over India is associated with cloud cover moving from eastward in the northern Indian region as seen in Fig. 1.2. This is the satellite imagery of an active WD travelling from the Mediterranean to the Indian region, which shows its evolution, migration and ultimately dissipation of a specific WD. Clouds associated with WDs are upper-tropospheric clouds associated with the SWJ and high clouds with some alto-clouds (Srinivasan 1971). These form as short term mesoscale clouds in the cirrus formation, form around regions of relatively strong winds, and are organized in bands. The study reported that, even if the SWJ is a quasi-stationary feature of the winter circulation over India, the clouds are sporadic in nature. These clouds form only when there are troughs or disturbances within the SWJ flow. This defines that the clouds are associated with the WD travelling in the SWJ. High and medium clouds form during the winter over northern India with variable formations as described by Rao and Moray (1971). These might form the vortex type cloud system of the extra-tropical cyclone or the frontal cloud system during the origin of a WD. Agnihotri and Singh (1982) described similar organized system of clouds which are similar to the clouds that develop during extra-tropical cyclones. Latitudinal and meridional bands of clouds form during the migration of the WD as described by Rao and Moray (1971). Srinivasan (1971) also described the formation of longitudinal or transverse bands

of clouds. Moreover, Agnihotri and Singh (1982) reported the formation of latitudinal bands which slowly migrate eastward along with the broad shallow troughs in SWJ. Further cloud types according to Rao and Moray (1971) were formed as the WD interacts with any form of orography; this further intensifies the cloud system to form an overcast mass of clouds, which were further described by Agnihotri and Singh (1982) as shapeless and extensive. Formation and migration of low-level clouds through the valleys of the Himalayan mountain range depends on the interaction of air flow from westerlies and the relative orientation of the mountain range (Barry 2008). The WDs generate synoptic level instability which is enhanced or suppressed by moisture and orography. So pockets of clouded regions form within the region where WD is located. These create the broken amorphous type of the cloud system which are the most common form of the cloud systems during a WD. This suggests that WDs cause sporadic precipitation over irregular spatial intervals rather than over continuous spatial terrain. However, not all the cloud systems form during each of the WDs. Depending on the synoptic conditions, the cloud systems associated with the WD attain the general geometry of the clouded area. These cloud systems are sporadic in occurrence over the Indian region and occur only with troughs of sufficient amplitude (Srinivasan 1971). The associated secondaries developed along with the primary WD also have associated cloud formation. The cloud system associated with the secondaries usually show well organized structure and continuity during the migration in the subsequent time periods (Agnihotri and Singh 1982). The cloud systems associated with the primary or induced WDs in the satellite imagery can be used to systematically track the WDs track, as well as the precipitation patterns associated with the WD. Research by Veeraraghavan and Nath (1989) also used the cloud-top temperatures of these cloud systems as an indicator of the precipitation occurring during an active WD. Further details on the satellite studies of WDs are provided in the subsequent chapter.

1.4 Structure of Western Disturbances

As just discussed, the WD is an extra-tropical cyclone developing as a trough or low pressure system in the westerlies associated with a mid-latitude frontal system. The disturbances in the jet stream form a wave-like pattern with the trough in the mid-troposphere forming the upper portion of the WD. This is the extra-tropical depression, but as suggested by Chitlangia (1976), the pattern of the core of a WD is more complex and differs from a typical two-layer model of an extra-tropical depression. Singh et al. (1981) described the depression or the trough lying between two ridges in the jet stream flow. Formation of the extra-tropical cyclone associated with this trough follows the life cycle as described by Bjerknes which forms a cut off cyclone (Shapiro and Grønås 1999). According to the theory of formation of extra-tropical cyclones, there is front development or frontogenesis occurring to form frontal zones. This cyclogenesis forms as a wave along the frontal zone. This disturbance in the upper layer of the atmosphere causes the increase of divergence which in turn

causes lower-level convergence and an increase in the vertical movement of air. The associated cold and warm front occlude near the cyclone to develop the extra-tropical frontal cyclone. This is a cut off cyclone which is symmetrical thermally and has maximum vertical velocities during its peak intensities (Singh et al. 1981). But the vertical structure of a WD as suggested is quite unique on its own. This section describes the structure of a WD in detail.

To understand the WD structure, the mid-troposphere provides indicators for WD migration in the SWJ. Figure 1.4 shows the 500 hPa (mid-troposphere) wind and geopotential height in an example of a WD occurring in February 2002. On 5 February 2002, a depression is seen north-west of India which develops into a deeper depression on the next day 6 February 2002. Further intensification leads to formation of cyclonic circulation that is characteristic of the WD. On 7 February 2002, intensification of cyclonic circulation over north-west India and Pakistan region at 500 hPa is seen. The cyclonic circulation on both 7 February 2002 and 8 February 2002 weakens by 9 February 2002. This shows the western “disturbance” which develops as an anomalous circulation pattern or disturbance in the westerlies. This disturbance has different forms and changes according to its intensity. This may be in the form of a wave perturbation in the SWJ shown as a dip or a curve in the weather charts around a low pressure region called the westerly trough or a low. It can be in the form of a western depression which shows a circulation pattern with at least two closed isobars. And in further intense cases, it can also be called an extra-tropical cyclone which has at least four closed circle isobars on the weather charts. The induced WDs or the secondaries that form are classified based on intensity as an induced low or induced cyclonic circulation. Further, this figure illustrates the WD as a mid-tropospheric cyclone, but as Singh and Kumar (1977) established, the WD is not only a well-organized upper- to mid- tropospheric phenomenon in westerlies, but it also includes a pre-existing surface low as a part of the WD structure. Dimri and Chevuturi (2014) described the WD structure in the vertical column in detail and this has been elaborated in this section below.

The geopotential-height anomaly describes the vertical distribution of the low-pressure region formed during a WD occurrence. Figures 1.5 and 1.6 depict the geopotential-height anomaly at different pressure levels for a WD case in February 2002, averaged over latitude and longitude respectively. The region shaded blue depicts the WD low. As noted in the Fig. 1.5, the low-pressure region of the WD is showing a tilt when seen in the vertical cross section. The vertical tilt shifts towards the west during the early stage of development of the WD, which shifts towards the east as the WD propagates and subsequently dissipates. In Fig. 1.6, clear and consistent northerly shift in the vertical dimension is seen during evolution of the WD. This suggests that the low at different pressure levels during a WD has a north-westerly tilt in the early days of the WD, which becomes northerly as the WD arrives at WHs and propagates to become a north-easterly tilt as the WD travels further eastward. This movement describes the motion of the WD over the course of its life cycle of origin-evolution-propagation-deterioration. The WDs are defined by two synoptic characteristics; an upper tropospheric depression in the STWJ (SWJ) and the pre-existing surface low (Singh and Kumar 1977). These extra-tropical syn-

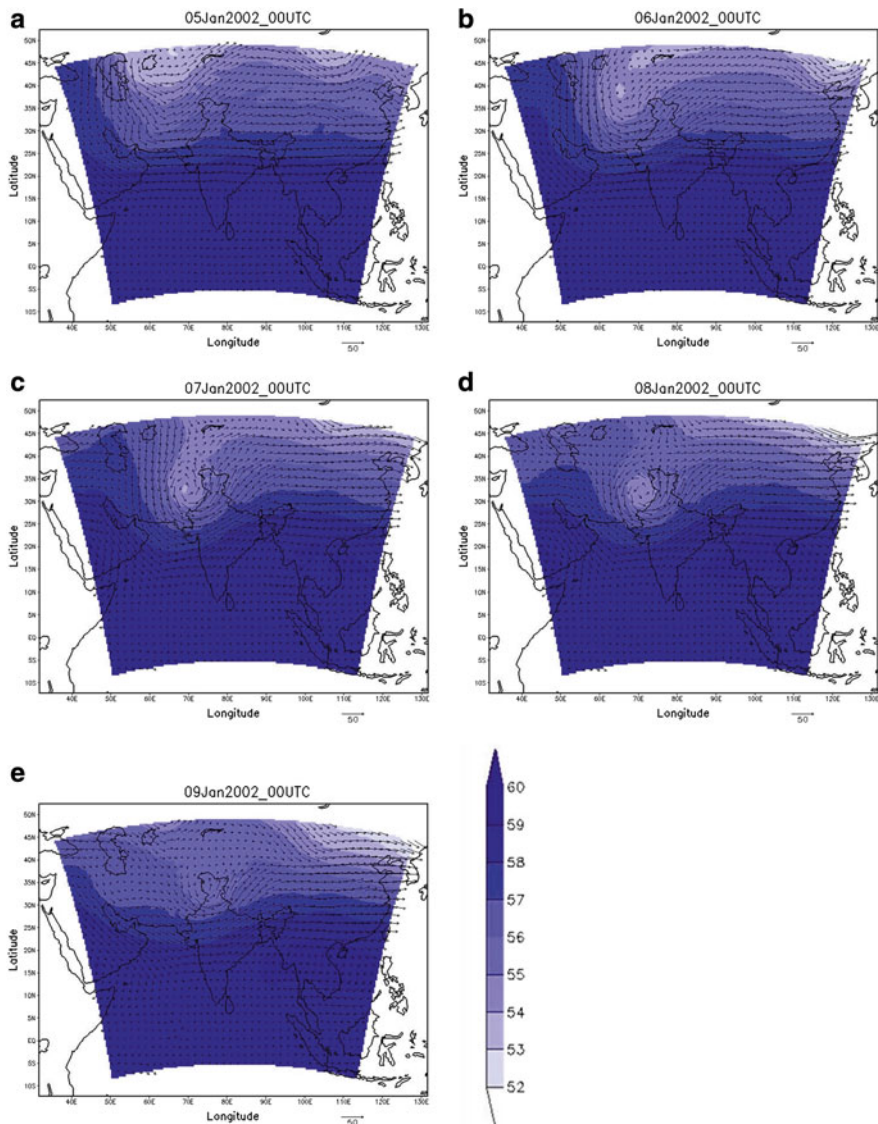


Fig. 1.4 500h Pa geopotential ($\times 10^{-2}$ m; shaded) and wind (m/s; arrow) for 05 February 2002 to 09 February 2002 with WRF model simulation (Dimri and Chevaturi 2014)

optic weather systems (low pressure systems) are brought by the SWJ stream from the Mediterranean region to the Indian region. The surface low already exists over western India, specifically over the Thar desert region of Rajasthan. The tilt of the low pressure system in the vertical axis can be attributed to the evolution of WD from west of India in the upper atmosphere and the stationary surface low seen over the India. During the lifetime of a WD, this tilt decreases or it disappears as the mid-

Fig. 1.5 Vertical distribution of geopotential height anomaly averaged over latitude (25°N–40°N) for WD in February 2002

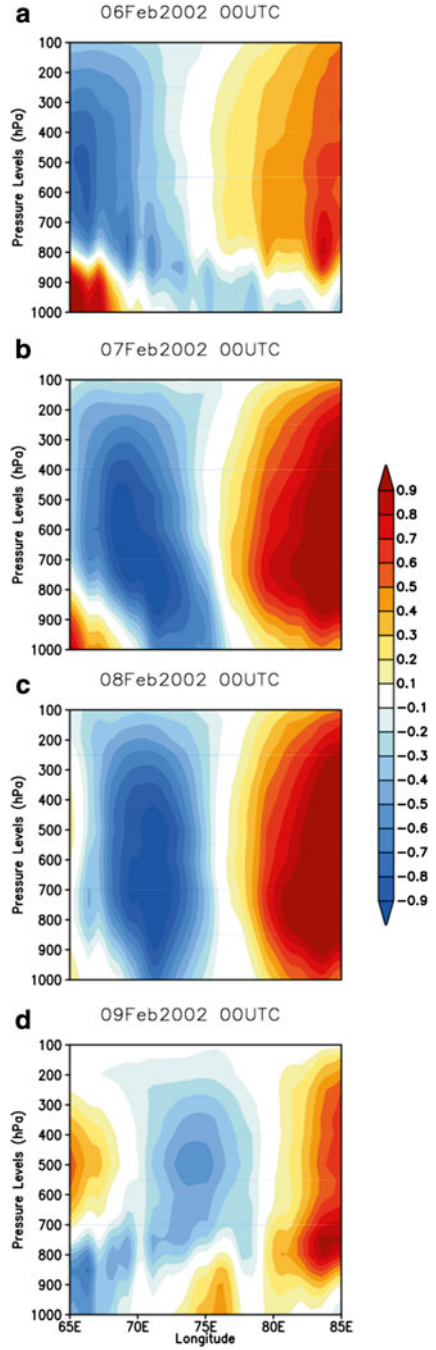
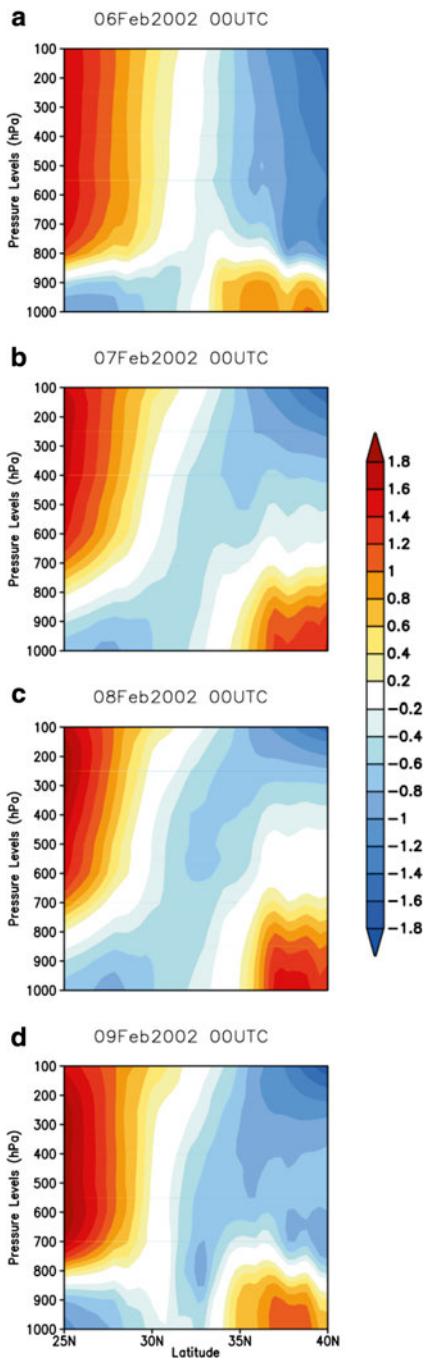


Fig. 1.6 Same as Fig. 1.5 but averaged over longitude (65°E–85°E)



tropospheric low travels towards the Himalayas. When the WD is situated exactly north of the surface low over the WHs, then the east-west tilt of the low is completely straight but the low still has a northerly tilt. As the WDs travel beyond WHs and further east, where they weaken, the tilt of the low-pressure system in the vertical axis becomes north-easterly. To conclude, the vertical dynamical structure of the WD of 5–8 February 2002 is examined in both respects, through the vertical distribution of a model-simulated geopotential anomaly on 7 February 2002 using the modeling framework of the Weather Research and Forecasting (WRF) in the study of Dimri and Chevuturi (2014). The vertical axis of the WD that links the surface low to the upper-air depression is tilted north-westward from the surface to the upper atmosphere. In the course of the WD evolution-propagation-demise, the surface low remains stationary but the upper-air depression moves eastwards in the upper level westerlies. Thus, subsequently the north-westward tilted axis straightens and further tilts north-eastward with time.

For a clearer understanding of the concept, Fig. 1.7 shows a conceptual model of a WD propagating west to east as a trough in the *SWJ*. The depression originating over the Mediterranean culminates in the formation of the *mid- to upper-level cyclonic circulation*, which is associated with a stationary *surface low* over the western Indian region. This causes a low pressure column to develop in the vertical direction which is *tilted* along the movement of the upper level disturbances. These wave-like disturbances interact with the orography of the *Himalayan terrain* to generate instability conditions over the northern Indian region and so form the winter storms. The orographic lifting, along this steep relief in addition to moisture incursion from the Arabian Sea, supports the development of convective available potential energy (CAPE) which is realized in the form kinetic energy required for storm development. The WD storms usually generate *precipitation* over the north-western Himalayas, which then dissipates as the WD moves eastwards. The dynamics of WDs and the orographic influence of the Himalayas on the WDs mentioned in this paragraph will be discussed in detail in the next chapter.

1.5 Western Disturbances and Linkages with Large-Scale Forcing

Many studies pertaining to the ISM are available whereas very little is known regarding the winter precipitation related WDs and its association to large scale flow. Rasmusson and Carpenter (1982) recognized the role of the El Niño – Southern Oscillation (ENSO) phases in defining the Indian winter monsoon (IWM). Meehl (1994) has addressed the evolution of winter and summer upperair flow in conjunction with Indian sub-continent heating. Yanai and Li (1994) investigated the phase relationship between the monsoon index, mean SST of various parts of the equatorial oceans, and Eurasian snow cover and found that snow cover leads both SST and monsoon index in a quasi-biennial range which is more complicated and suggestive

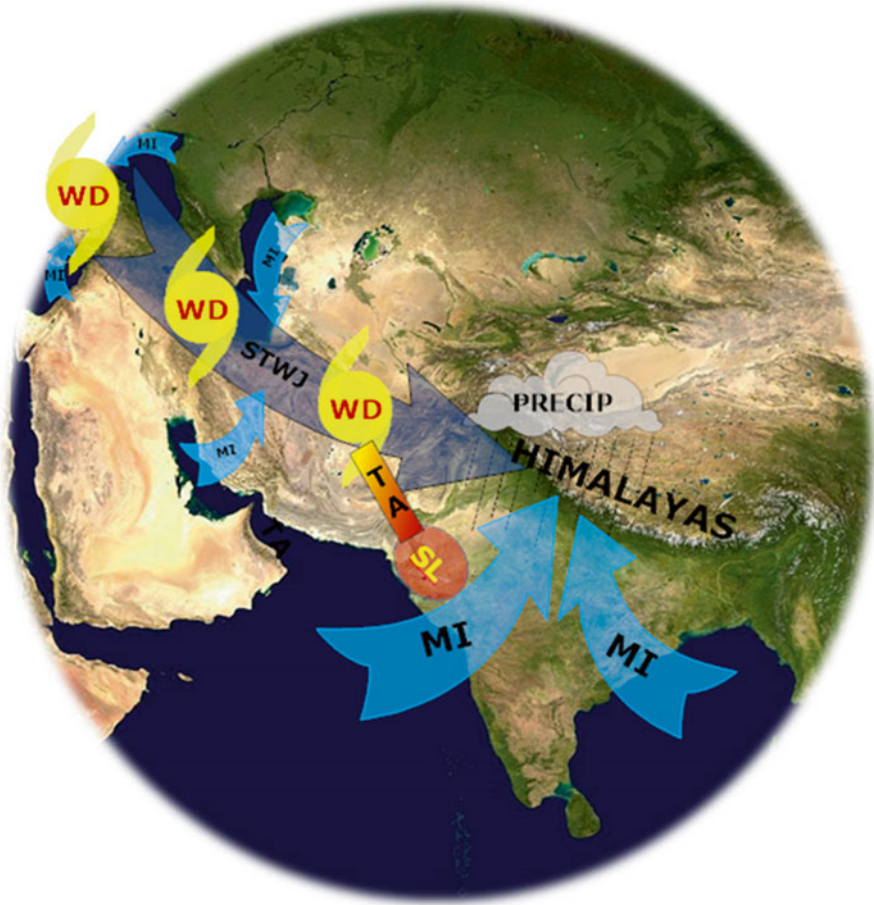


Fig. 1.7 Conceptual model of WDs (*MI*: Moisture incursion, *PRECIP*: Precipitation, *SL*: Surface low, *STWJ*: Sub-tropical westerly jet, *TA*: Westward tilted axis in vertical, *WD*: Upper air western disturbance)

of two-way interaction. Kawamura (1998) explained that, due to suppressed convection over the Indonesian region and the symmetric Rossby response due to attenuated Walker circulation associated with El-Nino conditions, this will result in conditions more conducive for cyclonic circulations over the Western Himalayas during wet years. Yang et al. (2002) noted a possible link of the Asian – Pacific – American climate with the East Asian jet stream during boreal winter. During years of high IWM precipitation, a higher magnitude (nearly on the order of 10) of kinetic energy flux convergence and stronger vorticity generation prevail than during dry years. In the case of surface and upper-air fields, this lowers sea-level pressure and strengthens westerlies over the Saudi Arabian region. It is important to mention that the WDs are embedded in the westerlies and hence, due to strengthening of these westerlies, strengthening of WDs also takes place (Dimri 2013b). In the upper air,

significant anomalous fields favor higher frequency and possible intensification of WDs during years of higher precipitation.

Roy (2006) provided comprehensive linkages of IWM with the different phases of ENSO, Pacific Decadal Oscillation (PDO), and local sea surface temperature. Syed et al. (2006) explained the intensification of WDs as they encounter a low-pressure trough, which is a dominant feature during positive Northern Atlantic Oscillation (NAO) and warm ENSO conditions. Further, examination of anomalous kinetic energy balance, vorticity, angular momentum, and the heat and moisture budget reveals that turbulent exchanges in the middle troposphere result in latent heat release and, during IWM, significant meridional moisture transport from the Arabian Sea to the western Himalayas due to the mean motion in the upper troposphere which takes place (Dimri 2007). The Himalayan glaciation itself has a positive feedback by increasing surface albedo (Bush 2000). Variations between sea-surface temperatures over the tropical Indian ocean impact winter precipitation over India. Increasing temperatures of the sea surface and reduced surface air temperatures over northern India intensify the SWJ, with the embedded disturbances leading to higher amounts of precipitation over the region (Yadav et al. 2007). A positive precipitation anomaly over northwest India is typically found in correspondence to subdued convection over the warm pool region. One proposed mechanism (Yadav et al. 2009) is that, in abnormally wet years, tropical cooling over the warm pool region due to suppressed convection generates an upper-level convergence (cyclonic circulation) anomaly over South Asia which intensifies the westerly jet stream over the Indian region. The Rossby-gyre dynamics, with strong vertical and westward meridional tilts in the tropical baroclinic atmosphere, forms cyclonic circulation anomalies in the upper troposphere due to a weak Madden-Julian Oscillation (MJO, Madden and Julian 1972) that intensifies the westerly jet stream over the Indian region (Dimri 2013a). The jet stream guides the WDs and hence increases precipitation over northwest India. Yadav et al. (2013) reported that the northern and central Indian winter precipitation becomes enhanced due to eastern Pacific El-Nino warming conditions. In association with the El-Nino, this warms the western Indian Ocean during winters and this strengthens the Hadley cell and causes subsidence over the central India. This sinking movement causes the intensification of the SWJ over northern India which further intensifies the surges/disturbances (WDs) embedded within it. This results in excess of precipitation over northern and central parts of India. Further details on the IWM will be given in the ensuing chapters.

References

- Academica Sinica (1957) On the general circulation over Eastern Asia (I). *Tellus* 9:432–446
- Agnihotri CL, Singh MS (1982) Satellite study of western disturbances. *Mausam* 33(2):249–254
- AIR Worldwide (2012) The impact of climate change on extra-tropical cyclones: a review of the current scientific literature. <http://www.air-worldwide.com/Publications/White-Papers/documents/The-Impact-of-Climate-Change-on-Extratropical-Cyclones---A-Review-of-the-Literature/>. Accessed on 24 Jan 2013

- Alexander G, Srinivasan V (1974) Winter – westerly jet streams and troughs in upper westerlies. Indian Meteorological Department: forecasting manual part III
- Attri SD, Tyagi A (2010) Climate profile of India. Meteorological monograph no environment meteorology –01/2010. http://www.imd.gov.in/doc/climate_profile.pdf. Accessed on 14 July 2012
- Bannon JK (1954) Note on the structure of the high altitude strong-wind belt in the middle east in winter. *Q J R Meteorol Soc* 80(344):218–221
- Barry RG (2008) Mountain weather and climate. Cambridge University Press, New York
- Benn DI, Owen LA (1998) The role of the Indian summer monsoon and the mid-latitude westerlies in Himalayan glaciation: review and speculative discussion. *J Geol Soc* 155:353–363
- Blanford HF (1884) On the connection of the Himalaya snowfall with dry winds and seasons of draughts in India. *Proc Roy Soc Lond* 37:3–22
- Bolch T, Kulkarni A, Kääh A, Huggel C, Paul F, Cogley JG, Frey H, Kargel JS, Fujita K, Scheel M, Bajracharya S, Stoffel M (2012) The state and fate of Himalayan glaciers. *Science* 336(6079):310–314
- Bugayev VA, Giorgio VA, Kozik EM, Petrosyants MA, Pshenitshnij AJ, Romanov NN, Tshernysheva ON (1957) Synoptic processes of Central Asia. Publishing Company of the Academy of Sciences of the Usbek Soviet Republic, Russia (in Russian)
- Bush AB (2000) A positive climatic feedback mechanism for Himalayan glaciation. *Quat Int* 65:3–13
- Chakravarti AK (1968a) Summer rainfall in India: a review of monsoonal and extramonsoonal aspects – I. *Atmosphere* 6(1):21–28
- Chakravarti AK (1968b) Summer rainfall in India: a review of monsoonal and extramonsoonal aspects – II. *Atmosphere* 6(3):87–114
- Chanysheva SG, Subbotina OI, Petrov UV, Egamberdiyev KT, Aizensh-tat BA, Leukhina GN (1995) Variability of the Central Asian Climate (in Russian). Central Asian Hydrometeorological Research Institute, 215 pp
- Chattopadhyay J (1970) Power spectrum analysis of atmospheric ozone content over north India. *Pure Appl Geophys* 83(1):111–119
- Chaudhury AM (1950) On the vertical distribution of wind and temperature over Indo-Pakistan along the meridian 76° E in winter. *Tellus* 2(1):56–62
- Chitlangia PR (1976) Mean model of western depression. *Indian J Meteorol Hydrol Geophys* 87(2):157–162
- Das S, Ashrit R, Moncrieff MW (2006) Simulation of a Himalayan cloudburst event. *J Earth Syst Sci* 115(3):299–313
- Dash SK, Singh GP, Vernekar AD, Shekhar MS (2004) A study on the number of snow days over Eurasia, Indian rainfall and seasonal circulations. *Meteorol Atmos Phys* 86:1–13
- Dash SK, Singh GP, Shekhar MS, Vernekar AD (2005) Response of the Indian summer monsoon circulation and rainfall to seasonal snow depth anomaly over Eurasia. *Clim Dyn* 24:1–10
- Dash SK, Kulkarni MA, Mohanty UC, Prasad K (2009) Changes in the characteristics of rain events in India. *J Geophys Res* 114(D10109):1–12
- Datta RK, Gupta MG (1967) Synoptic study of the formation and movements of western depressions. *Indian J Meteorol Geophys* 18(1):45–50
- De US, Dube RK, Rao GP (2005) Extreme weather events over India in the last 100 years. *J Indian Geophys Union* 9(3):173–187
- Defant F, Taba H (1957) The threefold structure of the atmosphere and the characteristics of the tropopause. *Tellus* 9(3):259–274
- Defant F, Taba H (1958) The breakdown of the zonal circulation during the period January 8 to 13, 1956, the characteristics of temperature field and tropopause and its relation to the atmospheric field of motion. *Tellus* 10(4):430–450
- Dimri AP (2006) Surface and upper air fields during extreme winter precipitation over the western Himalayas. *Pure Appl Geophys* 163:1679–1698
- Dimri AP (2007) A study of mean winter circulation characteristics and energetics over southeastern Asia. *Pure Appl Geophys* 164:1081–1106

- Dimri AP (2013a) Interannual variability of Indian winter monsoon over the western Himalaya. *Glob Planet Chang* 106:39–50
- Dimri AP (2013b) Intraseasonal oscillation associated with the Indian winter monsoon. *J Geophys Res* 118:1–10
- Dimri AP, Chevuturi A (2014) Model sensitivity analysis study for western disturbances over the Himalayas. *Meteorol Atmos Phys* 123(3–4):155–180
- Dimri AP, Niyogi D (2012) Regional climate model application at subgrid scale on Indian winter monsoon over the western Himalayas. *Int J Climatol* 33(9):2185–2205
- Duan A, Wu G (2005) Role of the Tibetan Plateau thermal forcing in the summer climate patterns over subtropical Asia. *Clim Dyn* 24:793–807
- Easterling DR, Evans JL, Groisman PY, Karl TR, Kunkel KE, Ambenje P (2000) Observed variability and trends in extreme climate events: a brief review. *Bull Am Meteorol Soc* 81(3):417–425
- Endlich RM, McLean GS (1957) The structure of the jet stream core. *J Meteorol* 14:543–552
- Flohn H (1968) Contribution to a meteorology of the Tibetan highlands. Atmospheric Science Paper No 130, 120 pp, Department of Atmospheric Science, Colorado State University, Fort Collins
- Gadgil S, Joshi NV (1983) Climatic clusters of the Indian region. *J Climatol* 3:47–63
- Ganju A, Dimri AP (2004) Prevention and mitigation of avalanche disasters in western Himalayan region. *Nat Hazards* 31:357–371
- Goswami BN, Venugopal V, Sengupta D, Madhusoodanan MS, Xavier PK (2006) Increasing trend of extreme rain events over India in a warming environment. *Science* 314(5804):1442–1445
- Hara M, Kimura F, Yasunari T (2004) The generating mechanism of western disturbances over the Himalayas. In: 6th international GAME conference, Japan. http://www.hyarc.nagoya-u.ac.jp/game/6thconf/html/abs_html/pdfs/T4HM09Aug04145134.pdf
- Hingane LS, RupaKumar K, RamanaMurty BV (1985) Long-term trends of surface air temperature in India. *J Climatol* 5(5):521–528
- Houze RA Jr (2012) Orographic effects on precipitating clouds. *Rev Geophys* 50:1–47
- Karl TR, Easterling DR (1999) Climate extremes: selected review and future research directions. *Weather and Climate Extremes*. Springer, Dordrecht, pp 309–325
- Kawamura R (1998) A possible mechanism of the Asian summer monsoon-ENSO coupling. *J Meteorol Soc Jpn* 76:1009–1027
- Koteswaram P (1957a) Mean zonal wind circulation over India. *Indian J Meteorol Geophys* 8:346
- Koteswaram P (1957b) Meteorological in relation to high level aviation. Indian Meteorological Department Publication, New Delhi, pp 101–108
- Koteswaram P, Parthasarathy S (1954) The mean jet stream over India in the pre-monsoon and post-monsoon seasons and vertical motions associated with sub-tropical jet streams. *Indian J Meteorol Geophys* 5(2):138–156
- Koteswaram P, Raman CRV, Parthasarathy S (1953) The mean jet stream over India and Burma in winter. *Indian J Meteorol Geophys* 4(2):111–122
- KrishnaKumar K, Rajagopalan B, Cane MA (1999) On the weakening relationship between the Indian monsoon and ENSO. *Science* 284(5423):2156–2159
- KrishnaKumar K, Rajagopalan B, Hoerling M, Bates G, Cane MA (2006) Unraveling the mystery of Indian monsoon failure during El Niño. *Science* 314(5796):115–119
- Kuang X, Zhang Y (2005) Seasonal variation of the East Asian subtropical westerly jet and its association with the heating fields over East Asia. *Adv Atmos Sci* 22:831–840
- Kucharski F, Bracco A, Yoo JH, Molteni F (2007) Low-frequency variability of the Indian monsoon-ENSO relationship and the tropical Atlantic: the “weakening” of the 1980s and 1990s. *J Clim* 20(16):4255–4266
- Lang TJ, Barros AP (2004) Winter storms in central Himalayas. *J Meteorol Soc Jap* 82(3):829–844
- Madden RA, Julian PR (1972) Description of global scale circulation cells in the tropics with a 40–50 day period. *J Atmos Sci* 29:1109–1123

- Malurkar SL (1947) Abnormally dry and wet western disturbances over north India. *Curr Sci* 16(5):139–141
- Mamgain A, Dash SK, Sarthi PP (2010) Characteristics of Eurasian snow depth with respect to Indian summer monsoon rainfall. *Meteorol Atmos Phys* 110(1):71–83
- Meehl JA (1994) Coupled ocean-atmosphere-land processes and South Asian monsoon variability. *Science* 256:263–267
- Mohanty UC, Madan OP, Rao PLS, Raju PVS (1998) Meteorological fields associated with western disturbances in relation to glacier basins of western Himalayas during winter season. Technical report, Centre for Atmospheric Science, IIT, Delhi, India
- Mohri K (1953) On the fields of wind and temperature over Japan and adjacent waters during winter of 1950–1951. *Tellus* 5(3):340–358
- Mohri K (1958) Jet streams and upper fronts in the general circulation and their characteristics over the Far East. *Geophys Mag (Tokyo)* 29:45–126
- Montgomery RB (1940) Report on the work of G. T. Walker. *Mon Weather Rev* 39(Suppl):26
- Mooley DA (1957) The role of western disturbances in the production of weather over India during different seasons. *Indian J Meteorol Geophys* 8(3):253–260
- Mull S, Desai BN (1947) The origin and structure of the winter depression of Northwest India. India Meteorological Department, Technical note No. 25, p 18
- Murray R (1953) Jet stream over the British isles during June 14–18, 1951. *Meteorol Mag* 82:971
- Nakamura H (1992) Midwinter suppression of baroclinic wave activity in the Pacific. *J Atmos Sci* 49:1629–1642
- Newton CW, Persson AV (1962) Structural characteristics of the subtropical jet stream and certain lower-stratospheric wind systems. *Tellus* 14(2):221–241
- Nigam S, Lindzen RS (1989) The sensitivity of stationary waves to variations in the basic state zonal flow. *J Atmos Sci* 46:1746–1768
- Nitta T, Nanbu M, Yoshizaki M (1973) Wave disturbances over the China continent and the Eastern China Sea in February, 1968. *J Meteorol Soc Jpn* 51:11–28
- Palmén E, Newton CW (1969) Atmospheric circulation systems: their structure and physical interpretation, International Geophysics Series, vol 13. Academic Press, New York/London
- Parthasarathy B, Munot AA, Kothawale DR (1994) All-India monthly and seasonal rainfall series: 1871–1993. *Theor Appl Climatol* 49(4):217–224
- Peel MC, Finlayson BL, McMahon TA (2007) Updated world map of the Köppen-Geiger climate classification. *Hydrol Earth Syst Sci Discuss* 4(2):439–473
- Pisharoty P, Desai BN (1956) “Western disturbances” and Indian weather. *Indian J Meteorol Geophys* 7:333–338
- Ramaswamy C (1956) On the sub-tropical jet stream and its role in the development of large-scale convection. *Tellus* 8(1):26–60
- Ramaswamy C (1962) Breaks in the Indian summer monsoon as a phenomenon of interaction between the easterly and the sub-tropical westerly jet streams. *Tellus* 14(3):337–349
- Ramaswamy C (1966) The problem of fronts in Indian atmosphere. *Indian J Meteorol Geophys* 17(2):151–170
- Rangachary N, Bandyopadhyay BK (1987) An analysis of the synoptic weather pattern associated with extensive avalanching in Western Himalaya. *Int Assoc Hydrol Sci Publ* 162:311–316
- Rao NSB, Moray PE (1971) Cloud systems associated with western disturbances: a preliminary study. *Indian J Meteorol Geophys* 22:413–420
- Rao YP, Ramamurti KS (1968) Climate of India. Indian Meteorological Department: Forecasting Manual Part I
- Rao VB, Rao ST (1971) A theoretical and synoptic study of western disturbances. *Pure Appl Geophys* 90(7):193–208
- Rao YP, Srinivasan V (1969) Discussion of typical synoptic weather situation: winter western disturbances and their associated features. Indian Meteorological Department: Forecasting Manual Part III

- Rasmusson EM, Carpenter TH (1982) Variations in tropical sea surface temperature and surface wind fields associated with the Southern Oscillation/El Niño. *Mon Weather Rev* 110(5):354–384
- Reddy SJ (2008) Climate change: myths and realities. Jeevananda Reddy
- Riehl H (1962) Jet streams of the atmosphere. Technical paper No. 32. Colorado State University
- Riehl H, Alaka MA, Jordan CL, Renard RJ (1954) The jet stream. *Meteorol Monogr* 2(7):100
- Roy SS (2006) The impacts of ENSO, PDO, and local SSTs on winter precipitation in India. *Phys Geogr* 27(5):464–474
- Roy SS (2009) Spatial variations in the diurnal patterns of winter precipitation in India. *Theor Appl Climatol* 96:347–356
- Saha SK, Halder S, KrishnaKumar K, Goswami BN (2011) Pre-onset land surface processes and ‘internal’ interannual variabilities of the Indian summer monsoon. *Clim Dyn* 36:2077–2089
- Schiemann R, Luthi D, Schar C (2009) Seasonality and interannual variability of the westerly jet in the Tibetan Plateau region. *J Clim* 22:2940–2957
- Serebreny SM, Wiegman EJ, Hadfield RG (1962) Some characteristic features of the jet stream complex during selected synoptic conditions. *J Appl Meteorol* 1(2):137–153
- Shapiro MA, Grønås S (1999) The life cycles of extratropical cyclones. American Meteorological Society, Boston
- Singh MS (1963) Upper air circulation associated with a western disturbance. *Indian J Meteorol Geophys* 14:156–172
- Singh MS (1971a) Study of the jet stream over India and to its north in winter: part I. *Indian J Meteorol Geophys* 22(1):1–14
- Singh MS (1971b) Study of the jet stream over India and to its north in winter: part II. *Indian J Meteorol Geophys* 22:149–160
- Singh MS (1980) Tropospheric structure and jet-streams over the Middle-East in winter. *Mausam* 31(2):241–246
- Singh MS, Agnihotri CL (1977) Baroclinity over India in winter and its relation to western disturbances and jet streams – Part I. *Indian J Meteorol Hydrol Geophys* 28(3):303–310
- Singh MS, Kumar S (1977) Study of western disturbance. *Indian J Meteorol Hydrol Geophys* 28(2):233–242
- Singh MS, Rao AVRK, Gupta SC (1981) Development and movement of a mid-tropospheric cyclone in the westerlies over India. *Mausam* 32(1):45–50
- Smith RB (1979) The influence of the mountains on the atmosphere. *Adv Geophys* 21:87–230. doi:10.1016/S0065-2687(08)60262-9
- Srinivasan V (1971) Some case studies of cirriform clouds over India during the winter period. *Indian J Meteorol Geophys* 22:421–428
- Srinivasan K, Ganju A, Sharma SS (2005) Usefulness of mesoscale weather forecast for avalanche forecasting. *Curr Sci* 88(6):921–926
- Subbaramayya I, Raju ASN (1982) A study of tropospheric wave disturbances over India in winter. *Pure Appl Geophys* 120(3):437–452
- Syed FS, Giorgi F, Pal JS, King MP (2006) Effect of remote forcings on the winter precipitation of central southwest Asia part I: observations. *Theor Appl Climatol* 86(1):147–160
- Thayyen RJ, Gergan JT (2010) Role of glaciers in watershed hydrology: a preliminary study of a “Himalayan catchment”. *Cryosphere* 4:115–128
- Thayyen RJ, Dimri AP, Kumar P, Agnihotri G (2012) Study of cloudburst and flash floods around Leh, India during August 4–6, 2010. *Nat Hazards*. doi:10.1007/s11069-012-0464-2
- Veeraraghavan K, Nath T (1989) A satellite study of an active western disturbance. *Mausam* 40(3):303–306
- Venkiteshwaran SP (1939) Rainfall due to winter disturbances and the associated upper air temperatures over Agra. *Proc Natl Inst Sci India* 5(1):117–121
- Venekar AD, Zhou J, Shukla J (1995) The effect of Eurasian snow cover on the Indian monsoon. *J Clim* 8:248–266

- Walker GT (1924) Correlation in seasonal variation of weather, X. Application to seasonal forecasting in India. *Mem India Meteorol Dept* 24:333–345
- Webster PJ, Magana VO, Palmer TN, Shukla J, Tomas RA, Yanai M, Yasunari T (1998) Monsoons: processes, predictability, and the prospects for prediction. *J Geophys Res* 103:14451–14510
- Wu G, Liu Y (2003) Summertime quadruplet heating patterns in the subtropics and the associated atmospheric circulation. *Geophys Res Lett* 30:1201. doi:[10.1029/2002GL016209](https://doi.org/10.1029/2002GL016209)
- Yadav RK, RupaKumar K, Rajeevan M (2007) Role of Indian Ocean sea surface temperatures in modulating northwest Indian winter precipitation variability. *Theor Appl Climatol* 87(1):73–83
- Yadav RK, RupaKumar K, Rajeevan M (2009) Increasing influence of ENSO and decreasing influence of AO/NAO in the recent decades over northwest India winter precipitation. *J Geophys Res* 114(D12):112
- Yadav RK, Ramu DA, Dimri AP (2013) On the relationship between ENSO patterns and winter precipitation over North and Central India. *Glob Planet Chang* 107:50–58
- Yanai M, Li C (1994) Interannual variability of the Asian summer monsoon and its relationship with ENSO, Eurasian snow cover and heating. In: *Proceedings of the international conference on monsoon variability and prediction, WMO/TD 619, vol I. World Meteorological Organization, Geneva*, pp 27–34
- Yanai M, Li C, Song Z (1992) Seasonal heating of the Tibetan Plateau and its effects on the evolution of the Asian summer monsoon. *J Meteorol Soc Jpn* 70:319–351
- Yang S, Lau KM, Kim KM (2002) Variations of the East Asian jet stream and Asian-Pacific-American winter climate anomalies. *J Clim* 15(3):306–325
- Yoshizaki M (1974) A study of wave disturbances over the China continent and the East China Sea in winter 1968. *J Meteorol Soc Jpn* 52(4):380–386

Chapter 2

Western Disturbances – Dynamics and Thermodynamics

Abstract To further expand our knowledge of the weather systems called western disturbances (WDs), in this chapter we present the dynamical basis of WDs. The mechanism of WD formation with details on the evolution of such storms are discussed, and a detailed explanation of the energetics and thermodynamics of the winter storms provided. The various studies on WDs using various tools such as satellite information or numerical modelling techniques are reviewed and summarized. Last but not the least, the influence of surface variability in terms of orography and land use – land cover impacts on WDs are in this chapter.

The previous chapter dealt with WDs in an introduction that detailed providing the typical structure and origin of these extra-tropical systems. To further expand our knowledge of these systems, this chapter develops the dynamical understanding of the WDs. The various studies on WDs using various tools such as satellite information or numerical modelling techniques are have been reviewed and summarized. And finally the influence of surface variability in terms of orography and changes in land use and land cover changes on WDs are discussed in this chapter.

Before proceeding with the working sections of the chapter detailing information about the WDs we briefly review the Himalayas. As will be discussed later, the Himalayas have a major impact on WDs and in further chapters we will note that there is a reciprocal impact from WDs on the Himalayas also. Hence, an introduction to the Himalayan mountain range is prudent. The Himalayas have been illustrated clearly in the Fig. 1.1 in the previous chapter. A detailed idea of the Himalayan extent and topography has been illustrated in Fig. 2.1. The Himalayas extend 2500 km which stretches from 34 to 36°N, 27° E and 27–28°N, 90° E with a width of 250–400 km (Barry 2008). West to east this mountain range is divided into regions called as the north-western Himalayas, central Himalayas and eastern Himalayas. Bordering on the northern edge of the Himalayas is the Tibetan Plateau. Moreover, the western part of the Himalayas is bordered by the Hindu-Kush range. According to Barry (2008), the Himalayas from north to south can be divided into three major ranges. The Greater Himalayas in the north have the highest mountains, with an average height of 6000 m. South of this range, in the middle, is the Lesser Himalayas with average peak height of 2000–3300 m. And down south the range is called the outer Himalayas or the Siwaliks which are shorter with peak height

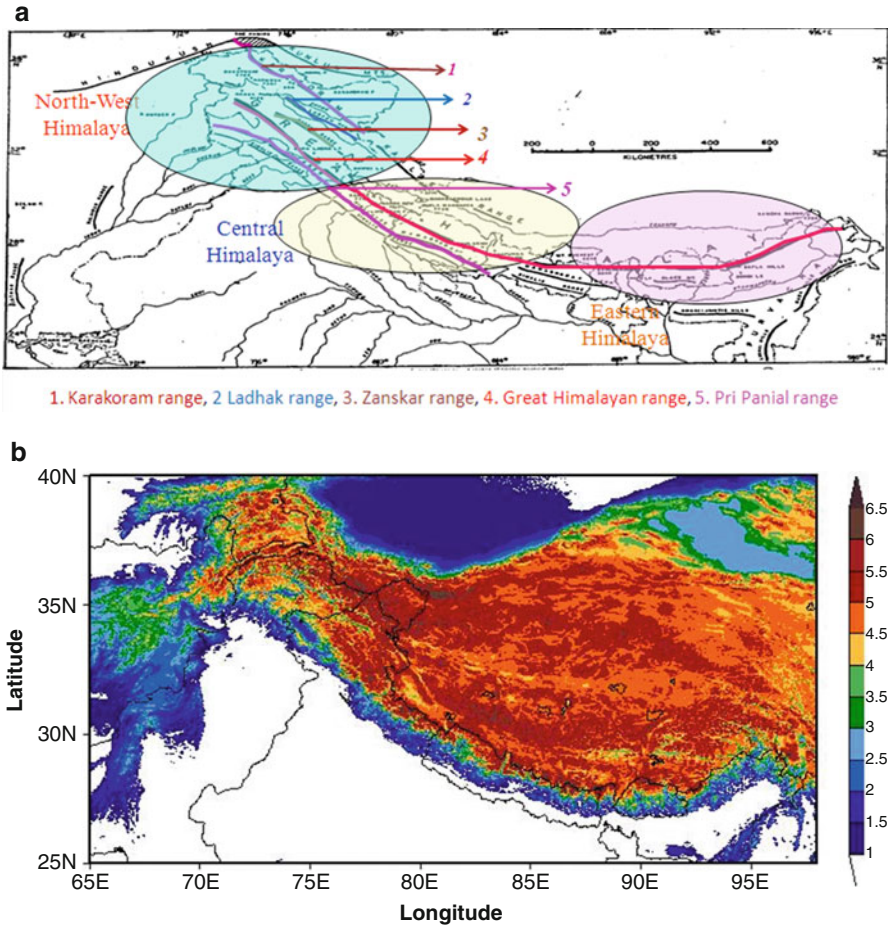


Fig. 2.1 (a) Schematic representation of cascading Himalayan mountain ranges (Pir Panjal- Great Himalaya-Zaskar-Ladhak-Karakoram) and western-central-eastern Himalayan region (b) Topographic ($\times 10^3$ m) overview of the Himalayas

averaging 900–1200 m. The Himalayas have a natural variability in land-cover patterns. Thus, the land-use and land-cover variability and topographic heterogeneity are the characteristic features of the Himalayas (Dimri 2012). The climatic conditions for the temperature parameter show variability over the Himalayan region due to the variation in the orography (Dimri 2004) and the land use (Dimri 2009), as also reported in the study Dash et al. (2007). Temperature predictably decreases with altitude, and the mountain range also shows a normal latitudinal gradient over the lower Himalayas. Precipitation patterns over the Himalayas also have a large variation due to the heterogeneous topography and variation in the surface cover (Dimri 2012). From an ecological stand point, the Himalayas have an outer monsoon forest, a zone of inner coniferous forest, and a border zone in the north of arid steppe.

With increased human intervention, there has been clear changes in the land-use and land-cover variability of the region especially because of more unplanned urbanization, agriculture and industrialization (Kala 2014).

The Himalayas, due to their unique geographical position, provide a physical barrier that plays an important role in global weather patterns (Fig. 2.1), acting as a heat source during the summer and a heat sink during the winter. Topographic heterogeneity, land-use variability, and varying snow-cover extent are important climate actors affecting the Indian summer monsoon (ISM) (Boos and Kuang 2010). During winter, the Himalayan region is prone to severe weather and the large amounts of snowfall produced by WDs (Schiemann et al. 2009). Regional spring snowmelt runoff contributes 15–44 % of the discharge to the tributaries of the Indus, and 6–20 % of the Ganges discharge (Ramasastry 1999). Spring runoff becomes especially important in the case of a delayed monsoon onset (Bamzai and Shukla 1999; Liu and Yanai 2002), and is a factor in pre-monsoon flooding and landslides (Agrawal 1999; Thayyen et al. 2012).

2.1 Dynamics of Western Disturbances

In this section we examine the dynamics, energetics and thermodynamics of WDs. WDs are synoptic systems with associated large-scale circulation patterns. Various process studies into the energy and water budgets for large-scale synoptic systems are required to determine the dynamics of the systems. After reviewing many papers, Gupta and Mandal (1987) as well as Raju et al. (2011) noted the importance of large-scale synoptic systems in the generation, transfer and transformation of kinetic energy in the middle latitudes and their various patterns in the lower latitudes. The available potential energy for the extra-tropical cyclonic weather systems is drawn from the latitudinal/meridional temperature gradient (between different latitudes) (Dimri et al. 2004). The difference in the temperatures between the tropics and mid-latitudes or even the polar region play a significant role in generating the extra-tropical cyclones. The literature review also suggested that the WD kinetic-energy budget will be a more interesting topic to study since WDs are systems that move in the borderline zone of tropics and extra-tropics (Raju et al. 2011). Although WDs are considered similar to extra-tropical systems, they differ from such systems because their frontal structures dissipate due to the friction of the surface as they migrate long distances. Also, their movement across Himalayan orography causes energy changes that are different than those seen in the usual mid-latitude systems. A synthesis of the various studies on WD kinetic-energy budget is provided here for a deeper understanding of the WDs.

A study by Ananthkrishnan and Keshavmurthy (1973) analysed the generation of kinetic energy over India during the winter season by diagnosing the meridional wind and the zonal wind flow. The study reported that the adiabatic kinetic energy within WDs is consumed by zonal wind flow along its track due to enhanced meridional wind flow and vice versa. Gupta and Mandal (1987) explained the behavior of

the kinetic-energy generation function during a WD. Their study revealed that the increase (decrease) in the kinetic energy content of the system could not be related directly to the positive (negative) contribution of the kinetic-energy generation function. Further, the zonal component of the kinetic energy generation function acted as a source, while the meridional component behaved as a strong sink in the upper levels throughout the life cycle of the system. Analysis of meteorological global reanalysis datasets enables researchers to examine the unique characteristics of specific synoptic events. Many of these reanalyses depict the large-scale circulation characteristics of WDs reasonably well despite weak constraints due to data paucity in the Himalayas (Mohanty et al. 1998, 1999). As an example, Roy and Bhowmik (2005) successfully used gridded datasets of the Indian Meteorological Department global- model output to thermodynamically analyse the WDs over the Delhi region. The study revealed that there is external advection of water vapor over a region as a consequence of the passage of WDs. The atmosphere during the winter season over the region is relatively dry and cannot result in precipitation due to convection at the local level. Hence, the external source of moisture incursion is a necessity for the WD related winter precipitation. In association with the moisture influx, convective activity is observed as the energy realized when the conditional instability is released, the latter termed the convective available potential energy (CAPE). The CAPE values increase during a WD passage, providing the required energy for the storm to form. According to Agnihotri and Singh (1987), during winters the shortwave solar radiation is absorbed mostly in the lower levels of the atmosphere due to the presence of the moisture. During WD occurrences due to low level moisture incursion, there is enhanced absorption of the incident solar radiation in the lower levels, which is another source of energy for the storm. Mohanty et al. (1999) performed a comparative analysis of the dynamical and thermodynamical characteristics between weak and active WD using observational analysis. The study reports higher amounts of precipitable water and higher convergence of horizontal heat flux during an active WD than in a weak WD. The role of the Himalayan orography in blocking and guiding the integrated moisture fluxes within the model reanalysis for an active WD over northern India is shown by Raju et al. (2011), confirming the early diagnosis of Ananthakrishnan and Keshavmurthy (1973). It reported that zonal and meridional formation of kinetic energy was in opposition to generation. The study also showed a strong rise in the convergence of the flux of kinetic energy and weak adiabatic production of kinetic energy during the passage of an intense WD. Towards the centre of the low pressure area of the WD, destruction of kinetic energy took place, whereas generation of the energy occurred west of the centre of an intense WD.

Access to satellite imagery changed tools and methodologies in weather forecasting and have proven to be essential elements of improved effectiveness (Houghton 1987). Studies related to the WDs using satellite data have provided detailed information on the topic. The first synoptic charts for India, with input from satellite imagery showing jets and cloud systems, were produced in 1970 (Srinivasan 1971). This study reported the formation of the clouds associated with troughs in the SWJ which is indicative of the precipitation associated with the WDs. Satellite

imagery and charts available were used to analyse the cloud bands associated with WDs, classifying cloud patterns in terms of the relationship between geometry and cloud area (Rao and Moray 1971). Such structure-based cloud imagery helped in assessing the evolution of WDs over time and provided an analysis of the life cycle of an evolving WD. Based on 10 years of satellite information, three broad categories were suggested by Agnihotri and Singh (1982). A significant finding of this study was that there are important secondary extra-tropical depressions traveling with large-scale westerlies and approaching northwest India. Detailed analysis of the cloud formation associated with the WDs are described in the previous chapter.

Other than using satellite imagery to study cloud systems associated with the WDs, this imagery has been used to analyse other details about these systems. Using NOAA-6 satellite products, Sharma and Subramaniam (1983) pointed out the linkages of WDs with the low-level easterly troughs responsible for intensification of the WD. They provided further support that this linkage caused expanded associated precipitation far to the south. A relationship between cloud-top temperatures and WD rainfall in the relatively drier month of November was proposed by Veeraraghavan and Nath (1989). They used Arkin's methodology to estimate the precipitation caused by WDs using the cloud-top temperatures. But this methodology did not provide accurate rainfall estimates when compared with the actual average rainfall based on the data provided by the gauge stations because the methodology was not used on a region of variable orography like Himalayas. Puranik and Karekar (2009) used satellite observations from multiple platforms to delineate the cold-air intrusion and the moisture pathways. Their objective was to demonstrate the capability of Advanced Microwave Sounding Unit -B (AMSU-B), flying onboard the NOAA satellite, to monitor WDs in five different microwave frequencies. Now data assimilation of satellite data into modelling techniques are providing yet greater accuracy for the model simulated outputs when compared with the observational analysis. Rakesh et al. (2009) is one of the studies including satellite data into numerical weather prediction.

Satellite information has been an important tool in studying the interaction of the mid-latitude systems with tropical systems. An important aspect of the interaction between the tropics and mid-latitudes is the emergence of cloud surges, which are due to the interaction of tropical and mid-latitude flows, and are clearly visible in satellite imagery. When the existence of large amplitude troughs in subtropical westerlies impinge on low-latitude synoptic disturbances, this first 'interaction' shows signs of cloud deformation north-eastward from the lower latitudes Kalsi and Halder 1992). Such interactions during summer monsoon months add to increased monsoonal flow. A similar case of tropical and extra-tropical interaction led to the massive disaster over the Kedarnath region in June 2013. Interaction between WD and MT caused the formation of dense clouding and resulting in the heavy precipitation observed over northern India (IMD 2013), as also seen by satellite imagery. This cloud system was termed a transient cloud system (Pandey and Pandey 2014; Chevuturi and Dimri in review). Detailed analysis of interaction of tropical and mid-latitude systems are described in the next chapter.

2.2 Modelling Studies Related to Western Disturbances

A survey of modelling attempts of WD events is described here. Table 2.1 presents the framework associated with various modelling studies and major findings of the studies. The main focus is on significant milestones in WDs' modelling studies that enhanced process understanding and model improvement. While greater understanding of the WDs needs no justification, model improvement is important for the improvement in forecasting and prediction of the WDs. The first mathematical description of cyclonic waves in the baroclinic westerlies was introduced by Charney (1947), which provided a theoretical basis for numerical weather prediction (Charney 1948; Charney et al. 1950). Here, we mainly rely on existing dynamical numerical models of WDs. Rao and Rao (1971) considered that the observed zonal wind profile is unstable with respect to the small superimposed disturbance, most notably for a perturbation wavelength of around 7000 km at 28°N. Such baroclinic instability is a possible mechanism for energy release and the development of a WD. They also analysed the periodicity and wavelength of the WD in the form of wave disturbances. They found out that WDs have a periodicity of about 9 days and a wavelength of about 6.0×10^6 m in early stages and 8.5×10^6 m in the later stages of development. Ramanathan and Saha (1972) applied a primitive equation in a barotropic model at 500 hPa to predict the evolution of WDs and investigated the role of initial and boundary conditions on forecast accuracy. The study used two cases of WDs to analyse the forecast ability of the model using east-west cyclic boundary conditions. They developed encouraging and important applications of dynamical models to predict WD movement. Chitlangia (1976) employed a moving coordinate system to study the mean structure of a WD. The study used data from six WD cases in the model. Hoskins and Karoly (1982), using a steady-state-linearized- five-layer baroclinic model, established the role of subtropical forcing to produce appreciable response in mid- and high latitudes. In low latitudes, it establishes that longer wavelengths propagate poleward and eastward, whereas shorter wavelengths are trapped in the equatorward side of the jet. This trapped jet enhances the evolution of embedded WDs. A comprehensive analysis of a WD simulated within a global spectral model reported by Dash and Chakrapani (1989) showed improvement in forecast skill with respect to geopotential heights and wind magnitude associated with a WD, and thus associated precipitation. deSilva and Lindzen (1993) investigated stationary waves in the northern hemisphere winter using stationary and time-dependent, linear primitive equation models. In tandem with Nigam and Lindzen (1989), they found that small displacements of the SWJ causes significant changes in stationary wave response right in the troposphere and in the lower troposphere. This behavior could be used for long-range forecasting of the associated synoptic weathers such as WDs. Predictability of precipitation associated with WDs increased with the introduction of boundary-layer and convection schemes in numerical models (Azadi et al. 2001; Das et al. 2003; Das 2005; Hatwar et al. 2005; Dimri and Chevuturi 2014; Chevuturi et al. 2014).

Table 2.1 Summary of the WD studies using modelling efforts

Reference	WD case discussed	Model used	Horizontal model Resolution	Parameterization Schemes		Significant findings
				Convective	PBLs0073	
Rao and Rao (1971)	11–17 Dec 1963	Observational data used				The WD development shows similar characteristics to a baroclinically unstable disturbance.
Ramanathan and Saha (1972)	22–25 Dec 1968; 11–14 Jan 1969	Primitive equation limited-area barotropic model	2.5°			Forecast of WD with the limited area model could generally predict the movement of WD, but required to improve resolution and reduce forecast error.
Chitlangia (1976)	4–5 Jan 1959; 3–4 Feb 1959; 20–21 Jan 1962; 25–26 Jan 1962; 23–24 Feb 1962; 19–20 Jan 1965	Moving coordinate system (empirical model)	1°			During a WD, the vertical structure of atmosphere shows more complex characteristics than an extra-tropical depression with a simple two layer model.
Dash and Chakrapani (1989)	27 Feb–3 Mar 1982	Global spectral model (IIT Delhi)				The forecast fields of 24 h accumulated precipitation and wind circulation patterns show agreement with the respective analysis.
Gupta et al. (1999)	27–30 Dec 1994; 8–10 Jan 1995; 15–17 Jan 1996; 19–21 Jan 1997	NCEP T80, 18 layer global spectral model (NCMRWF)	160 km			The model is able to forecast intensity and extent of winter systems 72h in advance but not able to provide point specific predictions.
Azadi et al. (2001)	18–21 Jan 1997	MM5 (V2.12)	60 km	Kuo, Grell, Kain-Fritsch, Betts-Miller	Blackadar, Hong-Pan	Hong-Pan PBL scheme and Betts-Miller cumulus scheme give better results as compared to the other parameterization schemes.

(continued)

Table 2.1 (continued)

Reference	WD case discussed	Model used	Horizontal model resolution	Parameterization Schemes		Significant findings
				Convective	PBLs/0073	
Das (2002)	14–16 Sep 2001	MM5	90 km, 30 km, 10 km	Grell	Hong-Pan	Results show that model forecasts of WD and associated wind and precipitation compare well with the observation over the region.
Das et al. (2003)	14–16 Sep 2001	MM5	90 km, 30 km, 10 km	Grell	Hong-Pan	Model forecasts WD features are well depicted 72h in advance of the system.
Dimri (2004)	21–25 Jan 1999	MM5 (V2.12)	90 km, 60 km, 30 km	Betts-Miller	Hong-Pan	Better representation of topographical features in the finer domain lead to improved simulation of WD and associated precipitation.
Dimri et al. (2004)	21–25 Jan 1999	MM5 (V2.12)	60 km	Betts-Miller	Hong-Pan	Model simulation captured the movement and intensity of WD along with representing some fine structure not observed in the verification analysis.
Dimri et al. (2006)	18–21 Jan 1997; 20–25 Jan 1999	MM5 (V2.12)	90 km, 60 km, 30 km	Kuo, Grell, Kain-Fritsch, Betts-Miller	Blackadar, Hong-Pan	Sensitivity analysis suggests that simulation of WD is better represented with combination of Hong-Pan PBL scheme and Betts-Miller convective scheme and finer horizontal model resolution.
Hatwar et al. (2005)	13–17 January 2002; 5–8 Feb 2002	IMD limited area analysis forecast system	1°	Model description in detail in Krishnamurti et al. (1990)		Precipitation patterns in the forecast compare well with the verification analysis but intensity of rainfall is under-predicted in the model output.

Azadi et al. (2005)	24 Mar 1993; 14 Feb 1995; 15 Jan 1996; 12 Mar 1998	MM5 (V2.12)	90 km, 60 km, 30 km	Betts-Miller	Hong-Pan	Model simulated synoptic system and associated features compares well with the analysis but shows slight bias which slows the system.
Das (2005)	14–16 January 2002	MM5	90 km, 30 km, 10 km	Grell	Hong-Pan	Forecasts upto 72 h show good capability of the model to predict rainfall over the mountainous regions.
Srinivasan et al. (2005)	13–15 Mar 2001; 13–17 Jan 2002; 16–20 Feb 2003	MM5 model (integrated with Snow cover model and statistical model)	30 km			Improved avalanche prediction was observed on application of model predicted meteorological parameters.
Semwal and Giri (2007)	30 Dec 2004–04 Jan 2005; 3–7 Feb 2007	ARPS (V5.1.5)	30 km	Kain-Fritsch		Model simulates spatial distribution of the precipitation well and shows heterogeneous precipitation distribution on comparison with observation analysis in cases of merging WDs.
Dimri and Mohanty (2009)	17–20 Jan 1997; 1–4 Feb 1997; 8–11 Feb 1997; 23–26 Feb 1997	MM5 (V2.12)	60 km	Betts-Miller	Hong-Pan	Simulation of active WDs with the model represent the associated mesoscale features well.
Hara et al. (2004)	27–31 Dec 1990	RAMS	100 km			A simulation of quasi-stationary cyclone over southern slope of Himalayas is depicted as a topographic Rossby wave.
Semwal and Dimri (2012)	1–4 Jan 2006; 31 Dec 2004–03 Jan 2005; 306 Feb 2005	ARPS (V5.1.5)	30 km, 10 km	Kain-Fritsch		Complex topography and local meteorological effects impact the prediction of heterogeneous precipitation distribution.

(continued)

Table 2.1 (continued)

Reference	WD case discussed	Model used	Horizontal model Resolution	Parameterization Schemes		Significant findings
				Convective	PBLs0073	
Rakesh et al (2009)	8–11 Feb 2007	MM5 using 3DVar assimilation (with MODIS derived data)				Forecast initialization with 3DVar approach shows improved results over simulation without incorporation of MODIS satellite datasets.
Dasgupta et al. (2012)	23 Apr 2004	MM5 (V3.4) using 3DVar assimilation	90 km, 30 km, 10 km	Grell	Non local closure scheme	Improvement of precipitation forecasts is observed in simulation with 3D Var assimilation.
Dimri and Niyogi (2012)	1980–2001	RegCM3	60 km, 10 km	Grell	Hollslag	Model dynamical downscaling captures the topography and precipitation interaction well with finer resolution showing better results over WH.
Dimri et al. (2013)	1990–2007	HadRM3 and REMO	0.23° (~2.5 km)	Mass flux (Gregory and Rowntree 1990) Mass flux (Tiedtke 1989) respectively		Regional climate models captured features of dynamic and orographic forcing along with the associated precipitation mechanisms of WDs.
Thomas et al. (2013)	17–18 Feb 2003; 21–22 Jan 2003; 10–11 Feb 2007; 27–28 Feb 2007; 11–12 Mar 2007	WRF (ARW)	45 km, 15 km	Grell Devenyi ensemble	Yonsei University (YSU)	For WDs simulations with ARW, RUC land surface parameterization is best suited.
Dimri and Chevuturi (2014)	13–17 January 2002; 5–8 Feb 2002; 11–13 Feb 2002	WRF (ARW)	81 km, 27 km, 9 km	Kain-Fritsch	Yonsei University (YSU)	Eta grid-scale cloud and precipitation microphysics scheme; Yonsei University scheme and Kain-Fritsch scheme is found to be the best suite for WD studies over the Himalayan region.

Benchmark studies for understanding the model of the physics and dynamics associated with WDs are reviewed next. From Azadi et al. (2001), Fig. 2.2a depicts the sea-level pressure chart during the 18–19 January 1997 WD event as seen in the observations reanalysis. In this figure, a clear surface low associated with the WD is observed. The corresponding MM5V3 (Mesoscale Model 5 Version 3) simulations for eight experiments with different combinations of planetary boundary layers and cumulus parameterization schemes are shown in Fig. 2.2b corresponding to the observation, Fig. 2.2a. This study provides guidance about the best combination of parameterization of physical processes from the various available options to configure the model to capture the dynamical structures of WDs. In this study, the analysis and prediction of field variables like sea level pressure, geopotential height, temperature, wind and precipitation are used as indicators of the best modelling output. Further, Dimri (2004), investigated the impact of topography and model resolution on the simulation of the WD on 23 January 1999 using MM5V3 and showed clearly that the evolution of the of WD in terms of its low pressure at 500 hPa is stronger when realistic topography is present (Fig. 2.3d, e, and f) than in a corresponding no topography experiment (Fig. 2.3a, b, and c). Similarly, more organized precipitation fields along the upwind slopes of the Himalayan complex are seen when realistic topography is present (Fig. 2.4d, e, and f) than in the corresponding no topography experiment (Fig. 2.4a, b, and c). Further, Dimri et al. (2004) study analysed the simulation of an intense WD using a mesoscale model (MM5) run at high resolution. According to the study, the model simulation at high resolution could capture the intensity and movement of the WD with accuracy. But the study of Azadi et al. (2005)

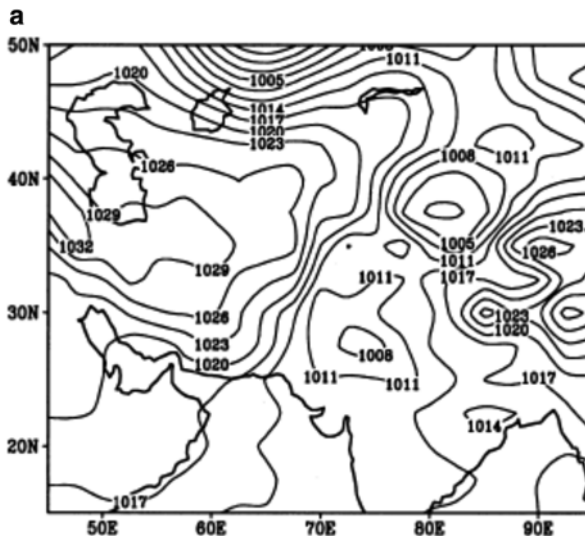


Fig. 2.2 Reanalysis of sea level pressure at 0000 UTC on (a) 19 Jan 1997 and (b) corresponding 24 h forecast of sea level pressure in 08 difference model experiments (Source: Met Appli. Azadi et al. 2001). Figure 1.3b is given on the next page

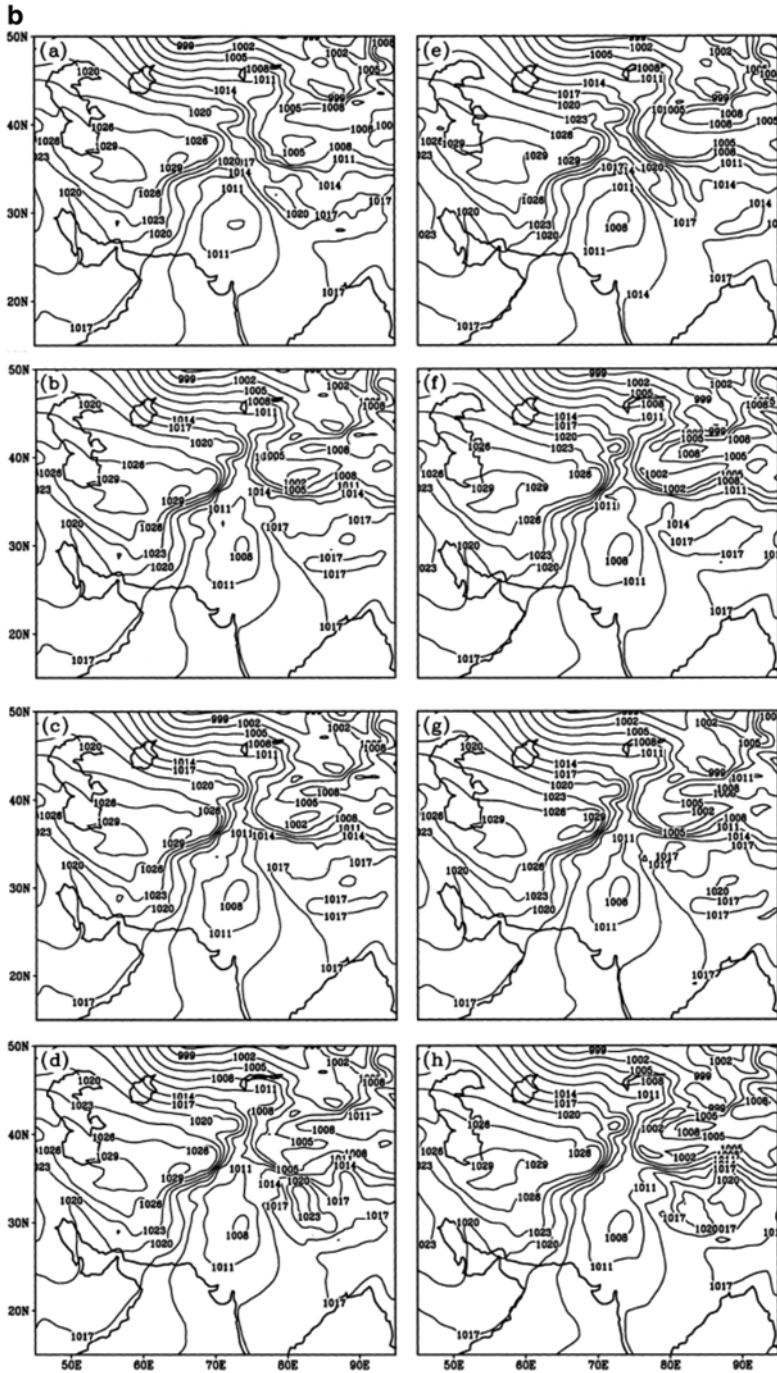


Fig. 2.2 (continued)

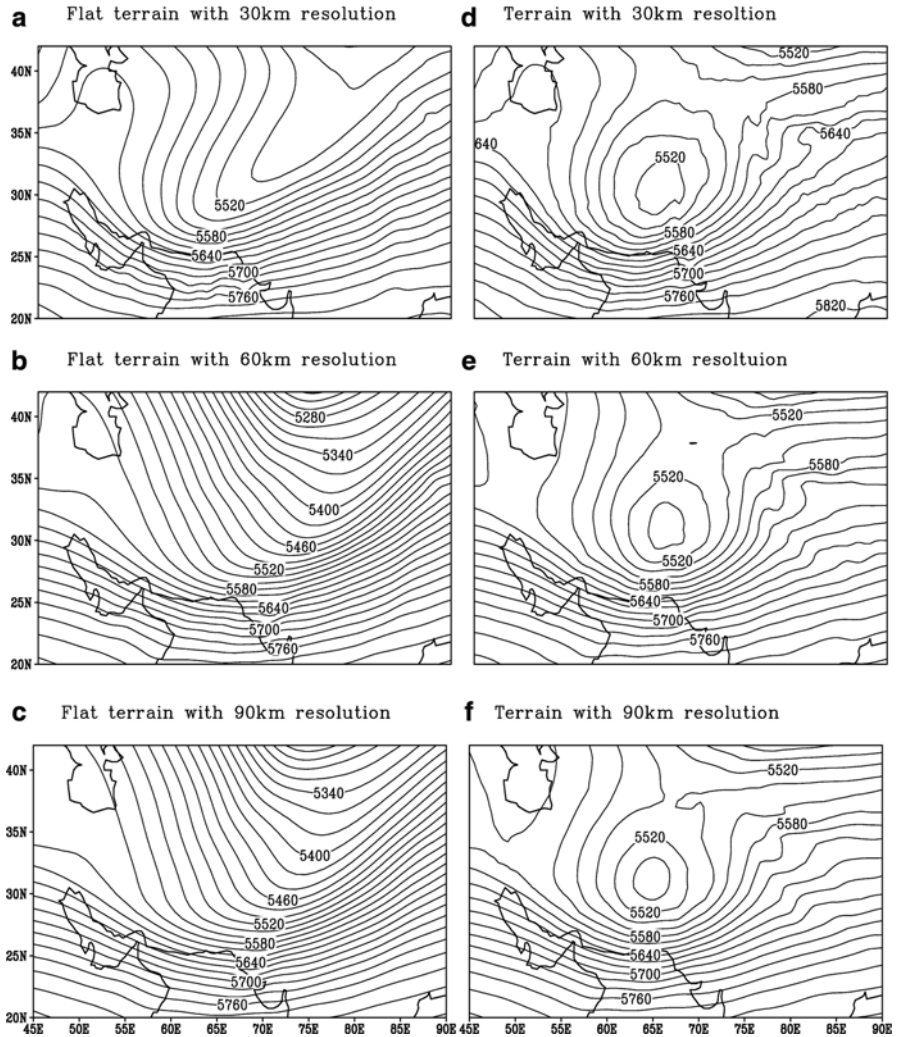


Fig. 2.3 500 hPa Geopotential height (m) after 48 h model forecast valid at 0000 UTC on 23 Jan 1999 over flat (a, b and c) and normal topography (d, e and f) with different model horizontal resolutions

showed that the same model could not accurately capture the advection during a WD and thus failed to simulate the observed speed of the system.

The associated intensification and modulation of the WD is further illustrated in Fig. 2.5a using results of WRF model simulations for the WD on 7 Feb 2002 and compared with the corresponding reanalyses results. Figure 2.5a depicts model-simulated 500 hPa wind, geopotential height, and wind speed which show similar cyclonic structure as in the corresponding with two reanalyses results presented in Fig. 2.5b and c respectively. The two reanalyses datasets are - Modern Era

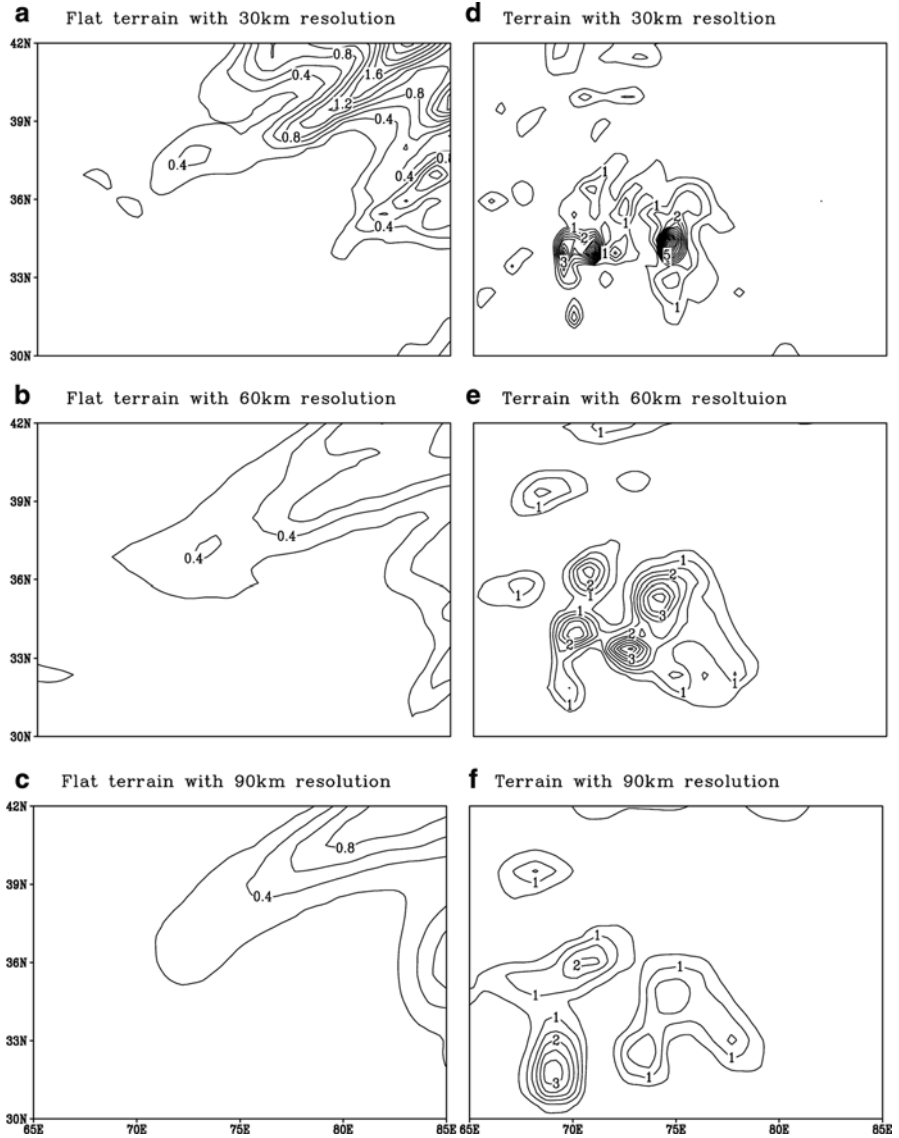


Fig. 2.4 Precipitation (cm/24 h) after 48 h model forecast valid at 0000 UTC on 23 Jan 1999 over flat (a, b and c) and normal topography (d, e and f) with different model horizontal resolutions

Retrospective Analysis for Research and Applications (MERRA) and National Center for Environmental Prediction – National Center for Atmospheric Research Reanalysis Project (NCEP-NNRPII). The wind speed shown in the shaded grey region depicts the flow intensifying along the cyclonic circulation. The overall wind pattern indicates that the model could simulate anomalous cyclonic circulation as

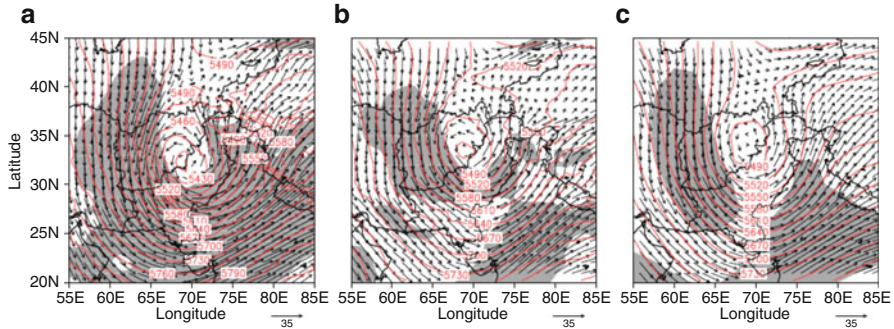


Fig. 2.5 500 hPa wind (m/s; arrow); geopotential height (m; red contour) and wind speed above 22 m/s (grey shed) in (a) model, (b) MERRA and (c) NCEP-NRPII on 07 Feb 2002 0000 UTC

seen in the corresponding verification analysis with higher magnitude. The corresponding geopotential field corroborates with the mid-tropospheric trough over the Indo-Pak region. The figure depicting model-simulated geopotential height is similar to the corresponding observational reanalysis. The trough/depression is depicted over Pakistan and north-west India which forms the cyclonic circulation. Correspondingly, the model also shows the high wind speeds due to the stronger storm simulation. The well-marked low developed over the region, and movement of the said low pressure system is depicted well in the model simulation. The model simulates a more intense storm, thus, over predicting all associated fields leading to stronger cyclonic circulation and stronger wind speed in comparison with the observation data. Corresponding thermodynamical factors, maximum convective available potential energy (CAPE) and convective instability (CINE) are presented in Fig. 2.6a and b respectively. It depicts the spatial distribution of CAPE and CINE on 7 February 2002 elongated along the Himalayan topography. These figures show that during passage, the WD interacts with topography generating enough energy for intensification of the winter storm, thus enhancing associated precipitation over northern India. Such interplay of the WD with topography provides an explanatory inference for the propensity of increased weather activity (Dimri and Niyogi 2012). Increase in CAPE is the release of energy from the instability in the atmosphere that is associated with the orographic lifting of unstable moist air. The kinetic energy generated through conversion of CAPE maintains the convective system during the WD occurrence. During the peak of the WD, CAPE provides support for intensification, which over time reduces significantly the dissipation of the energy and thus weakens the WD. Similarly there is also an increase in the CINE as seen in the figure across the region of WD occurrence. Though this parameter acts as an inhibiting agent for convection, the higher values of CAPE promote the WD. The high values of CINE in a region of high CAPE values indicates the development of the synoptic system in the vicinity. Overall there clearly is an increase in the values of CAPE and CINE in correspondence to the occurrence of precipitation.

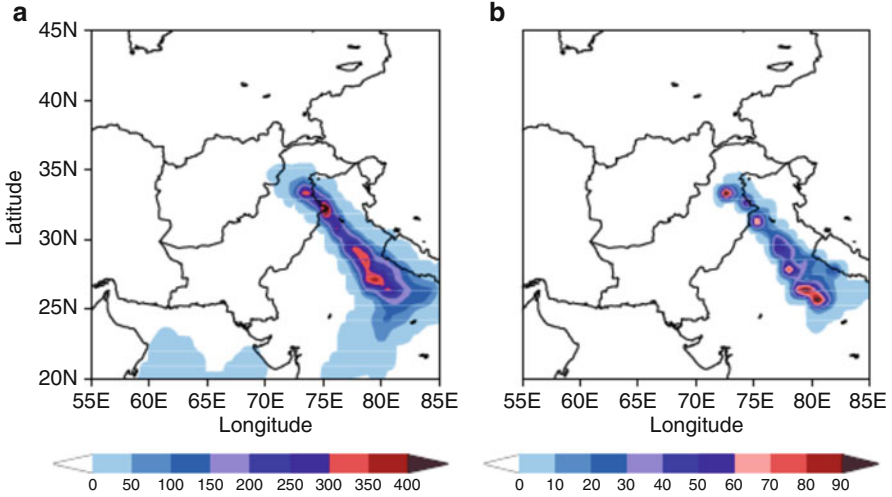


Fig. 2.6 Spatial distribution of model simulated maximum (a) CAPE (J/kg) and (b) CIN (J/kg) on 07 Feb 2002 0000 UTC

Roy and Bhowmik (2005) observed similar high values of CAPE and CINE associated with the days of occurrence of precipitation during WDs.

Another study by Chevuturi et al. (2014) was intended to analyse winter hailstorms over India using numerical weather prediction. This is still under the purview of our book as the study reported that the winter hailstorm was caused by the presence of a WD. Hailstorms are highly convective events and are uncommon during the cold and dry winter months. But this study describes how winter hailstorms are caused by the WD and in turn also provides a detailed description of the baroclinic conditions developed during a WD. We have mentioned the baroclinicity associated with the WDs before as described by Singh and Agnihotri (1977), but in this section we will describe the condition in much greater detail as per the study of Chevuturi et al. (2014). In the study, the vertical cross section of the field variable along the axis of core precipitation zone of the storm is shown in Fig. 2.7. The area-averaged values over the $1^\circ \times 1^\circ$ grid around the region of peak precipitation is shown in Fig. 2.8. The region over and around 77.2° E and 28.6° N would be considered the NCR (national capital region/New Delhi) or the region of study/interest. Over NCR the geopotential height anomaly shows an increase around 400–200 hPa (Fig. 2.7). This increase is associated with the dipping in the perturbation geopotential height contour lines. These changes are due to the tropopause fold penetrating the troposphere. The dip in the tropopause height values is also observed in the station data over New Delhi. This tropopause lowering is associated with baroclinic instability occurring over the region (Bush and Peltier 1994). The increased storm intensity over the region is caused by the baroclinic instability due to the passing WD and the development of cyclonic circulation. The mid-latitude migratory WD attains higher intensities in the form of a baroclinically unstable disturbance specifically over the

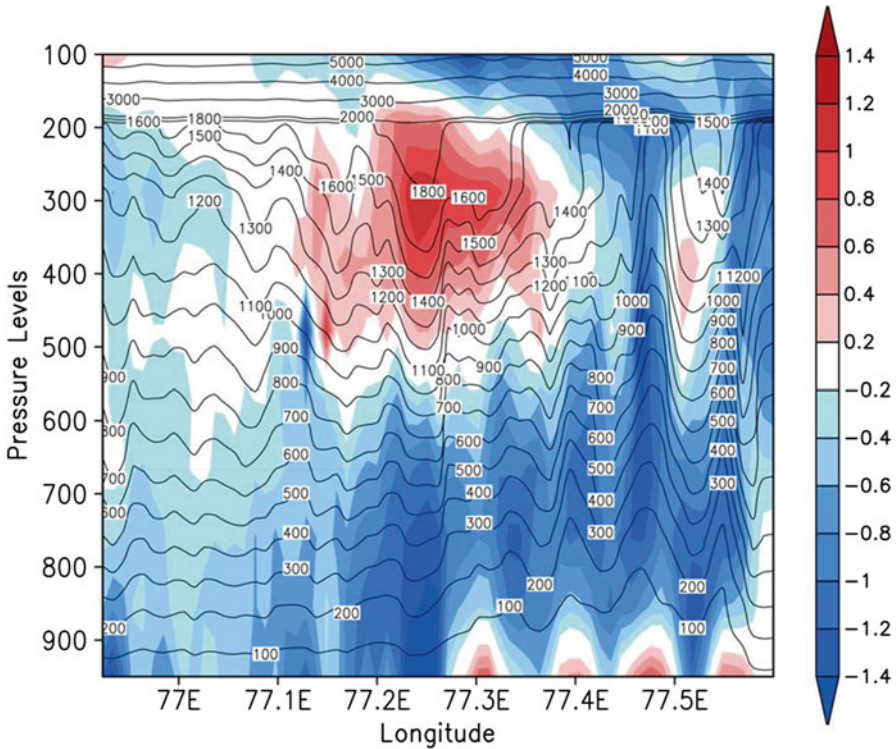


Fig. 2.7 Longitude-pressure cross section (at the line across peak precipitation spatial distribution of the storm) at 1700 UTC 17 Jan 2013 for geopotential height anomaly (*shaded*) and perturbation geopotential height (m; *contour*)

Indian region (Rao and Rao 1971; Singh and Agnihotri 1977). This instability in the mid- to upper-tropospheric levels generates the turbulent convective energy required for the development of updrafts during storm occurrence. With the availability of moisture in the atmospheric column, the instability leads to heavy precipitation. This is the usual baroclinic condition associated with a WD. While not all WDs over northern India lead to hail formation during winter, some of the intense WDs may lead to the hail formation. Heymsfield et al. (2005) describes how strong convective updrafts (with vertical wind speed greater than 5–10 m/s) suppress homogenous nucleation to form the ice particles which grow to form hail. However, lower wind speeds would not contain enough energy to develop a strong hailstorm. In cases of WDs occurrences where such updrafts are, the hail formation may be possible over northern India. The instability developed in the mid-tropospheric levels due to the WD increases the propensity for baroclinic atmosphere in the upper half of the troposphere. When the temporal variation of temperature profile of the region is analysed, a dip is observed in the $-60\text{ }^{\circ}\text{C}$ isotherm around 1600–1700 UTC (Fig. 2.8). This lowering corresponds to the tropospheric fold discussed before.

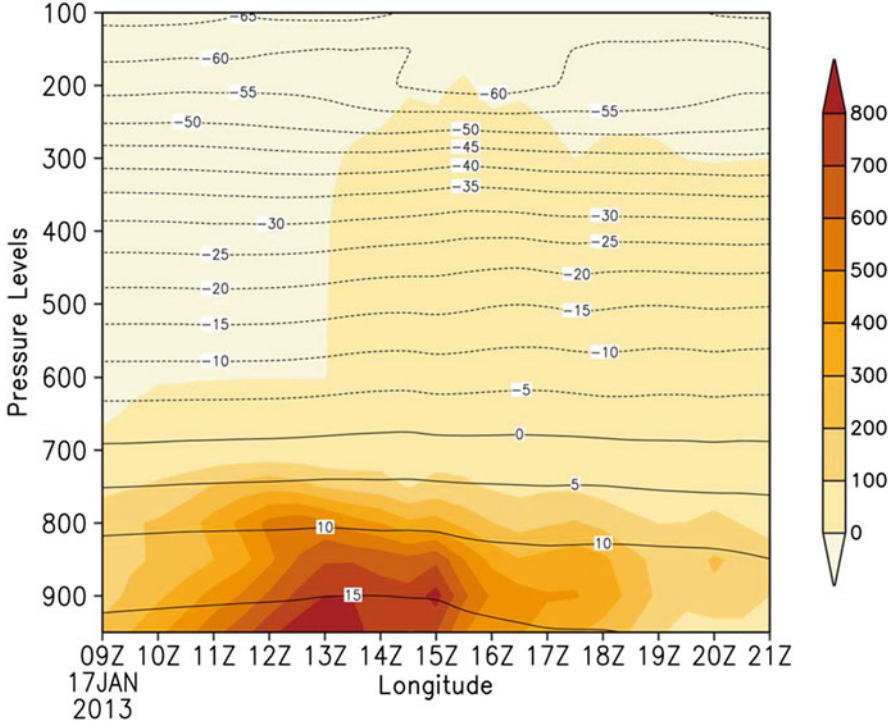


Fig. 2.8 Time-pressure cross section (area averaged over the grid around NCR) for CAPE (J/kg; shaded), temperature ($^{\circ}\text{C}$; black contours) and specific humidity (g/kg; blue contours)

The lowering in the tropopause causes the incursion of colder stratospheric layers into the warmer troposphere. This in turn causes development of a steep temperature gradient as seen in the figure, which enhances upper-level instability. Still the reasons for instability in the lower layers are yet not clearly addressed. To understand the lower layer instability, temporal variation in area-averaged CAPE and specific humidity are represented in the black and blue contours of Fig. 2.7 respectively. In this figure, an increase of moisture over NCR in the lower levels of the atmospheric column is observed along with development of CAPE from around 1300 UTC. The source of this low-level moisture incursion is primarily from the Arabian Sea and, to a lesser extent from the Bay of Bengal. The moisture convergence develops buoyancy which enhances the propensity of increase of CAPE in the atmospheric column. There is reduction in CAPE values in subsequent time periods after 1300 UTC. The increase of CAPE defines the potential energy that is available to drive a storm and release of CAPE in the form of kinetic energy promotes storm development. Along with this, the low-level moisture incursion provides the buoyancy required for the air parcel to rise. Thus, upper-level baroclinic instability is due to the presence of the WD embedded within the SWJ.

Various other studies examined the sensitivity to model the physics, spatial horizontal-model resolution, topography, domain, etc. towards the representation of WDs, and exhibited a systematic bias with the error in WD simulation increasing with integration time (Dimri and Mohanty 2009). These model biases can be reduced through the assimilation of satellite-derived atmospheric temperature profiles (Rakesh et al. 2009), surface observations (Dasgupta et al. 2012), and improved boundary conditions such as land-use maps (Thomas et al. 2013). This combination has provided significant improvement in the simulated precipitation intensity and dynamics associated with WD dynamical evolution from the forecasters' point of view and also the control factor of complex Himalayan topography within the model physics (Semwal and Dimri 2012). Accurate real-time prediction of WDs, which result in heavy snowfall and gale speed winds, allows for timely warnings of avalanches and landslides (Srinivasan et al. 2005). Dimri and Ganju (2007) and Dimri (2009) analysed the impact of orography and land-use interaction during mesoscale simulations using a regional climate model for WD simulation. Das et al. (2003) and Das (2005) were studies specifically directed to mesoscale modelling for forecasting of WDs over mountainous regions. These two studies identified model details for improved accuracy of mountain weather forecasting over the Indian region. Performance of the operational global circulation model called T80, used at National Centre for Medium Range Weather Forecasting (NCMRWF) for forecasting WDs, has also been studied (Gupta et al. 1999). They analysed four WD cases in detail to study the performance of the model for various qualitative and quantitative variables. The study showed an overall fair performance of the model, but still there was under prediction of the heavy precipitation event.

Even with some short-comings, there has been a marked improvement in the understanding of model simulation strategies in recent decades. This has enabled assessment of WD structure and dynamics with a level of detail that was very elusive earlier. These enhancements and improvements over time have been tabulated in the Table 2.1. These studies in the future will help forecasters in assessing these factors in advance through modelling efforts. Though there have been improvements, most studies still demonstrate deficiency in WD forecasting. Improvements have been suggested in the form of improved parameterization schemes specific for the mountainous regime of the Himalayas where the WDs occur. Improvements in developing a better observational network over this region, which has paucity of data, can improve the understanding of the weather systems impacting the region.

2.3 Interplay With Himalayan Orography and Land-use – Land-Cover Interactions

From the discussions in the previous and the current chapter, we can say that surface interactions have a significant impact on the extra-tropical systems, the WDs. Two types of surface interactions of WDs will be discussed in this section. The first is the

interaction with the orography or the height variability of the surface. Orography acts as a barrier to the circulation patterns and weather systems and so has a significant impact on their dynamics. The second is the interaction with variability in the land-use and land-cover patterns over the region impacted by the WDs. Land-surface interactions have more of a thermodynamical impact on the atmosphere above them. Overall these two interactions have a significant impact on not only the origin and structure but also the movement and intensity of the WDs.

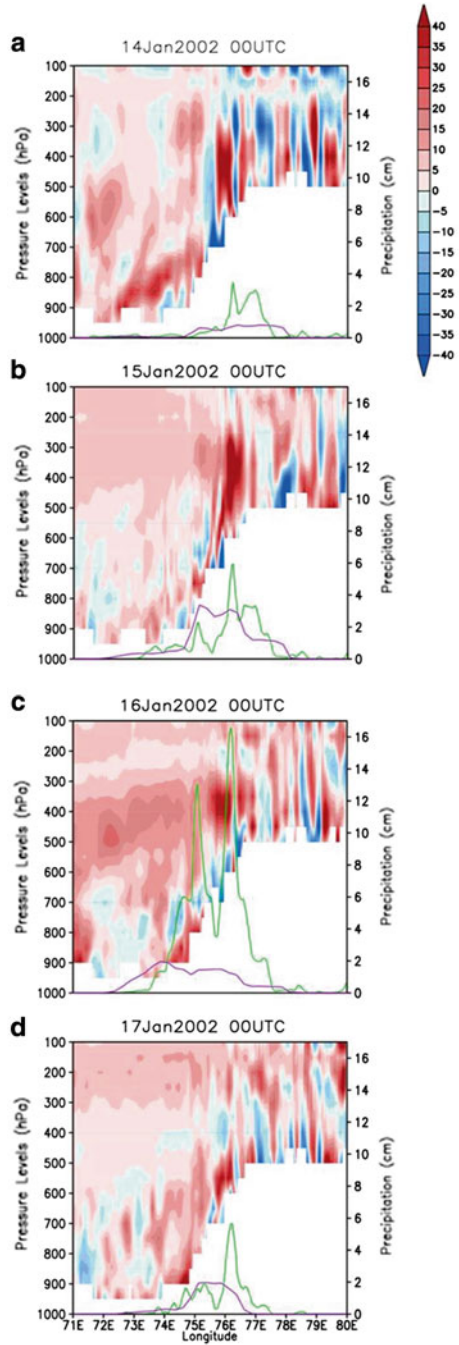
The first influence of orography is during the origin and migration of the WDs. After the formation of the depressions in the eastern Mediterranean, as these approach the highlands of Iran these systems break into two (Mull and Desai 1947). Their first portion moves north-eastwards towards northern Iran and is termed primary. Whereas the second portion moves over the Persian Gulf and southern Iran and is termed the secondary. This part of the depression is what ultimately forms the WDs that impact India. Though, this term secondary should not be confused with the secondaries of the induced WDs which have been discussed previously. The tendency of the parent depression to break up into the two depression due to the Iran Highlands is specific during winters since the SWJ lies over the region during this season. Further, during the migration of the depressions eastward, there is the possibility of orography influencing the structure of the WDs. Pisharoty and Desai (1956) reported that the weather systems that start out as frontal systems arrive over India in an occluded state without the frontal structure in the lower levels but the structure maintained in the higher levels of atmosphere. The rough orography of Iran, Afghanistan and Western Pakistan remove the frontal structure from the lower levels of this system due to friction. The distribution of orography within the path of the WD system tends to develop the secondaries as discussed before (Malurkar 1947). According to Mull and Desai (1947), as the depression center crosses near a mountain range, the cold front gets cut off from the warm front and the development of secondaries is possible. But for the orography to impact the WD depression, it is required that the system is sufficiently close to the mountain. A head-on interaction of the orography with the migrating depression may cause the depression to completely collapse if the depression height is lower than that of the mountain. Whereas if the height is higher, the lower portion of the depression is eroded (Mull and Desai 1947; Pisharoty and Desai 1956). This causes the reduction in the kinetic energy of the system which revives with the influx of fresh warm and moist air in the lower levels. This forms the occluded structure of the WD, with the frontal depression in the upper levels and low level buoyancy due to the moist-air incursion.

The final impact of orography on the WDs is the impact the Himalayas have on the WDs when the weather systems finally arrive over India and interact with the mountain range. The interplay of WDs with the topography of the Western Himalayas determines spatial and vertical distribution of precipitation. According to Dash et al. (2009), the rest of the Indian region receives most rainfall during monsoons but northwestern India receives up to 15 % of its annual precipitation during the winters and this is related to the interaction of WDs with the orography (Yadav et al. 2012). The annual precipitation pattern derived from Tropical Rainfall Measuring Mission (TRMM) satellite radar data shows gradients across the range,

from east to west, and fivefold differences between major valleys and their adjacent ridges (Barros et al. 2000; Lang and Barros 2002; Anders et al. 2006). Dimri and Chevuturi (2014) reported that the precipitation patterns associated with the WDs showed an axis along the Himalayan orography. The interannual variability of precipitation in the Nepal region of the Himalayas is dependent on the timing of the summer monsoon onset along the Himalayan range and is linked to the trajectories and strengths of the monsoon depressions forming over the Bay of Bengal (Lang and Barros 2002; Barros et al. 2006). Lang and Barros (2004) defined the WDs as “*westerly waves trapped and intensified by the unique large-scale topographic features, most notably the notch formed by the Himalayas and Hindu Kush mountains*”. The interannual variability of these systems is high and is dependent on the intensity of the circumpolar westerly jet and the location of the incoming disturbance with respect to the Tibetan Plateau. They also reported that orographic forcing is the dominant factor maintaining the precipitation due to WDs over the Himalayas. Evolution of the large-scale flow into an accurate geometric formation with respect to the orography causes significant precipitation over the region. Similarly, the orientation of major drainage basins and catchment areas can also lead to local differences in the distribution of precipitation (Barry 2008). The upper-level flow may interact with topography in variable ways to affect the low-level cloud motion in the valley. The precipitation to cloudiness scaling suggests a strong stationary behavior of orographic land-atmosphere interactions based on elevation class and ridge-valley scales (Barros et al. 2004). This is to be expected as topography plays a crucial role in modifying these WD weather systems (Dimri 2004). This study analysed the sensitivity of model simulation of WDs with horizontal model resolution. The reports suggested that finer resolutions simulate precipitation better as, at finer resolutions, the orographic effect and corresponding sub-grid mesoscale forcing are better represented within the model. Similar studies of Mohanty and Dimri (2004), Dimri (2009); Dimri and Mohanty (2009) described topographic interaction of WD cyclonic circulation and Himalayan orography. According to the studies, in the Himalayan mountainous region, the precipitation is location specific and dependent on the orography. Raju et al. (2011) studied the role of the Himalayan orography in blocking and guiding the integrated moisture fluxes during an active WD occurrence, as previously discussed. Though the Himalayas block the winter storms and cause precipitation on the windward side, exceptionally violent rainstorms can overcome orographic barriers and penetrate far into otherwise arid regions in the northwestern Himalayas at elevations above 3000 m (Bookhagen et al. 2005). Otherwise, in general, blocking effects prevail and penetration occurs along river valleys or mountain passes (Barros et al. 2006). Winter depressions are either strongly blocked or deflected by the Himalayan topography.

Orographic forcing of the Himalayas on the WDs has also been studied by Dimri and Chevuturi (2014) using a numerical simulation method. Figure 2.9 shows the vertical cross-sectional distribution of vorticity and precipitation along with topography across 33°N for a WD during January 2002. Here increased positive vorticity is observed over and along upslope orography particularly at 76.5° E from 14 January 2002 to 16 January 2002. Intensification of cyclonic circulation is associ-

Fig. 2.9 Vertical cross section of vorticity ($\times 10^5 \text{ s}^{-1}$, *shaded*), model precipitation (cm/day; *green line*) and observed precipitation (cm/day; *purple line*) along 33°N for the WD case studied

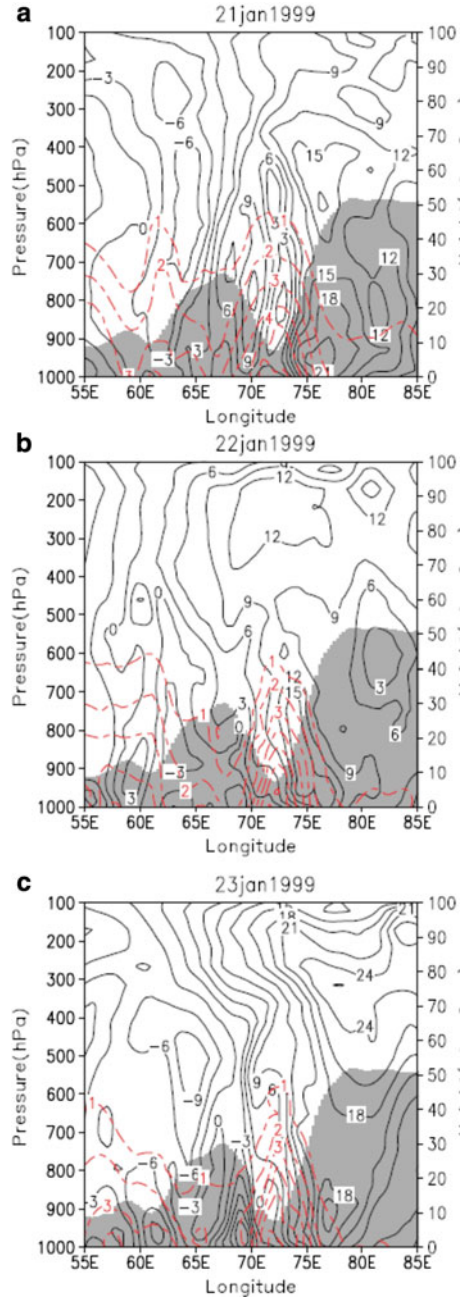


ated with increased positive vorticity, which in turn will intensify the WD and hence increase associated precipitation. It is also clearly seen that positive vorticity is closely associated with the maxima of precipitation. The distribution of vorticity along the rising topography of the Western Himalayan region causes the orographic forcing producing the precipitation by the WDs. It is seen that upslope increased cyclonic vorticity corresponds to increased precipitation which could be seen in increased precipitation in model fields and observation fields as well. Though quantitatively precipitation fields differ, their distribution along the topographic upslope and/or downslope is similar. This figure illustrates the precipitation forming mechanism along the upslope topography. There is also formation of an associated positive vertical wind flow along the topography which causes the rising air parcel. The increased vertical-velocity associated increase convective activity is noted along the region which further forms clouds and causes precipitation. Similar positive vorticity along the orography of the Himalayas during a WD occurrence was reported by Hara et al. (2004).

WD model simulations show that the implementation of a sub-grid land-use scheme leads to a more realistic simulation of precipitation and surface air temperature (Dimri 2009). The sub-grid scheme provides a more accurate representation of resolvable sub-grid-scale processes and atmospheric/surface circulations that result in a better representation of the storm. With a set of modelling experiments, Dimri and Niyogi (2012) provided insight into the interplay of topographic and WD circulation during the 21–23 January 1999 case. Figure 2.10a, b and c presents a longitude and vertical cross sectional distribution of meridional wind and air specific humidity at 34°N latitude at 0000 UTC on 21, 22 and 23 January 1999 respectively. This cross section was chosen because the highest topographic variability is seen across this latitude. Higher vertical wind shear in the lower troposphere and stronger meridional wind from the surface to 500 hPa along the Kashmir valley (~73° E) is discernible during the WD event. Also, contrast in meridional winds from the surface to 200 hPa is seen around ~67° E. Along the valley topographic boundaries, the wind is weaker, while in the middle of the valley, the wind is stronger. Also, an increase in air-specific humidity up to the mid-troposphere over the valley is clearly visible, which is lower along the valley topographic slopes/boundaries.

To investigate the precipitation mechanisms associated with WDs, a case during 20–22 December 2006 was investigated by Dimri et al. (2013). They documented the distribution of moisture variables and vorticity modulation due to topography in the intensification of WD. The Asian Precipitation -- Highly Resolved Observational Data Integration Towards Evaluation of the Water Resources (APHRODITE; Yatagai et al. 2012) (for the 24-h cumulative at 0000 UTC on 22 December 2006) shows a large daily precipitation event (see Fig. 2.11a). Note that the western Himalayan region has a limited observational network and most of the available reanalyses are based on the assimilation of satellite measurements, upper-air observations, and limited ground observations. Furthermore, the number of stations per grid cell is available for APHRODITE. This information was used to determine to what extent the gridded precipitation was determined from station data or derived using an interpolation between the stations. The climate over the western Himalayas

Fig. 2.10 Lon-pressure cross section vertical distribution at 34°N latitude of model simulated meridional wind (ms^{-1}) (continuous *black contour*) and air specific humidity ($\times 10^{-3}$) (broken *red contour*) at 0000 UTC during active WD **(a)** 21 Jan 1999 **(b)** 22 Jan 1999 **(c)** 23 Jan 1999 (*Left hand side* vertical axis corresponds to the pressure distribution and *right hand side* vertical axis corresponds to the topography $\times 10^2$ m)



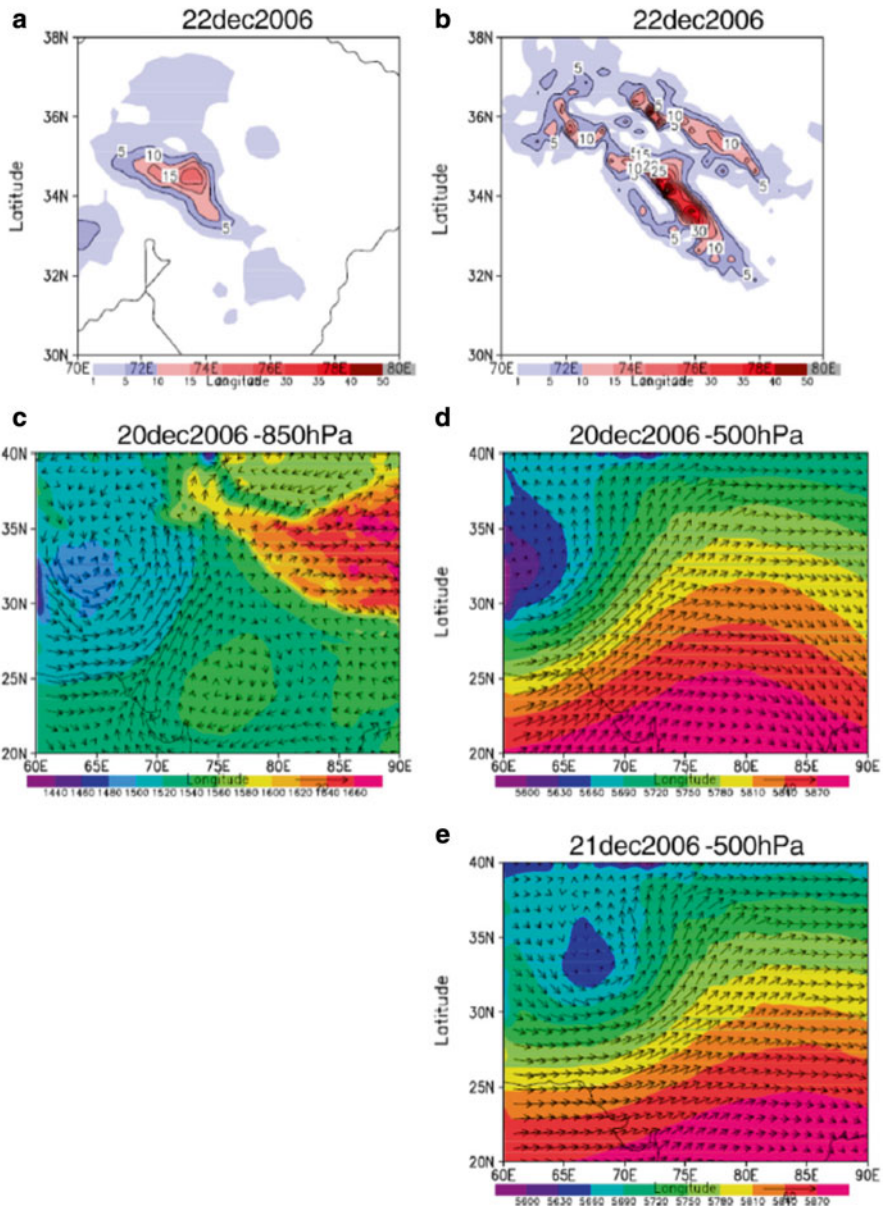


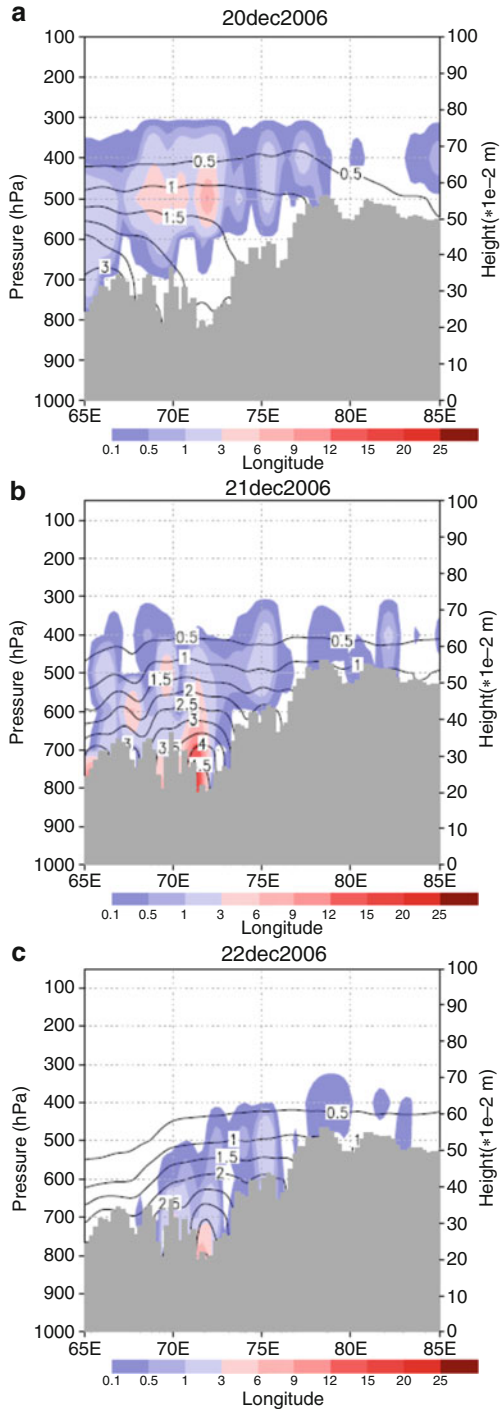
Fig. 2.11 Twenty-four hour cumulative precipitation on 22 December 2006 in (a) observational data (APHRODITE) and (b) the corresponding REMO simulated field, and geopotential height (m; *shade*) and vector wind (m/s; *arrow*) in the REMO simulation at (c) 850 hPa on 20 December 2006, (d) 500 hPa on 20 December 2006, and (e) 500 hPa on 20 December 2006

is colder and drier than that of other Himalayan regions, and therefore the daily time resolution of APHRODITE is more reliable than the monthly time resolution of other datasets and is, to date, the finer precipitation reanalysis available (25 km resolution). Also representation of vertical and horizontal discretization of topography in the analytical methodology makes this dataset comparably better than other observational reanalysis as it inputs the role of topography while preparing the reanalysis. The simulated precipitation from the Regional Climate Model (RCM)–REMO (Jacob et al. 2007) for this event is shown in Fig. 2.11b. The model simulation uses global ERA-Interim reanalysis data (Dee et al. 2011) to supply large-scale boundary conditions (LBCs). REMO uses the GTOPO30 topography data of the US Geological Survey (USGS). The domains were chosen to cover the whole area of India including the Himalayas. REMO RCM simulated the regional climate with a spatial resolution of 0.23° (~ 25 km). Such model resolution was chosen to match APHRODITE resolution. In the model and the corresponding observation, the peak precipitation appears across the Himalayan range, with the model showing the wet bias. The RCM geopotential height field at 850 hPa (Fig. 2.11c) shows a well-defined surface low associated with cyclonic circulation over 33°N , 65°E in the northwest of the western Himalaya two days earlier. The system develops on 20 and 21 December 2006 as it moves over the western Himalaya (Fig. 2.11d and e), indicating that such systems can be adequately depicted from the RCM's simulation. Figure 2.12 illustrates the vertical distribution of geopotential anomaly and specific humidity during that period. The clear influence of the topographic valley floor, upslopes, and downslopes are discernible in defining the spatial organization of precipitation.

The vorticity and relative humidity distribution over this period are presented in Fig. 2.13. The vertical deflection of flow induced by the topography results in adiabatic cooling, and, if sufficient moisture is available from clouds, will eventually lead to precipitation. Convergence on the upslope/windward side due to decreased velocity through orographic retardation will deform or slow down the flow, generating a mid-troposphere positive vorticity at the peak of the storm (Fig. 2.13a and b). Higher relative humidity is seen in the regions of positive vorticity (Fig. 2.13b and c). A weaker negative vorticity occurs along the topographic surface toward the windward side with positive vorticity over the leeward side and over the valley floors. The effects of stronger valley flows are twofold: first, these stronger valley flows reduce upslope moisture flow by channeling it, and second, the lateral circulations constrained by the valley boundaries provide conditions for precipitation formation. This suggests the models' robustness for mountainous regions at the event scale.

Important mountainous physical processes that need an explicit driving mechanism in the model physics are discussed and deliberated in Barros and Lettenmaier (1994), Leung and Ghan (1995) and Bindlish and Barros (2000). Barros and Lettenmaier (1994) had shown earlier efforts of modelling and certain type of precipitation over mountains and associated runoff. Lin et al. (2001) has shown

Fig. 2.12 Lon-pressure cross section vertical distribution at 34°N latitude of model simulated geopotential height (m; *continuous black contour*) and air specific humidity ($\times 1e-3$; *shaded*) at 0000 UTC during active WD (a) 20 Dec 2006 (b) 21 Dec 2006 (c) 22 Dec 2006 (*Left hand side* vertical axis corresponds to the pressure distribution and right hand side vertical axis corresponds to the topography $\times 10^2$ m)



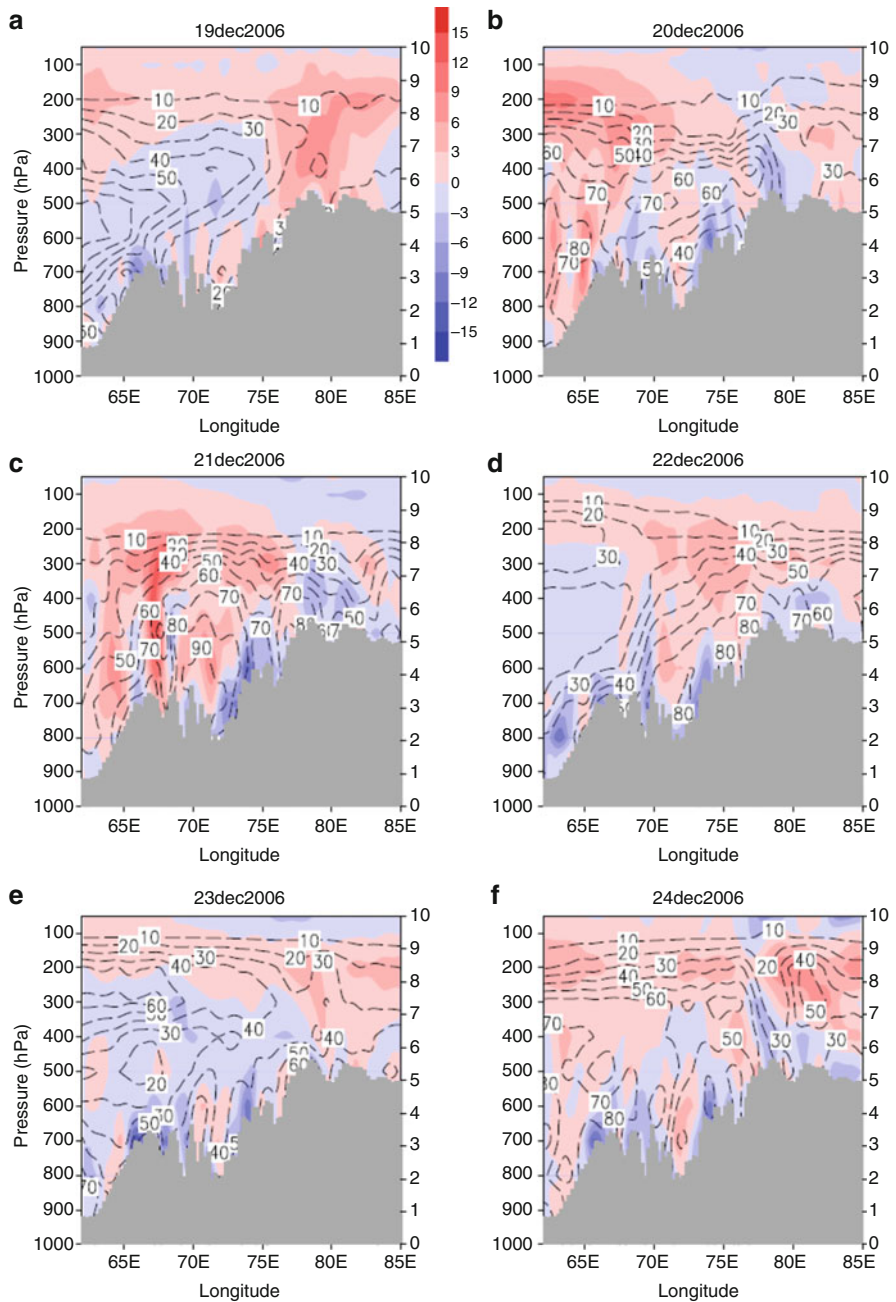


Fig. 2.13 Lon–pressure distribution of vorticity ($\times 1e-5/s$; *shade*), relative humidity (%; *broken contour*), and topography ($\times 10^3$ m; *shaded bar*) on (a) 19 December 2006, (b) 20 December 2006, (c) 21 December 2006, (d) 22 December 2006, (e) 23 December 2006, and (f) 24 December 2006 at 35°N Lat in the REMO simulation

environmental controls favoring heavy precipitation events over the mountainous regions. A theoretical framework of influence of stable moist airflow on precipitation over the mountains and its formulation in the idealized model condition is reviewed and proposed by Smith (2006). Roe (2005, p. 665) provided holistic review of the precipitation mechanism over mountains: ‘orographic precipitation is intrinsically a transient phenomenon, It tends to occur during the passage of a pre-existing weather disturbance, and precipitation rates can vary substantially during the course of a single storm as a synoptic conditions change...’. This review gave an insight about the orographic interaction and precipitation mechanism over the mountains. The most recent review by Houze Jr (2012, p. 42) has provided the latest insight into the orographic precipitation mechanism. ‘It provided variety of orographic effects that profoundly modify the structure of major precipitating cloud systems through combinations of dynamical response, terrain shape and size, and alteration of microphysical timescales...’.

The influence of various sections of the Tibetan Plateau and orography (referred as ‘regional mountain uplift’) is proposed by Chakraborty et al. (2002). He suggested that the presence of the western Tibetan Plateau is more instrumental to the formation of ISM than the eastern Tibetan Plateau. Boos and Kuang (2010) illustrated that the presence of the Himalayan orography and adjacent mountains sustain the present day strength of ISM. There is an important finding that the orographic insulation of low-entropy *extra-tropical air masses by the narrow mountain chains* (i.e. ‘thermal insulation’) rather than the diabatic heating of the entire elevated plateau maintains the ISM (Tang et al. 2013).

The above discussion is focused on the impact on the WDs themselves of the interactions between WDs and surface. These interactions might also have an impact on the orography and land surface. These impacts will be separately elucidated in the last chapter of this book.

References

- Agnihotri CL, Singh MS (1982) Satellite study of western disturbances. *Mausam* 33(2):249–254
- Agnihotri CL, Singh MS (1987) Absorption of short-wave radiation in the atmosphere over India in winter. *Mausam* 38(1):79–84
- Agrawal KC (1999) An introduction of avalanche forecasting and future trends. In: Dash SK, Bhadur J (eds) *The Himalayan environment*. New Age International Pvt. Ltd, New Delhi, pp 71–78
- Ananthkrishnan R, Keshavmurthy RN (1973) A preliminary study of the adiabatic generation and dissipation of kinetic energy by meridional and zonal winds over India and neighborhood during winter seasons. *Indian J Meteorol Geophys* 24:235–244
- Anders AM, Roe GH, Hallet B, Montgomery DR, Finnegan NJ, Putkonen J (2006) Spatial patterns of precipitation and topography in the Himalaya. In: Willett SD, Hovius N, Brandon MT, Fisher DM (eds) *Tectonics, climate, and landscape evolution*. Geological Society of America Special Papers 398, pp 39–53
- Azadi M, Mohanty UC, Madan OP, Padmanabhamurthy B (2001) Prediction of precipitation associated with western disturbances using a high-resolution regional model: role of parameterisation of physical processes. *Meteorol Appl* 7:317–326

- Azadi M, Mohanty UC, Madan OP (2005) Performance of a limited area model for the simulation of western disturbances. *J Aerosp Sci Technol* 2(2):29–35
- Bamzai AS, Shukla J (1999) Relation between Eurasian snow cover, snow depth and the Indian summer monsoon: an observational study. *J Clim* 12:3117–3132
- Barros AP, Lettenmaier DP (1994) Dynamic Modeling of Orographically-Induced Precipitation. *Rev Geophys* 32:265–284
- Barros AP, Joshi M, Putkonen J, Burbank DW (2000) A study of 1999 monsoon rainfall in a mountainous region in central Nepal using TRMM products and rain gauge observations. *Geophys Res Lett* 27:3683–3686
- Barros AP, Kim G, Williams E, Nesbitt SW (2004) Probing orographic controls in the Himalayas during monsoon using satellite imagery. *Nat Hazards Earth Syst Sci* 4:29–51
- Barros AP, Chiao S, Lang TJ, Burbank D, Putkonen J (2006) Tectonics, climate, and Landscape Evolution. In: Willett SD, Hovius N, Brandon MT, Fisher DM (eds) *Tectonics, climate, and landscape evolution*, Geological Society of America Special Paper 398. Geological Society of America, Boulder, pp 17–28
- Barry RG (2008) *Mountain weather and Climate*. Cambridge University Press, New York
- Bindlish R, Barros AP (2000) Disaggregation of rainfall for one way coupling of atmospheric and hydrological models in regions of complex terrain. *Glob Planet Chang* 25:111–132
- Bookhagen B, Thiede RC, Strecker MR (2005) Abnormal monsoon years and their control on erosion and sediment flux in high, arid northwest Himalaya. *Earth Planet Sci Lett* 231:131–146
- Boos WR, Kuang Z (2010) Dominant control of the South Asian monsoon by orographic insolation versus plateau heating. *Nature* 463:218–222
- Bush ABG, Peltier WR (1994) Tropopause folds and SynopticScale Baroclinic wave life cycles. *J Atmos Sci* 51:1581–1604
- Chakraborty A, Nanjundiah RS, Srinivasan J (2002) Role of Asian and African orography in Indian summer monsoon. *Geophys Res Lett* 29(20):50–1–50–4. doi:10.1029/2002gl015522
- Charney JG (1947) The dynamics of long waves in a baroclinic westerly current. *J Meteorol* 4:135–162
- Charney JG (1948) On the scale of atmospheric motions. *Geophys Publ* 17(2):1–17
- Charney JG, Fjørtoft R, Von Neumann J (1950) Numerical integration of the barotropic vorticity equation. *Tellus* 2:237–254
- Chevuturi A, Dimri AP (in review) Investigation of Uttarakhand (India) disaster- 2013 using Weather Research and Forecasting model
- Chevuturi A, Dimri AP, Gunturu UB (2014) Numerical simulation of a rare winter hailstorm event over Delhi, India on 17 January 2013. *Nat Hazards Earth Syst Sci* 14(12):3331–3344
- Chitlangia PR (1976) Mean model of western depression. *Indian J Meteorol Hydrol Geophys* 87(2):157–162
- Das S (2002) Evaluation and verification of MM5 forecasts over the Indian region. In *Proceedings of 12thPSU/NCAR mesoscale model users workshop*, Colorado, pp 77–81.
- Das S (2005) Mountain weather forecasting using MM5 modelling system. *Curr Sci* 88(6):899–905
- Das S, Singh SV, Rajagopal EN, Gall R (2003) Mesoscale modeling for mountain weather forecasting over the Himalayas. *Bull Am Meteor Soc* 84:1237–1244
- Dasgupta M, Das S, Ashrit R (2012) MM5 3D-Var data assimilation and forecast system over Indian Subcontinent – results from recent experiments. <http://www.mmm.ucar.edu/mm5/workshop/ws04/Session5/Gupta.Das.pdf>. Accessed on 19 Mar 2013
- Dash SK, Chakrapani B (1989) Simulation of a winter circulation over India using global spectral model. *Earth Planet Sci* 98(2):189–205
- Dash SK, Jenamani RK, Kalsi SR, Panda SK (2007) Some evidence of climate change in twentieth-century India. *Clim Chang* 85(3–4):299–321
- Dash SK, Kulkarni MA, Mohanty UC, Prasad K (2009) Changes in the characteristics of rain events in India. *J Geophys Res* 114(D10109):1–12

- deSilva AM, Lindzen RS (1993) On the establishment of stationary waves in the Northern Hemisphere winter. *J Atmos Sci* 50:43–61
- Dee DP, Uppala SM, Simmons AJ, Berrisford P, Poli P, Kobayashi S, Andrae U, Balmaseda MA, Balsamo G, Bauer P, Bechtold P, Beljaars ACM, van de Berg L, Bidlot J, Bormann N, Delsol C, Dragani R, Fuentes M, Geer AJ, Haimberger L, Healy SB, Hersbach H, Hólm EV, Isaksen L, Kallberg P, Kohler M, Matricardi M, McNally AP, Monge-Sanz BM, Morcrette JJ, Park BK, Peubey C, de Rosnay P, Tavolato C, Thépaut JN, Vitart F (2011) The ERA-Interim reanalysis: configuration and performance of the data assimilation system. *Q J R Meteorol Soc* 137:553–597
- Dimri AP (2004) Impact of horizontal model resolution and orography on the simulation of a western disturbance and its associated precipitation. *Meteorol Appl* 11:115–127
- Dimri AP, Mohanty UC, Azadi M, Rathore LS (2006) Numerical study of western disturbances over western Himalayas using mesoscale model. *Mausam* 57(4):579–590
- Dimri AP (2009) Impact of subgrid scale scheme on topography and landuse for better regional scale simulation of meteorological variables over the Western Himalayas. *Clim Dyn* 32:565–574
- Dimri AP (2012) Wintertime land surface characteristics in climatic simulations over the western Himalayas. *J Earth Syst Sci* 121(2):329–344
- Dimri AP, Chevuturi A (2014) Model sensitivity analysis study for western disturbances over the Himalayas. *Meteorol Atmos Phys* 123(3–4):155–180
- Dimri AP, Ganju A (2007) Wintertime seasonal scale simulation over Western Himalaya using RegCM3. *Pure Appl Geophys* 164(8–9):1733–1746
- Dimri AP, Mohanty UC (2009) Simulation of mesoscale features associated with intense western disturbances over western Himalayas. *Meteorol Appl* 16:289–308
- Dimri AP, Niyogi D (2012) Regional climate model application at subgrid scale on Indian winter monsoon over the western Himalayas. *Int J Climatol* 33(9):2185–2205
- Dimri AP, Mohanty UC, Mandal M (2004) Simulation of heavy precipitation associated with an intense western disturbance over western Himalayas. *Nat Hazards* 31:499–552
- Dimri AP, Yasunari T, Wiltshire A, Kumar P, Mathison C, Ridley J, Jacob D (2013) Application of regional climate models to the Indian winter monsoon over the western Himalayas. *Sci Total Environ* 468–469:S36–S47. <http://dx.doi.org/10.1016/j.scitotenv.2013.01.040>
- Gregory D, Rowntree PR (1990) A mass flux convection scheme with representation of cloud ensemble characteristics and stability dependent closure. *Mon Weather Rev* 118:1483–1506
- Gupta SC, Mandal GS (1987) Behaviour of kinetic energy generation function during a western disturbance in May 1982. *Mausam* 38(1):97–102
- Gupta A, Rathore LS, Singh SV, Mendiratta N (1999) Performance of a global circulation model in predicting the winter systems and associated precipitation over North West India during 1994–97. In: Dash SK, Bhadur J (eds) *The Himalayan environment*. New Age International Pvt. Ltd, New Delhi, pp 123–138
- Hara M, Kimura F, Yasunari T (2004) The generating mechanism of western disturbances over the Himalayas. In: 6th international GAME conference.
- Hatwar HR, Yadav BP, Rao YVR (2005) Prediction of western disturbances and associated weather over Western Himalayas. *Curr Sci* 88(6):913–920
- Heymsford AJ, Miloshevich LM, Schmitt C, Bansemmer A, Twohy C, Poellot MR, Fridlind A, Gerber H (2005) Homogeneous ice nucleation in subtropical and tropical convection and its influence on cirrus anvil microphysics. *J Atmos Sci* 62:41–64
- Hoskins BJ, Karoly DJ (1982) The steady linear response of a spherical Atmosphere to thermal and Orographic forcings. *J Atmos Sci* 38:1179–1196
- Houghton JT (1987) Importance of satellites for weather forecasting. *Nature* 326:450–450. doi:10.1038/326450a0
- Houze RA Jr (2012) Orographic effects on precipitating clouds. *Rev Geophys* 50:1–47
- IMD (2013) A preliminary report on heavy rainfall over Uttarakhand during 16–18 June 2013. http://www.imd.gov.in/doc/uttarakhand_report_04_09_2013.pdf, Accessed on 20 Mar 2014

- Jacob D, Bäring L, Christensen OB, Christensen JH, de Castro M, Déqué M, Giorgi F, Hagemann S, Hirschi M, Jones R, Kjellström E, Lenderink G, Rockel B, Schär C, Seneviratne SI, Somot S, van Ulden A, van den Hurk B (2007) An inter-comparison of regional climate models for Europe: model performance in present day climate. *Clim Change* 81:31–52. doi:[10.1007/s10584-006-9213-4](https://doi.org/10.1007/s10584-006-9213-4)
- Kala CP (2014) Deluge, disaster and development in Uttarakhand Himalayan region of India: Challenges and lessons for disaster management. *Int J Disaster Risk Reduct* 8:143–152
- Kalsi SR, Halder SR (1992) Satellite observations of interaction between tropics and mid-latitudes. *Mausam* 43(1):59–64
- Krishnamurti TN, Kumar A, Yap KS, Dastoor AP, Davidson N, Sheng J (1990) Performance of a high resolution mesoscale tropical prediction model. *Adv Geophys* 32:133–286
- Lang TJ, Barros AP (2002) An Investigation of the Onsets of the 1999 and 2000 Monsoons in Central Nepal. *Mon Weather Rev* 130:1299–1316
- Lang TJ, Barros AP (2004) Winter storms in central Himalayas. *J Meteorol Soc Jap* 82(3):829–844
- Leung LR, Ghan SJ (1995) A subgrid parameterization of orographic precipitation. *Theor Appl Climatol* 52:95–118
- Lin Y-L, Chiao S, Wang T-A, Kaplan ML, Weglarz RP (2001) Some common ingredients for heavy orographic rainfall. *Weather Forecast* 16:633–660
- Liu X, Yanai M (2002) Influence of Eurasian spring snow cover on Asian summer rainfall. *Int J Climatol* 22:1075–1089
- Malurkar SL (1947) Abnormally dry and wet western disturbances over north India. *Curr Sci* 16(5):139–141
- Mohanty UC, Dimri AP (2004) Location-specific prediction of the probability of occurrence and quantity of precipitation over the Western Himalayas. *Weather Forecast* 19(3):520–533
- Mohanty UC, Madan OP, Rao PLS, Raju PVS (1998) Meteorological fields associated with western disturbances in relation to glacier basins of western Himalayas during winter season. Technical report, Centre for Atmospheric Science, IIT, Delhi, India
- Mohanty UC, Madan OP, Raju PVS, Bhatla R, Rao PLS (1999) A study on certain dynamic and thermodynamic aspects associated with western disturbances over north-west Himalaya. In: Dash SK, Bhadur J (eds) *The Himalayan environment*. New Age International Pvt. Ltd, New Delhi, pp 113–122
- Mull S, Desai BN (1947) The origin and structure of the winter depression of Northwest India. India Meteorological Department, Technical note No. 25:18
- Nigam S, Lindzen RS (1989) The sensitivity of stationary waves to variations in the basic state zonal flow. *J Atmos Sci* 46:1746–1768
- Pandey P, Pandey AK (2014) Uttarakhand disaster of June 2013: Geological issues of a Himalayan state. Personal Communication.
- Pisharoty P, Desai BN (1956) “Western disturbances” and Indian weather. *Indian J Meteorol Geophys* 7:333–338
- Puranik DM, Karekar RN (2009) Western disturbances seen with AMSU-B and infrared sensors. *J Earth Syst Sci* 118(1):27–39
- Raju PVS, Bhatla R, Mohanty UC (2011) A study on certain aspects of kinetic energy associated with western disturbances over northwest India. *Atmós* 24(4):375–384
- Rakesh V, Singh R, Yliya D, Pal PK, Joshi PC (2009) Impact of variational assimilation of MODIS thermodynamic profiles in the simulation of western disturbance. *Int J Remote Sens* 30(18):4867–4887
- Ramanathan Y, Saha KR (1972) Application of a primitive equation barotropic model to predict movement of “Western Disturbances”. *J Appl Meteorol* 11:268–272
- Ramasastri KS (1999) Snow melt modeling studies in India. In: Dash SK, Bahadur J (eds) *The Himalayan environment*. New Age International, New Delhi, pp 59–70
- Rao NSB, Moray PE (1971) Cloud systems associated with western disturbances: A preliminary study. *Indian J Meteorol Geophys* 22:413–420

- Rao VB, Rao ST (1971) A theoretical and synoptic study of western disturbances. *Pure Appl Geophys* 90(7):193–208
- Roe GH (2005) Orographic precipitation. *Annu Rev Earth Planet Sci* 33:645–671
- Roy SS, Bhowmik SKR (2005) Analysis of thermodynamics of the atmosphere over northwest India during the passage of a western disturbance as revealed by model analysis field. *Curr Sci* 88(6):947–951
- Schiemann R, Luthi D, Schar C (2009) Seasonality and interannual variability of the westerly jet in the Tibetan Plateau region. *J Clim* 22:2940–2957
- Semwal G, Dimri AP (2012) Impact of initial and boundary conditions on simulations of western disturbances and associated precipitation. *Nat Hazards* 64(2):1405–1424
- Semwal G, Giri RK (2007) Precipitation simulation of synoptic scale systems over western Himalayan region using Advanced Regional Prediction System (ARPS) model. *Mausam* 58(4):471–480
- Sharma RV, Subramaniam DV (1983) The western disturbance of 22 December 1980: A case study. *Mausam* 34(1):117–120
- Singh MS, Agnihotri CL (1977) Baroclinity over India in winter and its relation to western disturbances and jet streams – Part I. *Indian J Meteorol Hydrol Geophys* 28(3):303–310
- Smith RB (2006) Progress on the theory of orographic precipitation. *Spec Pap Geol Soc Am* 398:1–16
- Srinivasan V (1971) Some case studies of cirriform clouds over India during the winter period. *Indian J Meteorol Geophys* 22:421–428
- Srinivasan K, Ganju A, Sharma SS (2005) Usefulness of mesoscale weather forecast for avalanche forecasting. *Curr Sci* 88(6):921–926
- Tang H, Micheels A, Eronen JS, Ahrens B, Fortelius M (2013) Asynchronous responses of East Asian and Indian summer monsoons to mountain uplift shown by regional climate modeling experiments. *Clim Dyn* 40:1531–1549
- Thayyen RJ, Dimri AP, Kumar P, Agnihotri G (2012) Study of cloudburst and flash floods around Leh, India during August 4–6, 2010. *Nat Hazards* 65:2175–2204. doi:[10.1007/s11069-012-0464-2](https://doi.org/10.1007/s11069-012-0464-2)
- Thomas L, Dash SK, Mohanty UC (2013) Influence of various land surface parameterization schemes on the simulation of the western disturbances. *Meteorol Appl*. doi:[10.1002/met.1386](https://doi.org/10.1002/met.1386)
- Tiedtke M (1989) A comprehensive mass flux scheme for cumulus parameterization in large scale models. *Mon Weather Rev* 117:1779–1800
- Veeraraghavan K, Nath T (1989) A satellite study of an active western disturbance. *Mausam* 40(3):303–306
- Yadav RK, RupaKumar K, Rajeevan M (2012) Characteristic features of winter precipitation and its variability over northwest India. *J Earth Syst Sci* 121(3):611–623
- Yatagai A, Kamiguchi K, Arakawa O, Hamada A, Yasutomi N, Kitoh A (2012) APHRODITE: constructing a long term daily gridded precipitation dataset for Asia based on a dense network of rain Gauges. *Bull Am Meteorol Soc*. doi:[10.1175/BAMS-D-11-00122.1](https://doi.org/10.1175/BAMS-D-11-00122.1)

Chapter 3

Western Disturbances – Indian Seasons

Abstract WDs usually impact India during the winter period. But there have been cases where western disturbances (WDs) with large amplitudes influenced the Indian weather during the other seasons also. This chapter discusses the impact of WDs during the different seasons of the Indian annual climatic cycle. India experiences four seasons during the annual cycle; winter, pre-monsoon, monsoon and post-monsoon. This chapter begins with a brief review of the four seasons of Indian climate with their associated major weather systems. Impact of WDs during each season are discussed individually under different sub-topics of the chapter. Detailed information on the interaction of WDs with every seasonal weather system is provided.

The Indian winter season occurs over the months of January and February; but, when the north-western India is taken into account, even December is included for consideration. This season is associated with the dry cold-air mass from the Siberian region flowing from the north (Attri and Tyagi 2010). Diurnal temperature shows large variation, along with the decreased average temperatures along with low humidity conditions during the season. Extremely low temperature conditions lead to cold waves over the region (De et al. 2005). The WDs usually impact northern India and cause wintertime precipitation over the region (Dimri and Chevuturi 2014) as previously discussed. Thus, this season in some cases can be termed as the northern Indian winter monsoon. WD-associated precipitation is the main source of snowfall over the Himalayas, and it replenishes the glaciers. Snow storms are considered severe weather events which may lead to other disasters like avalanches . Due to the availability of moisture in the environment after passing of a WD, the development of fog at a synoptic scale is common during this season (Dimri and Chevuturi 2014).

During the pre-monsoon (spring) season, the temperatures over the Indian sub-continent steadily increase. This is the warmest season of the annual climatic cycle, the with highest daily temperatures recorded (Kothawale et al. 2010). This is also known as the summer season, hot weather season or the thunderstorm season. This season is characterized by high temperatures interspersed with a few storms. In extreme conditions, positive departures from temperature normal due to heating of the land surface lead to heat-wave conditions during this season (De et al. 2005). These heat waves are associated with hot and dry winds leading to dust storms in the

northern plains. The pre-monsoon is also known for violent storms which occur during the convectively unstable atmospheric conditions that result, due to transient disturbances observed in the air mass caused by the surface heating (Romatschke and Houze Jr. 2011). These conditions are conducive for short-term high-intensity storms with associated thunder, lightning and in extreme cases hail (Houze Jr. 1981). Over eastern and north-eastern parts such storms are termed as Nor'westers (Attri and Tyagi 2010). Due to high temperatures over the sea surface, tropical cyclones develop during this time period (Singh et al. 2000). These low-pressure systems are associated with strong winds and heavy rains affecting the Indian coasts and islands and leaving in their wake heavy devastation (Singh et al. 2001). According to Wang et al. (2011), summer precipitation has two phases. The pre-monsoon phase preceding the monsoon trough generates very intense rainfall over small regions.

Monsoon is defined as the reversal of winds over a region that causes precipitation during a season Lau et al. 2012. The Indian summer monsoon or south-west monsoon is the most significant feature of Indian climate because it brings precipitation over the entire Indian landmass (Kumar et al. 1995). The summer monsoon over India is characterized by increased radiative heating during the pre-monsoon period (a heat low is formed over land surface) which leads to differential heating of the land and ocean, and causes the moisture-laden wind to flow from the ocean towards land. But, as this flow curls due to the coriolis force and due to the topography of the Indian peninsula, the south-west monsoon flow is divided into the Arabian Sea Branch and the Bay of Bengal Branch (Koteswaram 1958a; Ramage 1971; Sikka 1977). With the Himalayas acting as a barrier, precipitation due to this monsoon depression is confined to the Indian subcontinent. Individual disturbances during this period distribute precipitation on a spatio-temporal scale (Ananthakrishnan 1977; Ding and Sikka 2006). On a spatial scale, the monsoon at southernmost tip of India begins at the start of June and covers the whole of India by mid-July (Ananthakrishnan and Soman 1988). In contrast to the pre-monsoon phase, the monsoon phase is characterised by a larger area experiencing low-intensity rainfall (Wang et al. 2011) with some extreme events interspersed during the period. On a temporal scale, rainfall occurring over the central and west coasts of India is termed the active monsoon period whereas the rainfall low period is usually termed the break monsoon (Rajeevan et al. 2006). Extreme events during this time period are droughts or the high-intensity rainfalls which lead to floods or landslides (Bhalmea and Mooley 1980; Parthasarathy et al. 1987).

The post-monsoon (autumn) season over India is characterised by complete wind reversal and the retreat of the south-west monsoon winds which establishes the north-easterly winds. This is also termed the north-east monsoon, retreating south-west monsoon or, in some cases, the southern Indian winter monsoon. This season marks the gradual lowering of temperatures from hot to cold seasons and transitions from the south-west summer monsoon to the north-east winter monsoon (Singh and Sontakke 1999). Due to the retreat of monsoon from the Indian landmass, there is a reversal of lower-level winds from south-westerlies to north-easterlies. The heat low, Mascarenes high, Somali jet, Tibetan anticyclone, easterly jet stream over

south India and monsoon trough along the Ganges valley are replaced by the Siberian anticyclone, cold surges from the Siberian high, Western Pacific high, sub-tropical jet stream over north India and a monsoon trough over Indonesia during this season (Kumar et al. 2004). This causes precipitation over the north-eastern, eastern and southern parts of India. Most of the precipitation over Tamil Nadu, parts of Andhra Pradesh and Karnataka receive rainfall due to storms developing in the Bay of Bengal. In extreme cases there are heavy rainfall events along with strong winds and storm surges over eastern coastal India. But, on the other hand, during this season north and central India is associated with clear skies and a decrease in humidity (Attri and Tyagi 2010).

According to Dash et al. (2009), the monsoon season of June, July, August and September generates the maximum rainfall over most of the Indian region. During this period, approximately 80 % of the total annual precipitation occurs, except in Tamil Nadu and northwestern India. Tamil Nadu receives maximum rainfall during the post-monsoon season and northwestern India receives significant precipitation during the winter period due to the WDs. But the WDs' impact is not just limited to the winter months. After the general review of the climate of the Indian sub-continent, we will further describe the synoptic conditions caused due to the impact WDs during the different seasons of the Indian climate.

3.1 Winter

As discussed previously, WDs are weather systems that impact India, mostly northern India, specifically during the winter season. Though in a few rare cases WDs also impact other sections of India in other seasons, they usually dominate the Indian weather during winter. The previous two chapters that discuss the WDs in detail describe the typical WD condition in general. Since a typical WD occurs during the winter, this section provides only a short summary of WDs specifically during winter.

Due to the tilt of the Earth's axis, there are seasonal differences in the climate, primarily in the higher latitudes. As solar radiation peaks migrate from northern hemisphere to the southern hemisphere, there is also slight shift in the large-scale circulation patterns. The inter-tropical convergence zone (ITCZ) is a large-scale circulation pattern that shifts seasonally along with solar radiation peak. During northern-hemisphere winters, this ITCZ shifts southwards as the north pole of the earth tilts away from the sun. This results in the southward shift of other large-scale circulation patterns including the SWJ (Krishnamurti 1961). The WDs are wave disturbances migrating embedded within the SWJ. Due to the sub-tropical westerly jet shifting southwards towards the Indian region, these disturbances originating from Mediterranean Sea travel along the jet and influence northern India (Dimri 2013). This summarizes the reason why WDs usually impact India during winters. During winters, large amplitude WDs have a significant impact even over the southern Indian region. Sharma and Subramaniam (1983) discussed a case of a WD

over the Indian region and its interaction with lower-tropospheric easterlies in the Arabian Sea. These easterlies may lead to the intensification of the WDs and extend the precipitation due to a WD further south during winters. Similar in-phase superimposition between the westerly troughs from the higher latitudes and the easterly waves moving westwards in the equatorial latitudes has been reported by Pisharoty and Desai (1956). The pressure highs on both sides of the superimposed trough lines reinforce each other and, with possible moist-air incursion, intensify the precipitation caused by the WD during winters. But as suggested by this study, this superimposition is not only limited to the Arabian Sea, but also may impact regions of Central India and the even Bay of Bengal region. During northern-hemisphere summers, the ITCZ shifts northwards and causes the shift of the SWJ further north, above the Indian Himalayan region. This negates the influence of the WDs from the Indian region. There are some papers describing a similar impact of WDs over China during early summer periods, but with weaker impact due to lack of orography (Nitta et al. 1973; Yoshizaki 1974). But certain large amplitude waves of the WDs may also cause the extension of their influence towards lower latitudes even in the other seasons. These impacts will be discussed further in the next sections.

It has been extensively discussed that, during the winter season, the occurrence of WDs leads to winter-time precipitation. This is the major consequence of the WDs that have significant impacts. But other than precipitation, WDs also have an impact on the temperature patterns of the region affected. A migrating WD has an influx of warm moist air from the Arabian Sea and Bay of Bengal ahead of the depression, whereas, the rear of the depression has an inflow of cold and dry air from the northern latitudes. As a WD passes through the country, the region already impacted by the WD comes under the influence of the cold and dry air. The spread of this air flow leads to the formation of a cold wave condition (Mooley 1957). With the WD having already caused overcast skies, the cold conditions are enhanced with the incoming cold waves from the north (De et al. 2005). Prolonged cold-wave conditions are observed in cases with WDs having deep troughs to draw in the air flow from higher pressures in the north. Further, these cold waves are extended, if there is no successive WD, leading to the uninterrupted flow of cold air from the north and no inflow of warm air from the southern regions (Mooley 1957). So the absence of successive WDs maintains the prolonged cold wave conditions which is essential for the maintenance of the cold season. Clouds formed by the WDs have a moderating effect on the maximum temperatures during the winter season (Mooley 1957). Absence of WDs during winters for sufficiently long periods cause warmer periods due to radiative heating of the air mass which increases the temperatures. Contrastingly, the presence of multiple active WDs in quick succession may also lead to warm and moist conditions. As discussed previously, the region ahead of the front of the WD depression contains incoming warm moisture-laden air from the southern latitudes. Thus, if there are WDs occurrences one after the other, a continuous flow of the warm moisture air develops which generates warmer conditions during the winter season.

3.2 Pre-Monsoon

The pre-monsoon season is the hottest part of the entire annual cycle for most of South Asia. With anomalous high temperatures, this season can have recurring incidences of heat waves resulting in the whole season being hot and dry (Kothawale et al. 2010). The high temperatures generate sufficient energy for short bursts of thunderstorms, hailstorms and duststorms that affect the Indian subcontinent during this time period (De et al. 2005). Other than these generic storms, specific storms impact the eastern region of India which are called the Nor'westers. Nor'westers or Kalbaisakhis (calamities in the season of Baisakhi or the spring season) and storms which develop wind patterns from the north-westerly direction, hence the name. These sometimes develop characteristic the funnel-shaped clouds seen during a tornado (Pramanik and Alipore 1939; Srinivasan et al. 1973). All these storms are violent weather systems which may have quite a devastating impact. Though these have an independent impact on the Indian weather, these pre-monsoon weather systems are sometimes influenced by the presence of the WDs. Though unlike winter season, the influence is limited to northern regions only even with the passing of large amplitude WDs. During sporadic cases of the deep trough of WDs during the summer season, conditions can be generated for the development of cyclonic storms or deep depressions of small extent (Philip et al. 1973). These have a north-easterly migration and are much faster than typical tropical cyclones. They may develop both in the Bay of Bengal or the Arabian Sea (Pisharoty and Desai 1956; Niyas et al. 2009; Chakravarti 1968). Development of these depressions is rare, and more commonly the WDs affect storm formation in northern and eastern India during the hot-weather season, which is discussed in detail in the following paragraphs.

During the hot-weather period, the atmosphere is relatively dry, hot and very unstable. The WDs passing during this time period over northern India were observed to be closed cyclonic systems (Pisharoty and Desai 1956). The passage of the wave disturbances in the upper troposphere are thus often associated with the intensification of the unstable atmosphere that leads to these violent storms. This usually enhances any dust storm or thunderstorm over Pakistan and north-western India. The region preceding the upper level trough manifests high-level divergence which promotes lower-level convergence and ultimately leads to higher convective activity over the region. This enhanced convective activity or rapid rising of air masses leads to the occurrence of these storm systems ahead and along the WD path. According to Kalsi and Halder (1992) in certain cases, the WD trough during the pre-monsoon season shows deepening and oscillation over the Arabian Sea. North-eastward movement of the WD triggers convective activity along its track. This convective activity is caused by the low-level moist south-easterly flow in the front of the WD trough. This interaction of low-level and upper-level wind circulation generates high amounts of rainfall over a very large area in the form of thunderstorms. This substantiates the importance of WDs in enhancing convective activity during the pre-monsoon season over the northern Indian region.

Hailstorms over Northern India normally occur during the monsoon months, but at times a very few burst storms are observed during the pre-monsoon. Chevuturi and Dimri (2015) studied a severe hailstorm event over the National Capital Region (NCR, New Delhi) of India on 28 March 2013 using numerical simulation techniques. The findings suggested the rapid intensification of a localized storm event. The results depict the development of a pre-monsoon shower which is a convectively driven storm enhanced by the WD occurrence. With the development of instability and the release of convective available potential energy (CAPE), the storm evolved over the region. The WD enhances convective activity which achieves the hail formation processes typical of a storm reaching the upper tropospheric layers, where at top of the high clouds have the colder temperatures which promote hail formation. In this case, the moisture incursion, which initiates and maintains the hail formation and storm activity, was from the Arabian Sea. The enhanced convective activity generated hydrometeors, i.e. hail due to the cycling of the hail particles through the multiple cells of the storm clouds.

In the case of Nor'westers, these tornadic level storms are initiated by the interaction of the westerly to north-westerly winds at higher latitudes and moist winds from the Bay of Bengal which have southerly to south-westerly direction. These occur during the transition period between winter, which has the westerly wind dominating, and the monsoon, which has the prevalence of the south westerly winds. The presence of the upper-level cold north-westerly winds interacting with the lower-level south-westerly winds generates a high lapse rate in the atmospheric column. The lower-level winds are laden with moisture as these arrive from the Bay of Bengal, generating sufficient the moisture requirement and latent instability for the storm to develop (Pramanik and Alipore 1939). Any disturbance in the upper level flow enhances the storm activity over eastern and north-eastern India and the Bangladesh region by enhancing the upper-level divergence ahead of the WD trough (Srinivasan et al. 1973). The moist current drawn ahead of the WD trough is also responsible for the strengthening of the Bay of Bengal current that is necessary for the formation of the Nor'westers.

Previously discussed are the various influences of the WDs occurring during the pre-monsoon season. We will be describing their occurrence and impact during the monsoon season in the next section. But a study by Das et al. (2002) suggests that the frequency of the WDs occurring during the pre-monsoon season has a significant impact on the onset of monsoons. According to the study, the onset of monsoons over the northwestern part of India is delayed due to an increase in the frequency of WDs during the month of April or vice versa. However, this was a statistical study and did not provide detail on the cause of this correlation. Further, details of WD occurrence and monsoon onset will be described in the next section.

3.3 Monsoon

Although mid-latitude systems, i.e. the WDs, do not impact India during the monsoon season, some of the large amplitude troughs in the SWJ cause an interaction between the tropics and extra-tropical systems (Kalsi 1980). As with incoming sporadic WDs, there are varying impacts on the monsoonal circulation. One study suggested that in some rare cases the influence of WDs caused the onset of the monsoon either from the Arabian Sea or the Bay of Bengal (Bhullar 1952). Whereas another study, in contradiction, reported that the presence of a WD weakens the formation of the monsoon depression in the Bay of Bengal region and the onset of the monsoon occurred only after the WD had migrated further east (Chakravorty and Basu 1957). They also suggested that the increase in the number of eastern depressions generated in the Bay of Bengal during the monsoon season is associated with the decrease in the number of WDs impacting the region. Pisharoty and Desai (1956) also suggested that though the circulation changes in the Indian Ocean are responsible for the arrival of monsoons, the existence of WD may cause the delay in the arrival of the monsoon over the Indian subcontinent. It was also suggested that the monsoon would arrive over India after the passage of the WD. During the end of the monsoon period, the wave disturbances again start impacting the Indian region. The monsoon depressions, when interacting with the WD during the end of the season, are forced eastwards. This movement further causes the gradual withdrawal of monsoons from the north of India (Pisharoty and Desai 1956). These conditions might not always be the typical case for monsoon withdrawal, but the presence of a WD brings about a change in the circulation that might promote the monsoon withdrawal. Other than the onset and withdrawal of monsoon (in terms of attracting or repelling), the WDs have significant influence on the intensification or weakening of the monsoon after it enters the Indian subcontinent (Chakravarti 1968). The frequency and the track of the WDs are two major factors that influence the precipitation patterns caused by the monsoon. The different effects of interaction between the tropical (monsoons) and extra-tropical (WDs) systems produce different types of weather conditions (Kalsi and Halder 1992). These interactions have been termed as interactions between the tropics and mid-latitudes (ITML) that lead to the variation in the monsoonal precipitation pattern influenced by the WDs. According to two research studies (Pisharoty and Desai 1956; Rao 1976) these can be summarized as:

- (a) Intensifying rainfall in pre-existing weather systems (monsoons as well as WDs)
- (b) Developing and amplifying lower tropospheric troughs and convection
- (c) Causing the onset of the break monsoon conditions
- (d) Changing the path curvature of the lows, including the oscillation of the monsoon trough
- (e) Pulsatory extension of the monsoon (PEM) towards northern India

The first two cases are the intensification of the weather systems and amplification of other synoptic conditions. During the monsoon period there is interaction of the tropics and mid-latitudes (Kalsi and Halder 1992). The tropics over India are characterized by easterly winds and the mid-latitudes by a westerly flow separated by a subtropical anticyclone. If there is a large amplitude mid-latitude system passing through, then there are ITML systems. This interaction occurs over the baroclinic zones elongating the cloud-cover zones. The cloud patterns are of vertical type that sharpens the baroclinicity of the upper and middle troposphere over northern India. When large amplitude waves in the westerlies impinge on the lower latitudes, there is deformation of the clouds. Further, this causes a change in the lower-level circulation that results in the easterly flow extending northwards and interacting with the westerly flow of the upper to middle troposphere. This causes the enhanced convection and ultimately leads to intensification of weather systems and higher amounts of precipitation. Also, the WDs produced significant rainfall over the northwestern region of India during the monsoon season (BhaskaraRao and Venkataraman 1965). Upper-level divergence due to the trough in the westerlies pushed southwards and the lower-level convergence associated with the monsoon causes intensive rainfall. Other than the general intensification of the weather systems, there are two specific conditions of ITML which are the break monsoon conditions and the oscillation of the monsoon trough and PEM. We will address the two cases separately. Another major consequence of ITML over the monsoon period is the break monsoon period. We described the ISM in brief at the beginning of this chapter. The characteristic features of the monsoon circulation are the heat low, near equatorial trough and Mascarenes high, SWJ and tropical easterly jet streams, and the Tibetan high- and low-level jets. Due to large amounts of solar radiation during the summer, heating of the landmass over the continent causes the development of strong heat low in the lower atmosphere. A low pressure trough forms over the equator which migrates northwards to merge with the heat low. This enhancement of the low-pressure region over India draws the moisture-laden flow from the southern hemisphere. In contrast, over the southern hemisphere, an anticyclonic circulation develops a Mascarenes high-pressure region over the Madagascar coast. Further, in the upper layers of atmosphere over the southern portion of India, an easterly jet dominates, termed as the tropical easterly jet (TEJ), whereas the SWJ moves north of the India (Ding and Sikka 2006). There is an associated low-level jet (LLJ) which forms the south-westerly flow of the monsoon (Findlater 1969). This is a cross-equatorial jet stream that brings in the moisture-laden flow from the southern hemisphere (Joseph and Raman 1966). The monsoon draws large-scale convection and widespread precipitation over the Indian subcontinent. But within the monsoon period, there is intra-seasonal variability which shows brief periods of more rainfall, interspersed with slightly longer periods of drought (Blanford 1886). These periods are termed the active and break events respectively (Ramamurthy 1969; Rajeevan et al. 2010). The heat low which is pronounced over the Rajasthan region extends towards the east and forms a low-pressure region that has an east west direction (Ramage 1971). This is termed the monsoon trough (MT) and is vital for the monsoonal precipitation distribution. When this MT exists over the middle of the Indian

region, it causes precipitation over the major part of the subcontinent and these periods are termed the active events (Rajeevan et al. 2010). But the MT is a quasi-stationary system and shows oscillations and migrations. One such migration of the MT towards the foothills of the Himalayas causes drought like conditions over the rest of the Indian region and rainfall over the Himalayas and is aptly termed the break event (Ramamurthy 1969). Break events last for seven to ten days on the average. A WD as a trough in the SWJ arrives over the Tibetan high region where it slows down, producing the increase in its amplitude. This completely removes the Tibetan high and extends the wave of the WD much further southwards. This southward extension of the westerly wave disturbance causes the weakening of the upper-level easterly jet over the Indian region (Ramaswamy 1962). There is an associated migration of the MT towards the foothills of the Himalayas. Thus the whole atmosphere over the region shows a westerly wind movement. There is intensified meridional flow which causes northward flow of moisture (Kalsi 1980). This migration of the MT causes low rainfall over the central parts of India but heavy rainfall due to both the MT and WD over the Himalayas. With the eastward movement of the trough, there is also rainfall in the eastern parts of the country.

Other than the break-monsoon events, the WDs also have other impacts on the movement and intensity of the MT, e.g. interaction between the tropical and extra-tropical weather systems during summer generated floods over Pakistan during 2010. Hong et al. (2011) studied the synoptic conditions and concluded that the northward propagating monsoon surge coupled with the extra-tropical trough penetrating the region. This coupling promoted low-level convergence and increased vorticity and further increased the intensity of the monsoon surge and dragged it over the region. Further, coincidental La Nina conditions generated remote forcings of easterly wind further east which enhanced the moisture convergence over the Pakistan region. From the Indian perspective, according to Pisharoty and Desai (1956), a WD over the Gangetic plains in the month of June delays the migration of the MT towards Bihar and Uttar Pradesh. A WD also delays the migration of the MT towards the Konkan Coast from the Malabar Coast. The influence of the WD in preventing or slowing down the monsoons may not be so common, but even if rare, it has a significant impact. The presence of an active WD may also cause the extension of the Arabian Sea branch of the monsoon towards Punjab and Rajasthan before the movement of Bay of Bengal branch towards Uttar Pradesh (Pisharoty and Desai 1956). Only after the WD moves further east does the monsoon enter the Gangetic Plains of Punjab and the Himalayas of Kashmir. These describe the oscillation of the MT over the Indian region produced by the WD. But there is a different kind of change in the migration of the MT called the PEM which will be discussed in greater detail. According to Pisharoty and Desai (1956) and Mooley (1957) there is sometimes a pulsatory extension of the Bay of Bengal branch of the monsoon termed the PEM towards Punjab and then west into Uttar Pradesh (currently Uttarakhand) and the Kashmir region. The PEM was associated with enhanced monsoonal activity with heavy rainfall. An example of heavy rainfall due to a PEM in the recent records is the natural disaster affecting the Kedarnath region of Uttarakhand on 16–17 June 2014. The details of the PEM (Chevuturi and Dimri in review) and the cause of the disaster are discussed in detail next.

A natural disaster in the form of flash floods due to extreme precipitation occurred at Uttarakhand (Kedarnath), India, on 16–17 June 2013. According to Dube et al. (2014), Uttarakhand received 375 % more rainfall (340 mm) than its daily normal (65.9 mm) for the monsoon period. Early reports suggested a rapid advancement of the ISM, since it reached the western Himalayan region within fifteen days of its onset on 1 June 2013 on the Kerala coast of southern India (IMD 2013a), which usually takes around 25 days. The MT associated with the ISM showed westward to north-westward movement (Dube et al. 2014) and showed up as a low-pressure area developing in the Bay of Bengal of India on 13 June 2013. Further, this system intensified on 15 June 2013 when it was located in the east of India. On subsequent 2 days, it moved north-westward towards the Uttarakhand. IMD (2013a) reported the presence of a low-pressure area over eastern Rajasthan region (western India) in association with a trough in the mid-upper level westerlies on 16 June 2013, which formed a WD. The WD moved eastward in the subsequent days (Dube et al. 2014). The system reached Uttarakhand on the 16 June 2013, lasting over the region until 18 June 2013. Both the MT and WD systems arrived and remained over the Uttarakhand region from 16 to 18 June 2013. IMD (2013b) reported that the interaction between the two weather systems led to the formation of low-level convergence over the steep orography of Uttarakhand. Dense clouding and heavy precipitation was observed over northern India due to the moisture incursion from the south-westerly flow (IMD 2013b), as seen in the satellite image (Fig. 3.1). The very early migration of the monsoon trough (MT) towards northern India and its interaction with an incoming western disturbance (WD) formed a transient cloud system (TCS) that led to extreme precipitation. We discuss PEM dynamics in this section.

During the merging of MT and WD causing the PEM, following circulation patterns emerge. Monsoons are associated with south-westerly flow at the lower levels of the atmosphere, which is a cross-equatorial flow termed LLJ (Blanford 1884; Joseph and Raman 1966; Findlater 1969) and has a direct connection with monsoonal rainfall over peninsular India (Joseph and Sijikumar 2004). In the upper-troposphere, a trough is observed in the SWJ, which extends into north-western India. This is the WD travelling in the SWJ and its axis shows a slight eastward movement. A confluence of the two systems, the MT of ISM and the WD in the SWJ, occurred on 17 June 2013. Considering that the two systems are present in the lower and upper parts of troposphere respectively, this merging system extends right from the lower- to upper-troposphere. The trough in the middle atmosphere shows the merged low-pressure zones of both the MT and the WD trough. This trough is the cause of the development TCS (Fig. 3.1), formed along the same axis centered over Uttarakhand. These are the cloud systems formed during the ITML as described by Kalsi and Halder (1992).

Consistent with the dynamical understanding, the ISM shows warm advection whereas, as discussed in detail previously, the region ahead of the WD shows colder advection. In spatial extent, the clear zone of thermal-advection confluence is the zone of instability and frontogenesis (Singh and Agnihotri 1977). A clear zone of interaction between the two different systems (tropical and extra-tropical) is observed around the mid-troposphere when an incoming WD interacts during the

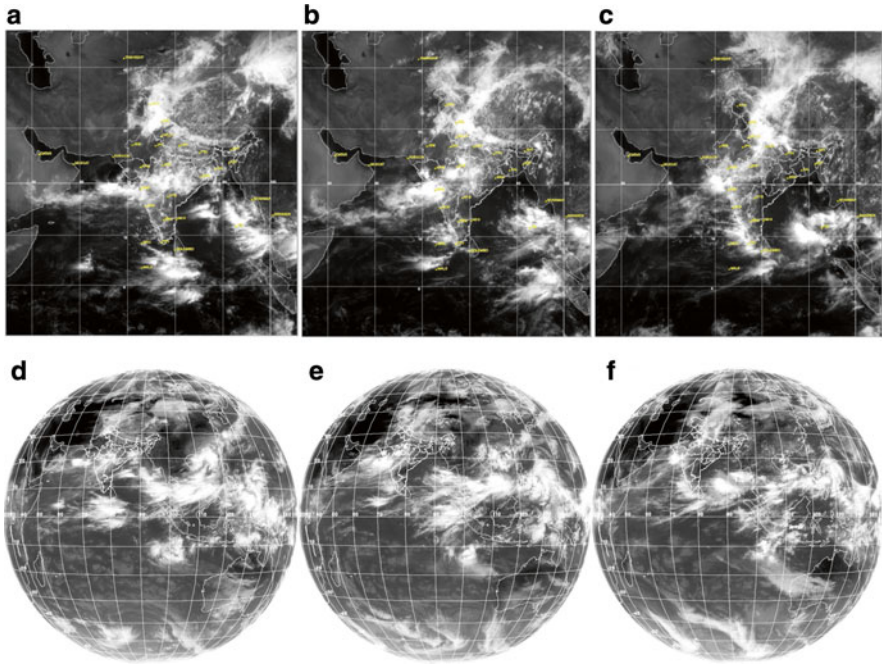


Fig. 3.1 Kalpana satellite images (Source: IMD 2013a, b) for (a) 15 June 2013 (0600 UTC), (b) 16 June 2013 (0600 UTC) and (c) 17 June 2013 (0600 UTC). (d–f) is same as (a–b) but with INSAT-3A with thermal infrared band

monsoon, leading to enhanced instability. The interaction of the MT and WD generates instability in the vertical column. As the potential instability declines, there is an increase in the deep-layer wind shear. In comparison, the deep-layer wind shear shows higher values than the low-level wind shear, signifying the deep convection observed during the storm. Instability (buoyancy) promotes the wind shear during storms (Weisman and Klemp 1982). Instability is promoted by moisture and temperature, but, in this case, also by the front formation with the interaction of two systems, further invigorating the precipitation forming mechanism. The next paragraph deals with this interaction of systems in detail.

The upper-level easterly winds are the tropical easterly jet (TEJ) as described by Koteswaram (1958b). This TEJ is an important part of the ISM, and it enhances convection by promoting the upper-level divergence (Sreekala et al. 2013). During the ITML, the westerly winds in the mid- to upper-troposphere dominate and ultimately overcome the TEJ. This westerly jet stream has already been discussed earlier as the SWJ. This SWJ moves north of India during the summer due to a shift in the ITCZ (Ding and Sikka 2006). Thus the troughs in the SWJ usually do not impact India during the summer. But, due to the fluctuations in the ridge and some disturbances having large enough amplitude and intensity, these might extend towards the northern Indo-Pakistan region (Ding and Sikka 2006; Ramaswamy

1962). In such situations, the TEJ gets weakened or replaced by the westerlies as was observed during this case. In the lower troposphere, orography dominates in the north-west due to the presence of the Himalayas, whereas in the south-east strengthening westerly flow is seen. If meridional wind is considered, a strengthening southerly wind is also observed. Thus, this combined flow is a south-westerly flow, which is a characteristic of ISM flow or LLJ, towards the Himalayan region. With the presence of SWJ trough or a WD which replaces the TEJ in the upper troposphere and lowlevel monsoonal flow, it exhibits some characteristics of the *break monsoon* period (Ramaswamy 1962; Bhatla et al. 2004). The upper tropospheric region also manifests southerly winds. Such a northward movement of meridional wind is associated with the break monsoon (Joseph 1978).

During the break monsoon, precipitation is common over the foothills of the Himalayas and rest of the India experiences dry conditions (Ramaswamy 1962; Bhatla et al. 2004). But according to IMD (2013a), the monsoon of 2013 showed no break periods and also precipitation was observed in some other parts of India, as well, during this time period. The interaction of the WD and the MT does generate a situation similar to the break period. But the question arises: what type of interaction of the WD and MT not only enhances the approach of the monsoon over India but also causes unusually high amounts of precipitation? Pisharoty and Desai (1956) in their paper briefly mentioned that WDs sometimes extend the Arabian Sea branch of the monsoon to north India before the Bay of Bengal branch in the early monsoon period. They termed it a *pulsatory extension of the monsoon* (PEM) towards north India. Mooley (1957) described a similar case (09 July 1953) of extension of the monsoon moist current towards former north-western Uttar Pradesh (currently Uttarakhand). This extension was said to be caused due by a WD leading to enhancement of precipitation over the region. But the PEM has not been much discussed in detail in the literature. PEM is characterized by suddenly enhanced precipitation over north-western India, which is extremely vulnerable to disasters due to such events. It is imperative to have a detailed understanding of such rare but extreme events due to their consequences. In the forthcoming portion of this monograph, the physics and dynamics of the PEM causing heavy precipitation over Uttarakhand is discussed in detail.

In Fig. 3.2, the analysis of geopotential height is represented. The geopotential height anomaly at each pressure level shows a lower geopotential height in the north-western upper-troposphere (with the presence of a WD) and higher geopotential height in the south-east lower-troposphere (with the presence of a MT). This indicates that the geopotential height lines are tilting down towards the south-east. This tilt can also be visualized in the perturbation geopotential height lines. This is causing *compression* in the pressure surfaces where the WD is present, and *rarifaction* around the location of the MT. The compression is caused by colder advection in the region and rarification is due to the layers becoming less dense with higher temperatures. Further, enhancement of both WD and MT is evident from Fig. 3.2a–c. This change in the thickness of the pressure surfaces leads to the development of changes in the geostrophic wind and occurs due to changes in temperature gradients. But from this figure we see two different systems in the opposite corners of the

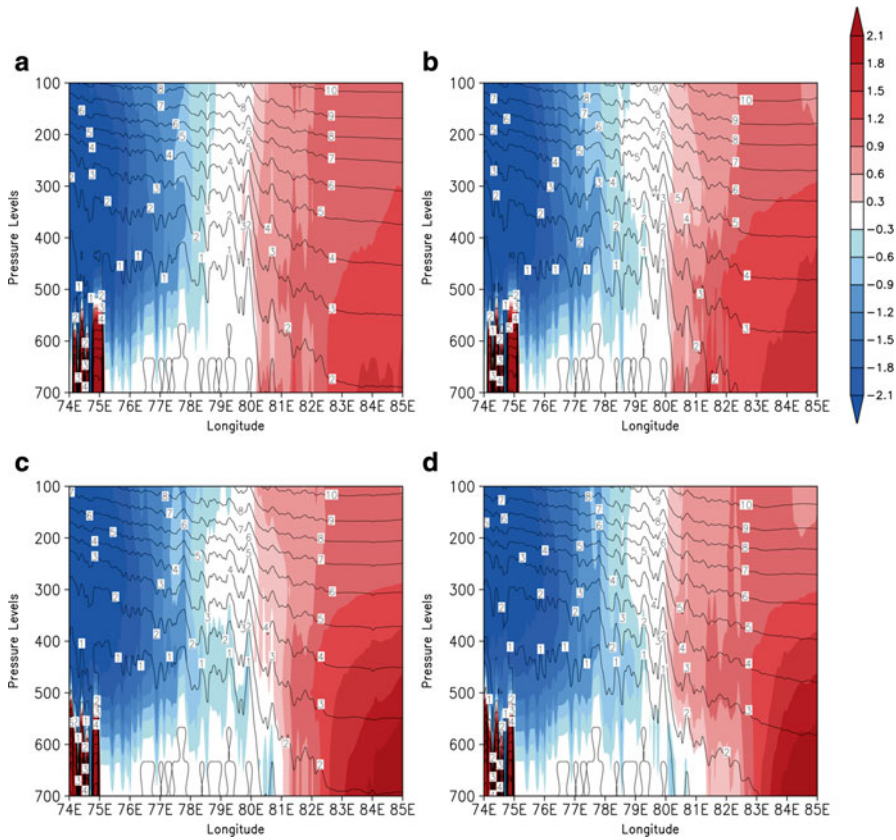


Fig. 3.2 Geopotential height anomaly (*shaded*) and perturbation geopotential height ($\times 10^2$ m/s; *contour*) over the axis normal to the formation of TCS for different time periods

graph. Black lines demarcating the systems are represented in Fig. 3.2c where a clear distinction of weather systems is seen. The lower-level south-west portion has orography whereas the upper-level northern part should be influenced by the WD. Here the upper-level WD is again divided into two portions; the warmer eastern part and the trailing colder western part. A WD is the form of frontal layer in the upper troposphere with a pre-existing low (Singh and Kumar 1977; Dimri and Chevaturi 2014).

Thus, there is a formation of an *occluded discontinuity* during the PEM at synoptic scale in the atmospheric column (Fig. 3.2c). The interaction of the weather systems forming the discontinuity with orography leads to lower-level convection enhanced by mechanical lifting and upper-level divergence due to the westerlies. The occluded discontinuity is located exactly over the Uttarakhand region (Fig. 3.2c) approximately between 79°E and 80°E. The discontinuity over the region is also leading to the high perturbation seen in the vertical atmospheric column between 79°E and 80°E. To further show that the occluded discontinuity is the

reason for the generation of the instability for storm formation, the reflectivity and hydrometeor mixing ratios are analyzed. From 16 June 2013 to 17 June 2013, a clear increase in the concentrations of hydrometeors is observed due to increasing reflectivity. This increase represents cloud formation and convective activity over Uttarakhand. This is an indication that the occluded discontinuity interacting with the orography culminates in heavy precipitation. Singh and Agnihotri (1977) stated that in winters WDs get their energy from baroclinic zones along the axis of the upper-level front (frontogenesis). In a slightly similar way, the occluded discontinuity also generates a baroclinic zone at the interaction point due to differences in the temperature gradient between the two weather systems and front formation within WD itself. These baroclinic zones give rise to enhanced instability in the atmosphere, which strengthens the precipitation-forming mechanism.

The thermal winds along with temperature advection is a representation of the advection due to the temperature gradient in two slices of the vertical atmospheric column; low to mid-troposphere (900–500 hPa) and mid to upper-troposphere (500–100 hPa). In the lower half of the troposphere, no clear representation is seen over Uttarakhand due to the presence of topography. But there is warm advection evident adjacent to the region. This warm advection with slight clock-wise motion of thermal winds contains veering winds. The horizontal movement of a low-level *warm and humid* air mass is observed and is associated with the MT. In the upper half of the troposphere, a clear frontal zone is seen over the Indo-Pakistan region, with cold advection trailing behind warm advection. The thermal winds signify a change in the geostrophic wind at different pressure levels. When the thermal winds are considered, a clear counter-clockwise movement is seen with height. This signifies backing winds, which also represent a cold air advection in the upper half of troposphere. Such a formation of a front with cold air advection is due to the trough in SWJ (WD formation). This zone of discontinuity between two air masses is due to the meeting of a tropical air mass with a middle latitude air mass which forms a baroclinic zone (Singh and Agnihotri 1977). This also explains the reason for the *early advance of the monsoon* which was reported in all studies. An enhanced thermal gradient is seen at the surface due to the northward-moving MT and at the cold front in the form of the eastward moving WD. This strong temperature gradient accelerates the rate of northward propagation of the MT towards north India. A temperature gradient within the atmosphere causes the differential densities of air within the atmospheric column. Heating causes rarification and cooling causes compression which produces varying thicknesses of pressure levels. Due to such density/thickness differences in the pressure column, the pressure surfaces or geopotential surfaces show a tilt (Fig. 3.2). Only horizontal temperature gradients and advection can cause such a tilt in geopotential surfaces and thus changing geostrophic winds with height. The thermal winds are a result of the vertically varying geostrophic wind. The stronger is the advection; the stronger is the change in the geostrophic wind with height; which forms stronger frontal zones. Also, since most of the mid-latitudes are in geostrophic balance, slight ageostrophic wind over the troughs and depressions in the pressure surfaces generates the synoptic scale

weather systems as seen in this case. The baroclinic zones between the fronts (especially in the region of occluded discontinuity) generates instability which is the source of the kinetic energy driving the storm and enhancing precipitation.

The heavy precipitation that caused devastation in Kedarnath was observed all over the Uttarakhand state. The interaction of WD and MT formed a cloud cluster directly over Uttarakhand termed the TCS, which caused the extreme precipitation. The formation of the TCS was attributed to the rapidly advancing PEM towards northern Indian in the early monsoon period. This was caused by the formation of an *occluded discontinuity or front* over north India. WDs usually do not impact India during summer due to a northward shift of the SWJ. In summers some WDs, with larger amplitudes of upper-level troughs, migrate over the Indo-Pakistan region. Eastward-moving WDs in the upper levels have cold-air mass advection towards the warmer air mass, forming strong temperature gradients leading to frontogenesis associated with cold fronts. The low-level warm and humid air mass associated with the MT acts similar to a warm front. With a northward PEM, a warm and humid air mass interacts with the cold front associated with the eastward moving WD (Fig. 3.3). The movement of the cold front over this warm and humid low-level flow forms an occluded front which develops deep instability at the lines of discontinuity. This thermal forcing develops a pseudo-frontal system between the low and upper levels of the atmosphere. The enhanced temperature gradient of such a front

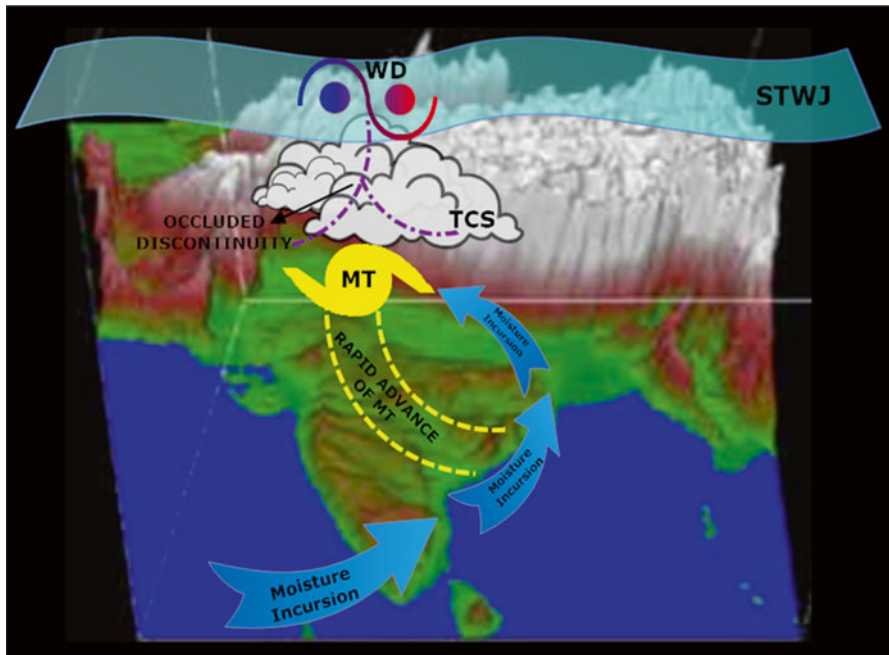


Fig. 3.3 Conceptual model of the PEM towards Himalayas

causes a stronger pressure gradient leading to a faster northward approach of the MT. Also, the formation of a strong occluded front augments instability more than simple convective instability. This generates the formation of a large organized storm (rather than multiple small storm cells) which caused the high-intensity precipitation over a large region.

In addition to these effects of WDs directly impacting the ISM due to their occurrence during monsoon season and their subsequent interaction with the tropical systems, there are also indirect consequences of WDs on the ISM. Anomalous heavy snow in the Himalayas during winter or spring has long been regarded as a possible precursor of deficient Indian monsoon rainfall during the subsequent summer (Godbole 1973; Hahn and Manabe 1975; Das and Bedi 1978; Yanai et al. 1992). However, the teleconnection mechanisms by which snow anomalies in the Tibetan Plateau affect the summer monsoon, and its dependence on the spatial variability of the snowpack remains largely unknown. But many studies have been performed to understand the dependence of summer monsoon intensity on the snow depth of the Eurasian snow cover, which includes the Himalayan snow cover. Kripalani et al. (2002) suggested that snow depth over Eurasia impacts the low-level jet which is a characteristic feature of the monsoons. Sankar-Rao et al. (1996) hypothesized that the high snow amounts lead to the generation of the high-pressure perturbation over the north of India in the lower levels of the atmosphere and the lower-pressure anomaly in place of the upper-level monsoon high. These two changes weaken the subsequent ISM. As this snow cover is caused by the winter precipitation associated with the WDs, there is a possibility of a relation between the WDs and the ISM. In fact, Dash et al. (2005, 2006) reported that the variability in the snow depth over Eurasia is associated with variability in the mid-latitude circulations in the winter season, which may be precursors to the variability of the monsoon circulation and in turn the ISM rainfall.

The Himalayan snow cover during winter is a key factor in long-range forecasting of ISM rainfall (Vernekar et al. 1995; Kripalani et al. 1996; Dash et al. 2004, 2005; Manguin et al. 2010). A model study by Turner and Slingo (2011) revealed a Blanford-type mechanism involving reduced surface sensible heat and longwave fluxes, reduced heating of the troposphere over the Tibetan Plateau, and consequently a reduced meridional tropospheric temperature gradient that weakens the monsoon during early summer (Blanford 1884; Fasullo 2004). Snow albedo is shown to be key to this mechanism, explaining around 50 % of the perturbation in sensible heating over the Tibetan Plateau and accounting for the majority of cooling throughout the troposphere. Various model experiments undertaken to understand ISM forecasting on seasonal-to-interannual variability (Cane 1991) using Pacific ocean trade winds, show that weak trade winds, when imposed on the ocean models, result in *heavy winter snowfall regime and subsequent weak summer monsoon* (Barnett et al. 1989). Bamzai and Shukla (1999) reported a statistically significant correlation between western Eurasian snow cover and the subsequent ISM rainfall. Kripalani and Kulkarni (1999) found a significant negative correlation between the winter snow depth of western Eurasia and the subsequent ISM rainfall, whereas the eastern Eurasian snow depth had a positive correlation with the monsoon rainfall.

With the higher snowfall amounts in winter, there is a possibility that decreased surface temperatures over India cause weakening of the heat low and in turn weaken the ISM. The relationship between snow cover and the ISM may change in the future as more dust and black carbon from anthropogenic sources deposited on the snow reduce its albedo (Gautam et al. 2013).

3.4 Post-Monsoon

The post-monsoon season is the season during which the withdrawal of the ISM takes place. As mentioned before, this is the reversal of the monsoonal winds. As monsoon is a term that defines reversal of large-scale circulation, even this reversal can be termed as a monsoon which is called the north-east monsoon as the direction of wind flow is from the north-east. The withdrawal of the ISM leads to heavy precipitation over peninsular India, mainly over the eastern coastal regions such as coastal Andhra Pradesh and the Tamil Nadu region (Srinivasan and Ramamurthy 1973; Dhar and Rakhecha 1983). Further, this season is known for the occurrence of the tropical cyclones, since these storms form usually during the late summer and the autumn (Niyas et al. 2009). Seven percent of all global tropical cyclones form in the north Indian Ocean. Maximum cyclone formation in the north Indian Ocean occurs during the pre-monsoon (especially in the month of May) (Philip et al. 1973) and post-monsoon (October and November) (Singh et al. 2001). The cyclonic disturbances have five to six times higher frequency of formation over the Bay of Bengal than over the Arabian Sea (Niyas et al. 2009). During the advance or retreat of the monsoon, the ITCZ exists near the equatorial region of the oceans surrounding the India coasts, which promotes the initiation and intensification of low-level cyclogenesis into cyclones (Srinivasan and Ramamurthy 1973). According to Barry (2008), the transition of upper-air easterly winds to the sub-tropical westerly jet during autumn period is sudden as compared to the gradual transition observed during the spring.

WDs are not known to have a significant impact on the heavy precipitation caused due to the north-east monsoon over the Tamil Nadu region. As during this time the ICTZ is still shifting southwards and the SWJ is still north of India, only the WDs of very large amplitude impact the convective disturbances that far south over the Tamil Nadu region. But the WDs might affect the precipitation associated with the northeast monsoon over the Tamil Nadu region, if there is a superimposition of the westerly trough with the easterly waves, which sometimes also happen in winter (Pisharoty and Desai 1956). Superimposition during this season must be over the Bay of Bengal region between tropical marine air and dry northerly air. Possible asymptotic confluence occurs on the western side of the easterly wave trough and the rear of the westerly wave trough. This confluence of the air masses with variable temperature and moisture causes intensification of the rainfall on the western side of the easterly trough which is over the Tamil Nadu region. On the other hand, the WDs may have a more significant impact on the tropical cyclones that form during

this time period. We have already discussed the impact of WDs on the tropical depressions that form during the pre-monsoon season. In this section we describe the impact of WDs on the tropical cyclones that form during the post-monsoon season.

Tropical cyclones interacting with the WDs may result in changes in the intensity, structure and the track of the tropical cyclones. Kalsi and Halder (1992) reported the occurrence of cases where the mid-latitude westerlies caused the shearing off of tropical cyclones. Mandal et al. (1990) and Kalsi and Halder (1992) described the tropical cyclone of 2 February 1987 over the Bay of Bengal shearing off and weakening due to the mid-latitudes. Further, WDs with extended troughs towards the lower latitudes cause changes in the track of the tropical cyclones of the Bay of Bengal as well as the Arabian Sea. The changes in the path or re-curvature are sudden phenomena, and the tropical cyclone remains active even after the storms re-curve (Pisharoty and Desai 1956). The re-curvature of the tropical cyclones can also be due to semi-permanent highs, but during such conditions, due to upper level convergence, the tropical storm might lose its intensity. However, during the re-curvature due to a WD, the upper-level divergence is maintained, and the tropical cyclone remains active.

The presence of a westerly trough may also cause intensification of the tropical cyclones, because the westerly trough lines extend southwards between region of semi-permanent highs. If such an extension of the westerly trough interact and interlocks with the easterly trough of the southern latitudes, this causes intensification of both the troughs (Pisharoty and Desai 1956). In contrast, the westerly trough west of the tropical cyclone develops a strong outflow channel towards the westerlies (Kalsi and Halder 1992). A tropical low moving westward may also arrive vertically under the rear of trough (at the rear of the WD which has the anticyclonic flow). This causes the westerly trough to be in the east of the tropical cyclone. In such situations in the Bay of Bengal, the tropical low evidently intensifies into a tropical cyclone (Pisharoty and Desai 1956). Kalsi and Jain (1989) discussed another mechanism of tropical cyclone intensification due to WDs. Sometimes close proximity occurs between the cold upper-tropospheric low and the low-level warm tropical cyclone. This proximity causes the sudden sinking of the upper low which intensifies the tropical system. The cold air pool blocked by the westerlies causes sub-tropical genesis of the cyclone at the base of the mid-tropospheric trough in the westerlies. This sub-tropical genesis causes rapid onset of the cyclone which has an extensive belt of precipitation (Kalsi and Halder 1992). In addition to intensification of the tropical cyclones, the westerly troughs may also cause changes in the forward speed of the tropical systems. An extra-tropical vortex of the WD north of a tropical depression might cause abnormally fast movement of that tropical system. The rapid movement of tropical depression and its merger with the northern vortex ultimately leads to the further intensification of the depression into a tropical cyclone.

References

- Ali K, Momin GA, Tiwari S, Safai PD, Chate DM, Rao PSP (2004) Fog and precipitation chemistry at Delhi, North India. *Atmos Environ* 38(25):4215–4222
- Ananthakrishnan R (1977) Some aspects of the monsoon circulation and monsoon rainfall. *Pure Appl Geophys* 115(5–6):1209–1249
- Ananthakrishnan R, Soman MK (1988) The onset of the southwest monsoon over Kerala: 1901–1980. *J Climatol* 8:283–296
- Attri SD, Tyagi A (2010) Climate profile of India. Meteorological Monograph No. Environment Meteorology –01/2010. http://www.imd.gov.in/doc/climate_profile.pdf. Accessed on 14 July 2012
- Bamzai AS, Shukla J (1999) Relation between Eurasian snow cover, snow depth and the Indian summer monsoon: an observational study. *J Climatol* 12:3117–3132
- Barnett TP, Dumenil L, Schlese U, Roekler E, Latif M (1989) The effect of Eurasian Snow cover on regional and global climate variations. *J Atmos Sci* 46:661–685
- Barry RG (2008) Mountain weather and climate. Cambridge University Press, New York
- Bhalme HN, Mooley DA (1980) Large-scale drought/flood and monsoon circulation. *Mon Weather Rev* 108:1197
- Bhatla R, Mohanty UC, Raju PVS, Madan OP (2004) A study on dynamic and thermodynamic aspects of breaks in the summer monsoon over India. *Int J Climatol* 24(3):341–360
- Bhullar GS (1952) Onset of monsoon over Delhi. *Indian J Meteorol Geophys* 3:25–30
- Blanford HF (1884) On the connection of the Himalaya snowfall with dry winds and seasons of draughts in India. *Proc Roy Soc Lond* 37:3–22
- Blanford HF (1886) Rainfall of India. *Memories of India Meteorology Department* 2:217–448
- Cane MA (1991) Chapter 11: Forecasting El-Nino with a geophysical model. In: Glantz M, Katz R, Nicholls N (eds) Teleconnections connecting world-wide climate anomalies. Cambridge University Press, Cambridge, MA, pp 345–369
- Chakravarti AK (1968) Summer rainfall in India: A review of monsoonal and extramonsoonal aspects – II. *Atmos* 6(3):87–114
- Chakravorty KC, Basu SC (1957) The influence of western disturbances on the weather over northeast India in monsoon months. *Indian J Meteorol Geophys* 8(3):261–272
- Chevuturi A, Dimri AP (2015) Numerical simulation of a hailstorm event over Delhi, India on 28 Mar 2013. In: High-impact weather events over the SAARC region. Springer International Publishing, Cham, pp 49–61
- Chevuturi A, Dimri AP (in review) Investigation of Uttarakhand (India) disaster- 2013 using Weather Research and Forecasting model
- Das PK, Bedi HS (1978) Inclusion of Himalayas in a PE model. *Indian J Meteorol Hydrol Geophys* 29:373–383
- Das MR, Mukhopadhyay SR, Dandekar MM, Kshirsagar SR (2002) Pre-monsoon western disturbances in relation to monsoon rainfall, its advancement over NW India and their trends. *Curr Sci* 82(11):1320–1321
- Dash SK, Singh GP, Vernekar AD, Shekhar MS (2004) A study on the number of snow days over Eurasia, Indian rainfall and seasonal circulations. *Meteorol Atmos Phys* 86:1–13
- Dash SK, Singh GP, Shekhar MS, Vernekar AD (2005) Response of the Indian summer monsoon circulation and rainfall to seasonal snow depth anomaly over Eurasia. *Clim Dyn* 24:1–10
- Dash SK, ParthSarthi P, Panda SK (2006) A study on the effect of Eurasian snow on the summer monsoon circulation and rainfall using a spectral GCM. *Int J Climatol* 26(8):1017–1025
- Dash SK, Kulkarni MA, Mohanty UC, Prasad K (2009) Changes in the characteristics of rain events in India. *J Geophys Res* 114(D10109):1–12
- De US, Dube RK, Rao GP (2005) Extreme weather events over India in the last 100 years. *J Indian Geophys Union* 9(3):173–187
- Dhar ON, Rakhecha PR (1983) Foreshadowing northeast monsoon rainfall over Tamil Nadu, India. *Mon Weather Rev* 111:109–112

- Dimri AP (2013) Interannual variability of Indian Winter Monsoon over the Western Himalaya. *Glob Planet Chang* 106:39–50
- Dimri AP, Chevuturi A (2014) Model sensitivity analysis study for western disturbances over the Himalayas. *Meteorol Atmos Phys* 123(3–4):155–180
- Ding Y, Sikka DR (2006) The Asian monsoon; synoptic systems and weather. Springer Praxis Books, Berlin, pp 131–201
- Dube A, Ashrit R, Ashish A, Sharma K, Iyengar GR, Rajagopal EN, Basu S (2014) Forecasting the Heavy Rainfall during Himalayan Flooding – June 2013. *Weather Clim Ext*. doi:[10.1016/j.wace.2014.03.004](https://doi.org/10.1016/j.wace.2014.03.004)
- Fasullo J (2004) A stratified diagnosis of the Indian monsoon-Eurasian snow cover relationship. *J Climatol* 17(5):1110–1122
- Findlater J (1969) Inter-hemispheric transport of air in the lower troposphere over the western Indian Ocean. *Q J R Meteorol Soc* 95:400–403
- Gautam R, Hsu NC, Lau WKM, Yasunari TJ (2013) Satellite observations of desert dust-induced Himalayan snow darkening. *Geophys Res Lett* 40:988–993. doi:[10.1002/grl.50226](https://doi.org/10.1002/grl.50226)
- Godbole RV (1973) Numerical simulation of the Indian summer monsoon. *Indian J Meteorol Geophys* 24:1–14
- Hahn DG, Manabe S (1975) The role of mountains in the south Asian monsoon circulation. *J Atmos Sci* 32(8):1515–1541
- Hong CC, Hsu HH, Lin NH, Chiu H (2011) Roles of European blocking and tropical-extratropical interaction in the 2010 Pakistan flooding. *Geophys Res Lett* 38(13)
- Houze RA Jr (1981) Structures of atmospheric precipitation systems: a global survey. *Radio Sci* 16(5):671–689
- IMD (2013a) 2013 Southwest Monsoon end of season report. <http://www.imdpune.gov.in/end-of-season-report2013.pdf>. Accessed on 20 Mar 2014
- IMD (2013b) A preliminary report on heavy rainfall over Uttarakhand during 16–18 June 2013. http://www.imd.gov.in/doc/uttrakhand_report_04_09_2013.pdf, Accessed on 20 Mar 2014
- Joseph PV (1978) Sub-tropical westerlies in relation to large scale failure of Indian monsoon. *Indian J Meteorol Hydrol Geophys* 29(1–2):412–418
- Joseph PV, Raman PL (1966) Existence of low level westerly Jet stream over peninsular India during July. *Indian J Meteorol Geophys* 17:407–410
- Joseph PV, Sijkumar S (2004) Intra seasonal variability of the low level Jet stream of the Asian summer monsoon. *J Climatol* 17:1449–1458
- Kalsi SR (1980) On some aspects of interaction between middle latitude westerlies and monsoon circulation. *Mausam* 31:305–308
- Kalsi SR, Halder SR (1992) Satellite observations of interaction between tropics and mid-latitudes. *Mausam* 43(1):59–64
- Kalsi SR, Jain RK (1989) On some aspects of marginal cyclones. *Mausam* 40(1):47–50
- Koteswaram P (1958a) The Asian summer monsoon and the general circulation over tropics. *Monsoons of the World*. India Meteorological Department, New Delhi, pp 105–110
- Koteswaram P (1958b) The easterly jet stream in the tropics. *Tellus* 10(1):43–57
- Kothawale DR, Revadekar JV, Kumar KR (2010) Recent trends in pre-monsoon daily temperature extremes over India. *J Earth Syst Sci* 119(1):51–65
- Kripalani RH, Kulkarni A (1999) Climatology and variability of historical Soviet snow depth data: some new perspectives in snow-Indian monsoon teleconnections. *Clim Dyn* 15(6):475–489
- Kripalani RH, Singh SV, Vernekar AD, Thapliyal V (1996) Empirical study on Nimbus-7 snow mass and Indian summer monsoon rainfall. *Int J Climatol* 16:23–34
- Kripalani RH, Singh SV, Vernekar AD, Thapliyal V (2002) Relationship between Soviet snow and Korean rainfall. *Int J Climatol* 22:1287–1424
- Krishnamurti TN (1961) The subtropical jet stream of winter. *J Meteorol* 18:172–191
- Kumar KK, Soman MK, Kumar KR (1995) Seasonal forecasting of Indian summer monsoon rainfall: a review. *Weather* 50:449–467
- Kumar OSRU, Naidu CV, Rao SRL, Rao B (2004) Prediction of southern Indian winter monsoon rainfall from September local upper-air temperatures. *Meteorol Appl* 11(3):189–199

- Lau WK, Waliser DE, Goswami BN (2012) South Asian monsoon. Intraseasonal variability in the atmosphere-ocean climate system. Springer, Berlin/Heidelberg, pp 21–72
- Mamgain A, Dash SK, Sarthi PP (2010) Characteristics of Eurasian snow depth with respect to Indian summer monsoon rainfall. *Meteorol Atmos Phys* 110(1):71–83
- Mandal JC, Kalsi SR, Veeraraghavan K, Halder SR (1990) Some aspects of Bay of Bengal cyclone of 29 January to 4 February 1987. *Mausam* 41(3):385–392
- Mooley DA (1957) The role of western disturbances in the production of weather over India during different seasons. *Indian J Meteorol Geophys* 8(3):253–260
- Nitta T, Nanbu M, Yoshizaki M (1973) Wave disturbances over the China Continent and the Eastern China Sea in February, 1968. *J Meteorol Soc Jap* 51:11–28
- Niyas NT, Srivastava AK, Hatwar HR (2009) Variability and trend in the cyclonic storms over north Indian ocean. *Met. Monograph No. Cyclone Warning*. http://www.imdpune.gov.in/ncc_rept/Met_Monograph%20No.%203_2009.pdf. Accessed on 27 Mar 2012
- Parthasarathy B, Sontakke NA, Munot AA, Kothawale DR (1987) Droughts/floods in summer monsoons season over different meteorological sub-divisions of India for the period 1871–1980. *J Climatol* 1:57–70
- Philip NM, Srinivasan V, Ramamurthy K (1973) Low pressure areas, depressions and cyclonic storms in the Indian sea areas during the pre-monsoon season. Indian Meteorological Department: Forecasting Manual Part III
- Pisharoty P, Desai BN (1956) “Western disturbances” and Indian weather. *Indian J Meteorol Geophys* 7:333–338
- Pramanik SK, Alipore C (1939) Forecasting of Nor’westers in Bengal. *Proc Nat Inst Sci* 5:43
- Rajeevan M, Bhate J, Kale JD, Lal B (2006) High resolution daily gridded rainfall data for the Indian region: analysis of break and active monsoon spells. *Curr Sci* 91(3):296–306
- Rajeevan M, Gadgil S, Bhate J (2010) Active and break spells of the Indian summer monsoon. *J Earth Syst Sci* 119(3):229–247
- Ramage CS (1971) Monsoon meteorology, vol 15, International geophysics series. Academic, San Diego
- Ramamurthy K (1969) Some aspects of the “Break” in the Indian Southwest Monsoon during July and August. Indian Meteorological Department: Forecasting Manual Part IV
- Ramaswamy C (1962) Breaks in the Indian summer monsoon as a phenomenon of interaction between the easterly and sub-tropical westerly jet streams. *Tellus* 3:337–349
- Rao YP (1976) Southwest monsoon. Meteorological monograph synoptic meteorology no. 1. India Meteorological Department, New Delhi
- Romatschke U, Houze RA Jr (2011) Characteristics of precipitating convective systems in the South Asian monsoon. *J Hydrometeorol* 12:3–26
- Sankar-Rao M, Lau MK, Yang S (1996) On the relationship between Eurasian snow cover and the Asian summer monsoon. *Int J Climatol* 16:605–616
- Sharma RV, Subramaniam DV (1983) The western disturbance of 22 December 1980: a case study. *Mausam* 34(1):117–120
- Sikka DR (1977) Some aspects of the life history, structure and movement of monsoon depressions. *PAGEOPH* 115:1501–1529
- Singh MS, Agnihotri CL (1977) Baroclinity over India in winter and its relation to western disturbances and jet streams – Part I. *Indian J Meteorol Hydrol Geophys* 28(3):303–310
- Singh MS, Kumar S (1977) Study of western disturbance. *Indian J Meteorol Hydrol Geophys* 28(2):233–242
- Singh N, Sontakke NA (1999) On the variability and prediction of rainfall in the post-monsoon season over India. *Int J Climatol* 19(3):309–339
- Singh OP, Khan TA, Rahman MS (2000) Changes in the frequency of tropical cyclones over the North Indian Ocean. *Meteorol Atmos Phys* 75(1–2):11–20
- Singh OP, Khan TA, Rahman MS (2001) Has the frequency of intense tropical cyclones increased in the north Indian Ocean? *Curr Sci* 80(4):575–580
- Sreekala PP, Rao SB, Arunachalam MS, Harikiran C (2013) A study on the decreasing trend in tropical easterly jet stream (TEJ) and its impact on Indian summer monsoon rainfall. *Theor Appl Climatol*. doi:10.1007/s00704-013-1049-z

- Srinivasan V, Ramamurthy K (1973) Discussion of typical synoptic weather situations : Weather over the Indian Seas during the post-monsoon Season. Indian Meteorological Department: Forecasting Manual Part III
- Srinivasan V, Ramamurthy K, Nene YR (1973) Summer – Nor' westers and Andhis and large scale convective activity over peninsula and central parts of the country. Indian Meteorological Department: Forecasting Manual Part III
- Turner AG, Slingo JM (2011) Using idealized snow forcing to test teleconnections with the Indian summer monsoon in the Hadley Centre GCM. *Clim Dyn* 36:1717–1735
- BhaskaraRao NS, Venkataraman KS (1965) A study of effect of upper level divergence on rainfall distribution over NW India, venkataraman. *Indian J Meteorol Geophys* 16
- Vernekar AD, Zhou J, Shukla J (1995) The effect of Eurasian snow cover on the Indian monsoon. *J Climatol* 8:248–266
- Wang SY, Davies R, Gillies RR, Jin J (2011) Changing monsoon extremes and dynamics: example in Pakistan. In: Zhao J, Higgins W (ed) NOAA NWS. Science & Technology Infusion Climate Bulletin. pp 61–68
- Weisman ML, Klemp JB (1982) The dependence of numerically simulated convective storms on vertical wind shear and buoyancy. *Mon Weather Rev* 110(6):504–520
- Yanai M, Li C, Song Z (1992) Seasonal heating of the Tibetan Plateau and its effects on the evolution of the Asian summer monsoon. *J Meteorol Soc Jap* 70:319–351
- Yoshizaki M (1974) A study of wave disturbances over the China continent and the East China Sea in winter 1968. *J Meteorol Soc Jap* 52(4):380–386

Chapter 4

Western Disturbances – Indian Winter Monsoon

Abstract In this chapter, wintertime dynamics associated with large-scale flow and western disturbances (WDs) influencing winter precipitation is proposed and termed ‘Indian winter monsoon’. In Indian meteorological research, the northeast monsoon and Indian winter monsoon terms are interchangeable. In addition, winter precipitation – the Indian winter monsoon – is assumed to be similar to an extra-tropical cyclone traveling in large-scale westerlies. With concurrent research and the changing global context, increased understanding of the Indian winter monsoon is imperative. This chapter delineates the Indian winter monsoon while differentiating it from the northeast monsoon which so far is the prevalent term used in Indian meteorological parlance. Therefore, the present chapter provides comprehensive details on defining the Indian winter monsoon.

The Indian subcontinent is characterized by unique geographic positioning. The north is surrounded by the mighty Himalayas and the south by ocean. Such situations, along with many the seasonal changes, give rise to different weather patterns over the Indian subcontinent. The Indian summer monsoon (June, July, and August – JJA) (ISM) has been studied and discussed along with its varying dimensions (Annamalai et al. 2007; KrishnaKumar et al. 1999, 2006; Turner et al. 2007; Saha et al. 2011) such as the Tibetan high, which also well plays a significant role in defining the strength of ISM (Yasunari et al. 1991; Wu and Qian 2003; Sato and Kimura 2007). In the case of the northeast monsoon (NEM), Kripalani and Kumar (2004), Kumar et al. (2007) and Yadav (2012) have deliberated upon its dynamics comprehensively. On another regional scale, non-monsoon periods as well are of great importance for the Indian region. In winter (December, January, and February–DJF), accumulation in the form of snow provides important feed to the north Indian rivers, glacier etc. (Dai 1990; Lang and Barros 2004; Yadav et al. 2013; Dimri 2014). This precipitation is mainly contributed by the extra-tropical cyclones called WDs (Dimri and Mohanty 2009; Dimri et al. 2013). Though there are various studies available on the ISM and NEM, very limited information is available on the Indian winter monsoon (IWM) (Dimri 2004, 2006, 2012, 2013a; Yadav et al. 2013). Only very few studies have focused on the IWM variability (Laaat and Lelieveld 2002; Dimri 2012, 2013a, b, 2014; Yadav et al. 2013).

4.1 Introduction

Many studies have defined dominant intraseasonal (ISO) modes that vary at different time scales for ISM (Hartmann and Michelsen 1989; Goswami and Mohan 2001; Hoyos and Webster 2007). Though the interannual variations (IAVs) in the IWM are in phase with ENSO forcings (Yadav et al. 2010; Dimri 2012, 2013a), much less has been explained concerning its ISOs behavior (Dimri 2014). Since most of the Indian economy and agriculture is driven by ISM and derived from to its broader impact, most of the research is focused on understanding and defining the ISM. Apart from the contribution to winter precipitation over the northern Indian region, interaction of IWM with the northern Indian Himalayas topography and land use, paucity of observations, solid – liquid precipitation ratio and snow-covered land-surface interactions are research questions that still need to be debated. With concurrent research and the changing global context, the impacts of sub-continental-scale circulation changes during the IWM over northern India are imperative. In order to define the IWM, this chapter elaborates on the potential role of sub-continental and global-scale circulation changes and interannual and intraseasonal behavior associated with the IWM. Such deliberation will provide new dimensions and definition to the understanding of IWM in Indian meteorological parlance which has been missing thus far. The following sections sequentially deliberate upon the important dynamics associated with the IWM.

To understand the winter precipitation over the northern Indian region dataset in this chapter, these sources are used: Asian Precipitation – Highly-Resolved Observational Data Integration Towards Evaluation of Water Resources (APHRODITE, Yatagai et al. 2012), Global Precipitation Climatology Project (GPCP, Adler et al. 2003), Global Precipitation Climatology Centre (GPCC, Rudolf et al. 2005) and Climate Research Unit (CRU, New et al. 2000). Corresponding winter precipitation over the western Himalayas (WH) is shown in Fig. 4.1a. The reason for using multiple sets of precipitation data is to assess the spatial variability in different precipitation fields over the WH region. It is important because this region has a paucity of observations and possesses land-use heterogeneity and topographic variability. Wind, moisture and geopotential fields are taken from the National Center of Environmental Prediction/National Center for Atmospheric Research (NCEP/NCAR) (Kanamitsu et al. 2002). Sea-surface temperature (SST) is incorporated from the Hadley Center, UK (Hadley Center 2006). Outgoing long-wave radiation (OLR) from the National Oceanic and Atmospheric Administration (NOAA) in the US (Liebmann and Smith 1996) is also used to identify such seasonal and ground dependency. Data from 28 winters (1979–2007) for geopotential height, wind, stream function, moisture flux etc. are considered to examine ISOs associated with the IWM.

Most of the algorithms used in preparing precipitation reanalyses generate ‘synthetic’ precipitation values which sometimes deviate from the real observations. To remove this ‘probable’ bias of inadequate representation, a mask field of a 10 mm/month precipitation threshold is used. Also, precipitation, OLR, and reanalysis of

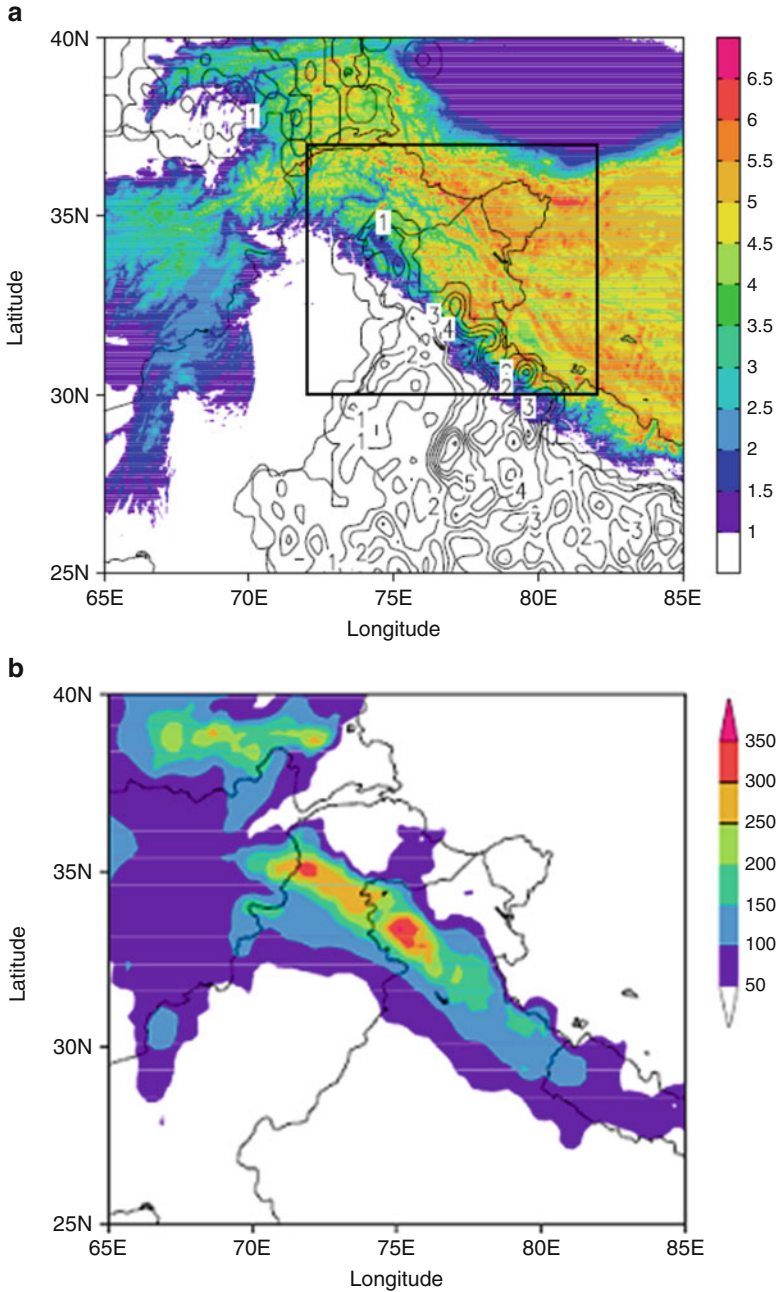


Fig. 4.1 (a) Topography ($\times 1e-3$ m; *shaded*) and ratio of 0.05° grids for stations (%; *contour*) over the western Himalayas. The area of 30°N , 72°E to 37°N , 82°E is considered in the present chapter; (b) winter season precipitation climatology (mm/DJF) based on APHRODITE precipitation observed data reanalysis

daily data anomalies are homogenized and deseasonalized. For each year, the first three harmonics of the annual cycle (about 120 days) are subtracted from the anomaly time series to homogenize it. Then to deseasonalize/detrend the time series, sub-monthly (7–25 days) perturbations were computed by applying a Lanczos filter (Duchon 1979). In the WH, the region from 30°N 72°E to 37°N 82°E (indicated by the box in Fig. 4.1a) was chosen to analyse winter precipitation and associated IAV and ISO. This region was chosen because the area receives the highest winter precipitation and is topographically variable. Figure 4.1b shows the seasonal precipitation climatology based on reanalysis of APHRODITE observations. Winter precipitation climatology is distributed across and along the WH topographic orientation. Precipitation maxima at ~34°N 76°E and ~35°N 72°E are observed. This climatology was compared with the other reanalysis data (GPCP, GPCC, and CRU). Correlations of greater than 0.8 were recorded between APHRODITE data and these reanalysed data. Over the WH, spatial precipitation patterns of precipitation in all four gridded precipitation reanalyzes are similar. Of these four reanalyzes, APHRODITE reanalysis is used for further analysis and discussion because they have the finest spatial resolution. It should be noted that over such a region, some data may be ‘synthetic’ due to the various algorithms used while preparing the reanalysis of precipitation fields. However, this issue is beyond the scope of the present chapter.

4.2 Interannual Variability of the Indian Winter Monsoon

A physical mechanism of the IWM over the WH with reference to excess/deficit years and their year-to-year variability is discussed based on the period 1980–2007 (28 years). In the following paragraphs, explanations with specific reference to the sub-continental and global-scale circulation changes are provided followed by deliberations on the role of the sea-surface warming/cooling phase and associated circulation patterns in defining winter precipitation over the WH.

Interannual variability associated with IWM over the WH is explained with composite sets of wet and dry years with the study area shown in Fig. 4.1. Based on ± 0.5 standard deviation, wet (1983, 91, 92, 95, 98, 2005) and dry (1985, 88, 97, 2000, 01, 06) precipitation years are chosen. The region from 30°N 72°E to 37°N 82°E (marked by the box in Fig. 4.1a) is selected as it receives the highest winter precipitation. Seasonal and monthly area-averaged winter precipitation anomaly is shown in Fig. 4.2a. There are years having excess and deficit precipitation over the region. Corresponding wet-dry composite precipitation differences, with 99 % confidence, are depicted in Fig. 4.2b. It shows that the significant region of higher precipitation is oriented along the WH topography which corroborates with Dimri and Niyogi (2012). On global-scale circulation patterns, 200 hPa zonal wind differences between wet and dry year composites show southward movement of the SWJ over and across the Indian subcontinent (Fig. 4.3a). In the mid-latitude region, steep pressure-gradient anomalies attribute to these stronger westerlies (Raman and

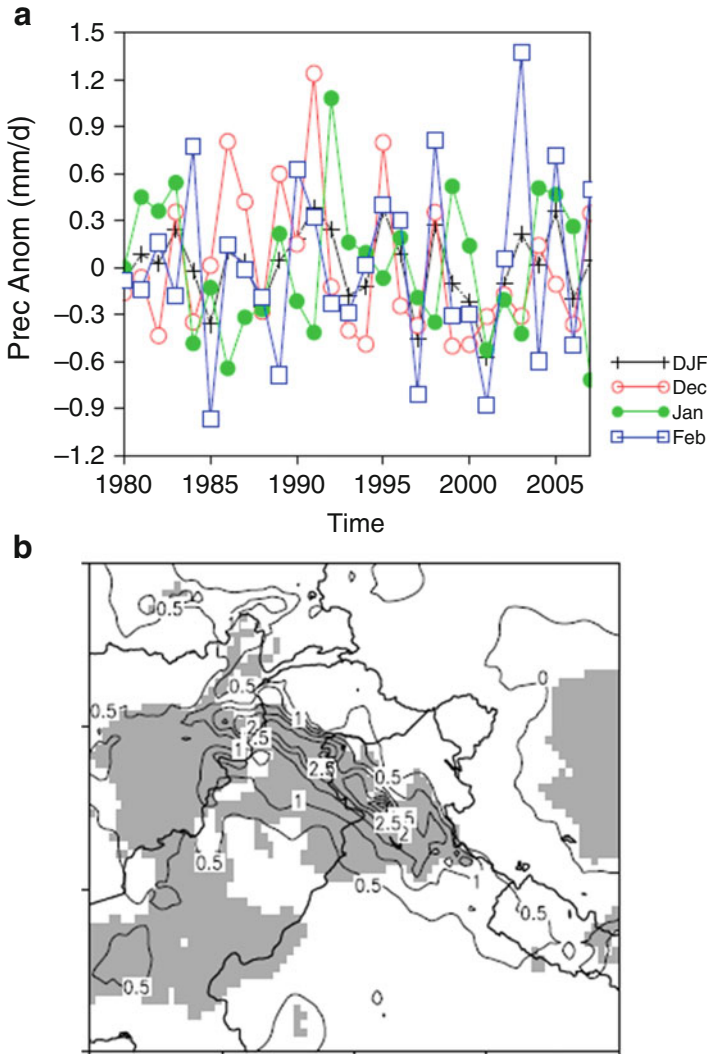


Fig. 4.2 (a) The monthly (Dec, Jan, and Feb) and seasonal (DJF) precipitation (mm/d) anomaly in APHRODITE observational reanalysis and (b) difference in 3-month (Dec, Jan, and Feb) average wet- and dry-year composites precipitation (*shaded*) and region with 99 % confidence level (*within contour*)

Maliekal 1985). At 500 hPa (Fig. 4.3b), significant lower geopotential is visible right from Saudi Arabia to the head of the Arabian Sea extending along 10°N to 30°N. Weaker westerlies dominate from the Black Sea region to the northwest Indian and Tibetan Plateau region in and around 30°N. During wet years, at lower level (850 hPa – Fig. 4.3c) over the head of the Arabian Sea, a weak anomalous cyclonic surface low persists. Such mid-tropospheric circulations provide necessary

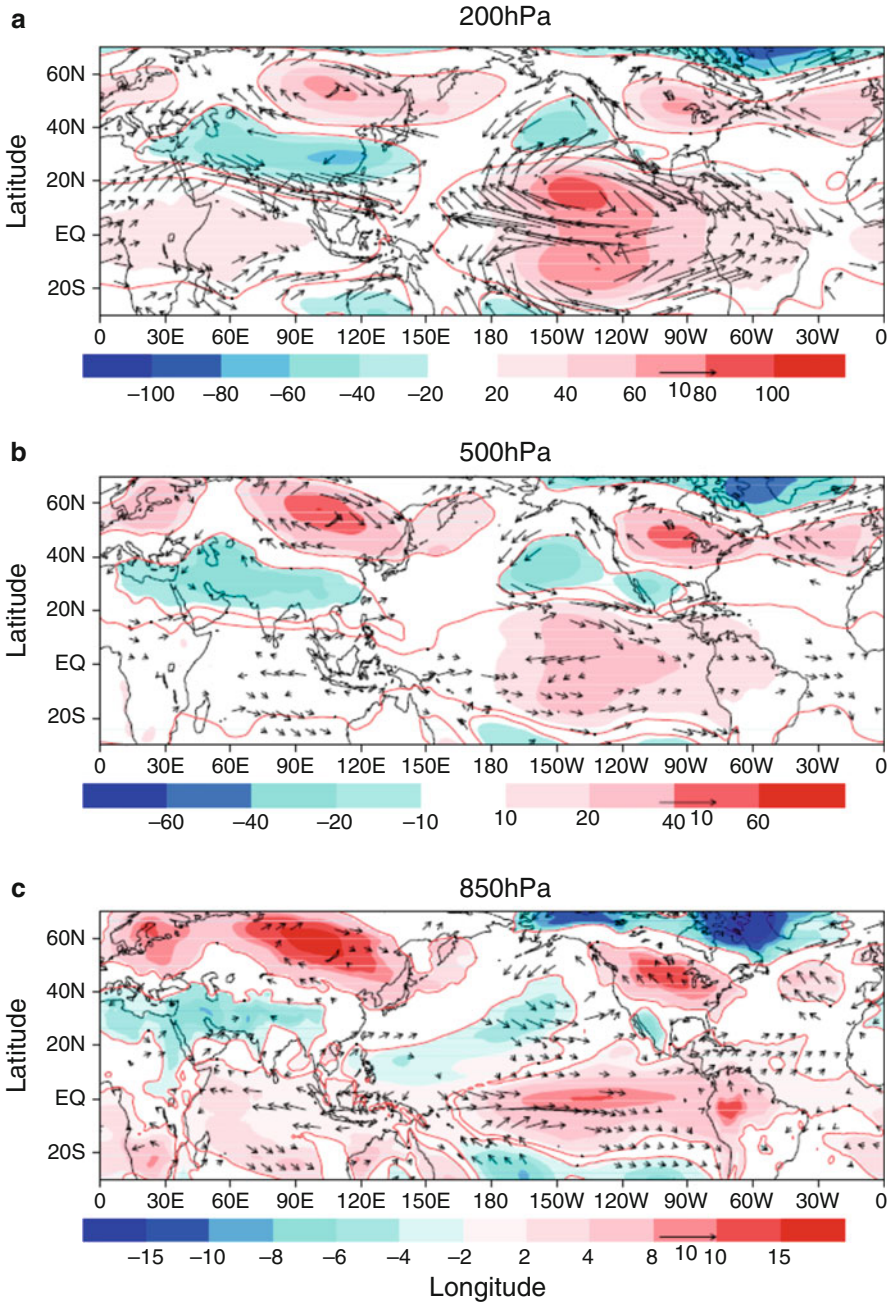


Fig. 4.3 Difference between 03 (DJF) month average wet and dry composites of wind (m/s; contour; winds above 99 % significant level are plotted) and geopotential height (m; shaded; region within contour corresponds to 99 % significant level) at (a) 200 hPa (b) 500 hPa and (c) 850 hPa

convergence augmenting the precipitation mechanism by enhancing moisture supplement from the Caspian and Arabian Seas. Further, an axis of anomalous anticyclone dominates along $\sim 60^{\circ}\text{N}$ 120°E at 200 hPa exists (see Fig. 4.3a). Another anomalous anticyclone extends from the central African continent to the Indian Ocean and up to Indonesia. A strong anomalous cyclone separates these two anomalous anticyclones and overruns the Indian subcontinent. In wet years, due to such enhanced anomalous highs and lows, the SWJ shifts southwards. The upper-level circulation patterns persist down into the mid-troposphere as well during the wet winters (Fig. 4.3b). Such stronger meridional pressure gradients provide favorable conditions for frontal WDs formations. During winter, these characteristic fronts in mid-latitude westerlies generate troughs in a sequential manner, and this is responsible for the genesis of a number of WDs. In wet years, at 850 hPa, stronger anomalous cyclonic circulation at and around $\sim 18^{\circ}\text{N}$ 62°E dominates (Fig. 4.3c). Slower westerlies around the equator and a deepening of northwesterlies over the Arabian Sea exist during wet years. Such deepening brings in moisture flux over the WH during the wet years. In addition, vertical distributions of cyclonic formations immediately west of the WH create favorable conditions for higher precipitation. Anomalous velocity potential and corresponding OLR at upper troposphere are presented in Fig. 4.4a and b for wet and dry year composites, respectively. In wet times, significant strong inflow (outflow) over the equatorial western (eastern) Pacific dominates (Fig. 4.4a). In dry year composites, a weak convergent source over the equatorial central Pacific is apparent (Fig. 4.4b). In addition, during wet years, the equatorial central (western) Pacific is associated with increased (decreased) convective activity. Further, lower-level increased (decreased) convection over the equatorial eastern (western) Pacific is associated with strong upward (downward) motion. In boreal winter, such situations attribute to enhanced north-south circulation in the upper tropospheric branch of the zonally-symmetric Hadley circulation. Corresponding OLR distributions show strong (weak) convection followed by pronounced (reduced) cloud formation and hence reduced (enhanced) OLR over the equatorial central (western) Pacific region (Fig. 4.4a). A slightly decreased OLR over the WH and western Indian Ocean, which also corresponds to increased cloud formation, is also observed. The upper-tropospheric anomalous stream function (representing rotational part of wind) with the corresponding anomalous OLR is depicted for wet and dry year composites (Fig. 4.4c, d respectively). A well-defined anomalous cyclonic core is seen over the WH. In addition, an upper-tropospheric low/cyclonic circulation dominates from the Mediterranean Sea to the western Pacific. ElNiño formed enhanced cooling over the western equatorial tropical Pacific and hence the corresponding Rossby responses (Kawamura 1998) creates cyclonic formulations over the WH. In this dry situation, anticyclonic/divergent circulation dominates over the WH (Fig. 4.4d.)

The antecedent dependency of the IWM is investigated here. The lagged correlation between winter precipitation over the WH and sea-surface temperatures for 28 years (1980–2007) is presented in Fig. 4.5. The IWM shows persistent and strong correlation with equatorial warming in previous seasons. Significant strong (negative) positive correlation with the eastern (western) equatorial Pacific warming

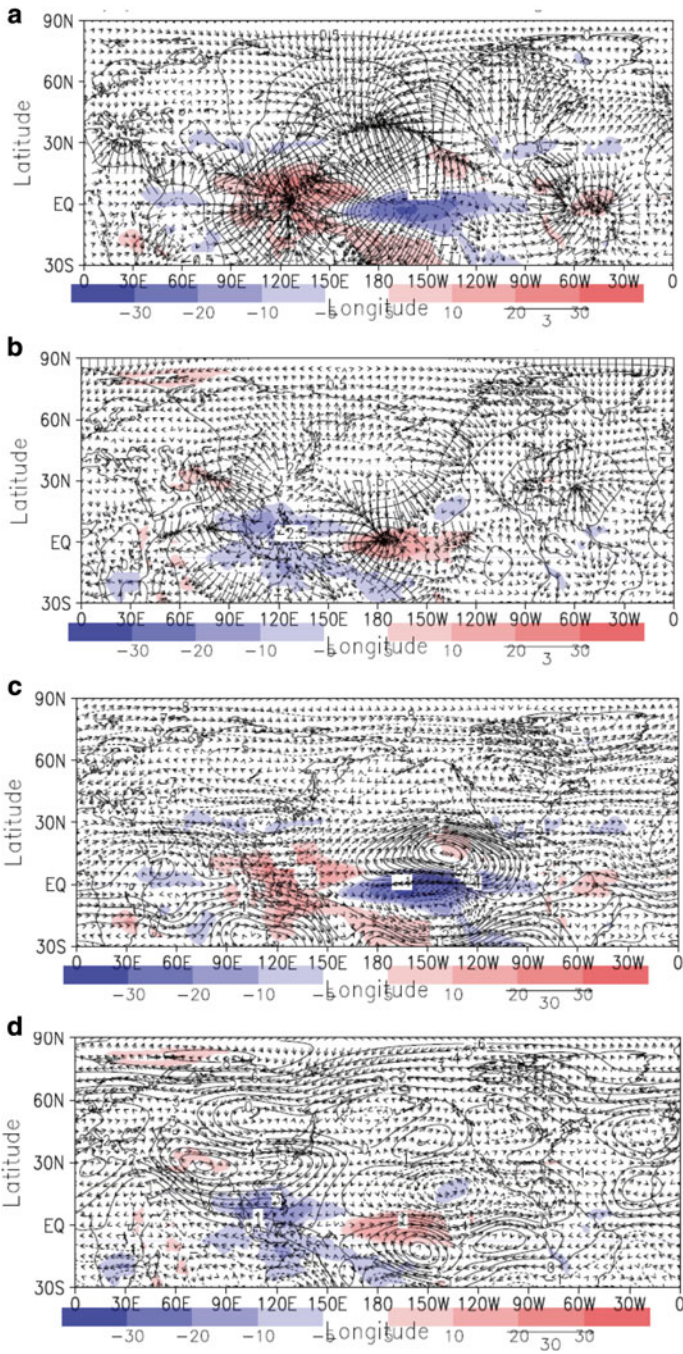
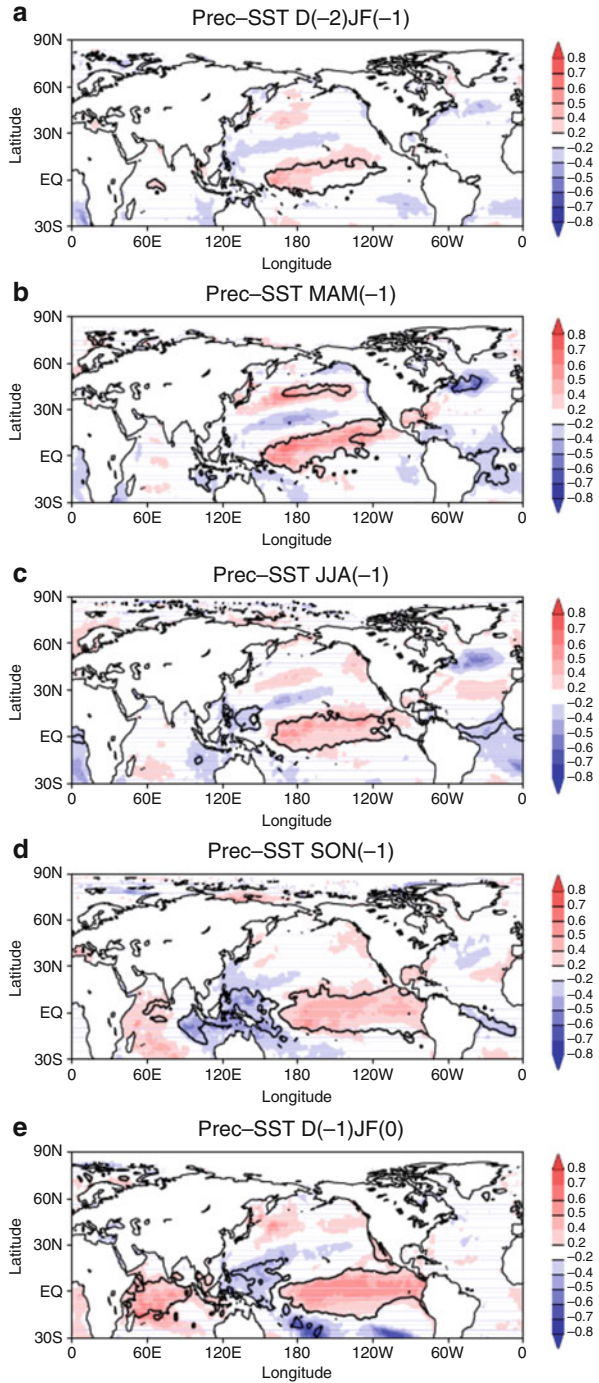


Fig. 4.4 Seasonal anomalous velocity potential ($\times 1e-6$ m²/s; contour) with corresponding anomalous divergent wind (m/s; arrow) at $\sigma=0.1682$ and anomalous outgoing longwave radiation (W/m²; shade) for (a) wet and (b) dry year composites and seasonal anomalous stream function ($\times 1e-6$ m²/s; contour) with corresponding anomalous rotational wind (m/s; arrow) at $\sigma=0.1682$ and anomalous outgoing longwave radiation (W/m²; shade) for (c) wet and (d) dry year composites

Fig. 4.5 Correlation between 28 years (1980–2007) area averaged winter precipitation $-D(-1)$ JF(0) – (mm/d) with sea surface temperature ($^{\circ}$ C) during (a) D(-2)JF(-1) (b) MAM(-1) (c) JJA(-1) (d) SON(-1) and (e) D(-1) JF(0). (Figures in bracket correspond to sea surface temperature with previous and corresponding seasons). Region within contour corresponds to 99 % significant level

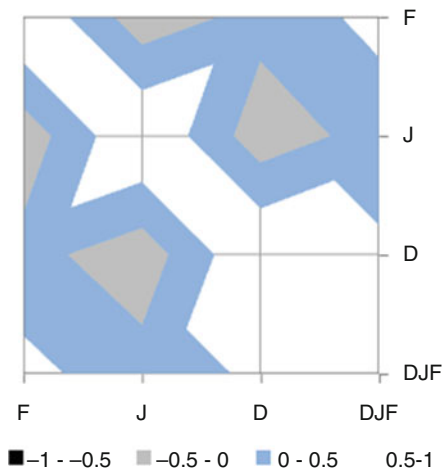


(cooling) is seen already by the previous winter (concurrent summer) season (Fig. 4.5a–e). This significant positive correlation with Indian Ocean warming increases (Fig. 4.5d, e) corresponds to the buildup of the IWM by the previous season (September, October, and November). By winter, equatorial eastern (western) Pacific warming (cooling) with the equatorial Indian-Ocean warming corroborate to create a stronger IWM. Warming over the Indian Ocean enhances the northward gradient for mass transfer and hence increased response of the Hadley cell. This robustness, in tandem with functioning of the enhanced Hadley cell and the attenuated Walker circulation, corresponds to the strengthened increased IWM, which previously was not well known (Oort and Yienger 1996; Mitras and Clement 2005).

4.3 Sub-seasonal Oscillation Associated with the Indian Winter Monsoon

As discussed in the preceding section, monthly (December, January, and February) interannual variabilities in precipitation are positively correlated with the corresponding seasonal (DJF) interannual variability in precipitation, but they are not in phase with each other. January interannual variability is negatively correlated with December and February interannual variabilities (Fig. 4.6). Seasonal (DJF) interannual precipitation variability is positively correlated with individual monthly interannual precipitation variability (0.60 for December, 0.20 for January, and 0.65 for February: Fig. 4.6). December and February show a higher degree of correlation than does January. It was found, however, that monthly anomalous interannual variabilities in the winter months (December, January, and February) were negatively correlated with one another. January interannual variability was negatively correlated with interannual variability in December (−0.29) and February (−0.30). ENSO

Fig. 4.6 Correlation between seasonal (DJF) and monthly (Dec, Jan, and Feb) interannual precipitation variability based on APHRODITE



forcing has a similar behavior during the whole season (DJF), and thus the reason that the January interannual variability is opposite to that of December and February is unclear. To address this question, a seasonal and monthly composite analysis for selected extreme precipitation years is performed to explain it further during the IWM. In the following paragraphs, discussion of the linkages of the IWM with global and local forcings to determine the reasons for the contrasting behavior of monthly interannual variabilities is presented.

4.3.1 Wet and Dry Winters over the WH and Its Associated Circulation

Initially, the corresponding composite monthly anomalous precipitation distribution during wet (Fig. 4.7a, b, and c) and dry (Fig. 4.7d, e, and f) years was analyzed. To remove the effect of inadequate in situ observations from the observational reanalysis, field masking with a 10 mm/month threshold was employed. The result indicates that January anomalous precipitation is reduced (enhanced) more during wet (dry) years (see Fig. 4.7b, e) than in December (Fig. 4.7a, d), and February (Fig. 4.7c, f). The January composite precipitation for wet (dry) years shows less (more) precipitation than the December and February values. In the case of composite precipitation for dry years, January shows a relatively higher anomalous precipitation when compared with December and February. Such contrasting sub-seasonal behavior during IWM is presented, deliberated and a rationale for such patterns and associated variability is developed.

During extreme winter, significant anomalous cyclonic circulation associated with the IWM exists over the Himalayas due to suppressed convection over the western equatorial tropical Pacific (Kawamura 1998; Dimri 2012, 2013a). To assess this dynamical role during the excess and deficit IWM, Fig. 4.8 presents wet-minus-dry composites at the 200 hPa height (contours) and wind (vector) for December (Fig. 4.8a), January (Fig. 4.8b), and February (Fig. 4.8c), respectively. The hatched region corresponds to a $\geq 95\%$ significance level. Similarly, only wind data at the $\geq 95\%$ significance level is shown. Broad differences between the wet and dry monthly composites indicate that, in the upper troposphere, a significant anomalous cyclonic circulation extending up to the South China Sea prevails over the Himalayas during December and February, which weakens during January and is not significant. Another anomalous anticyclonic circulation located over the Siberian region during December weakens and becomes more elongated during January and shifts northward during February. During January, a well-defined anomalous anticyclonic circulation exists over the North African region to the west of the Himalayas. Corresponding wind fields suggest that, over the north Himalayas/Tibetan Plateau, slower westerlies prevail during wet years. In particular, slower westerlies dominate during December and February. In the mid-troposphere, at 500 hPa, anomalous cyclonic circulation over and around the WH prevails during December and January

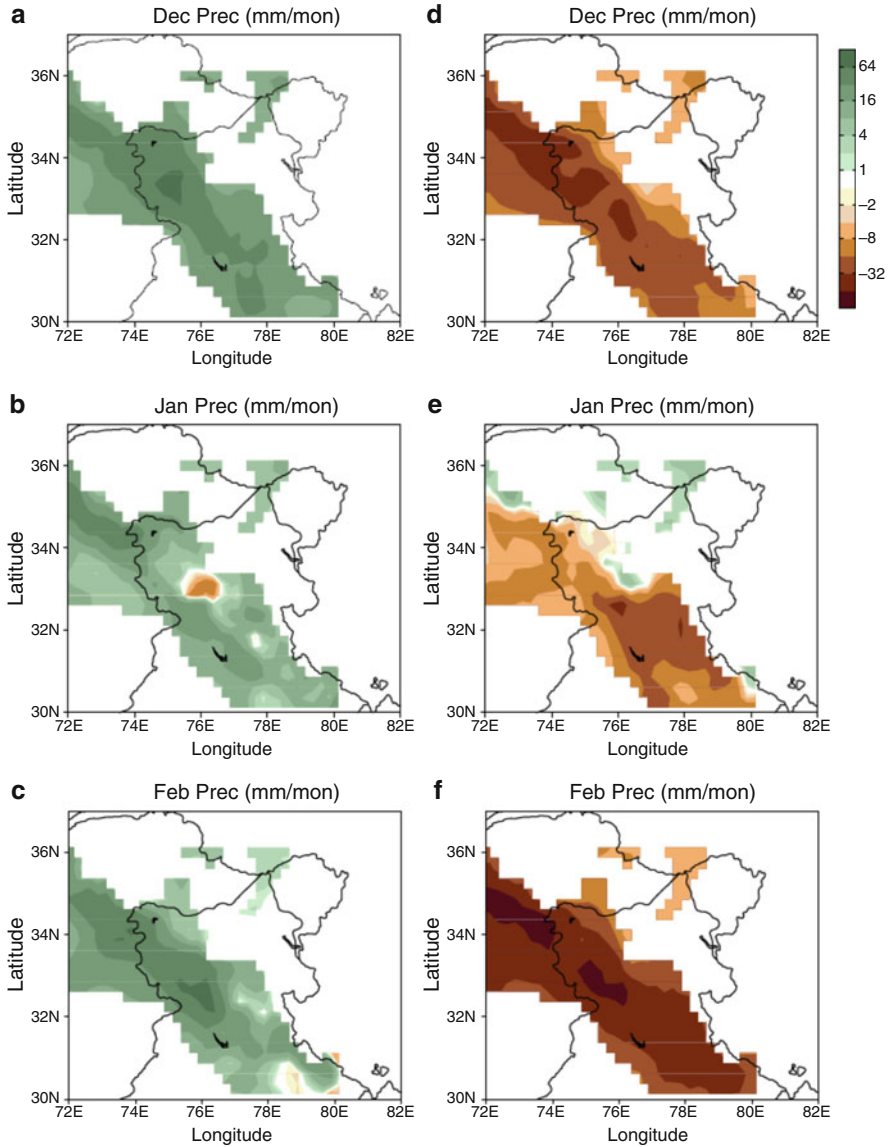


Fig. 4.7 Cumulative average monthly anomalous precipitation (mm/month) during wet composites of (a) Dec, (b) Jan, and (c) Feb and for dry composites of (d) Dec, (e) Jan, and (f) Feb. Masking with 10 mm/month was employed

(data not shown). Detailed scrutiny indicates that, during December, an elongated significant anomalous cyclonic circulation spreads over the west of the Himalayan region and then decays during January. However, an anomalous anticyclonic circulation over the Caspian Sea region prevails, which strengthens during January and

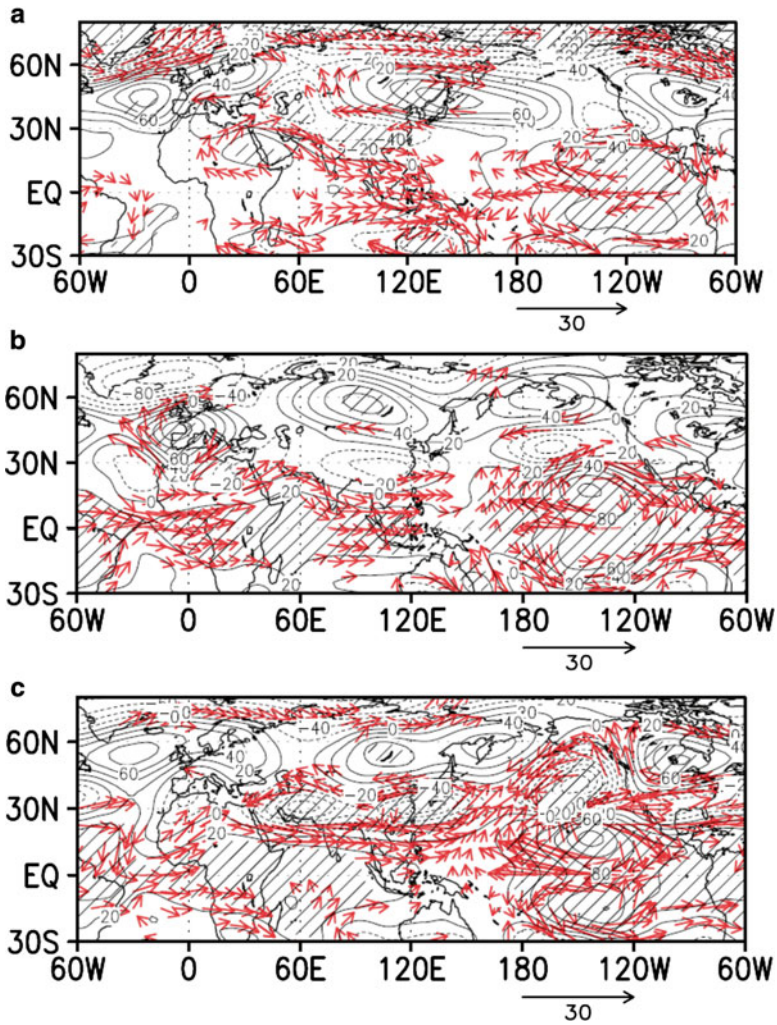


Fig. 4.8 Monthly difference in (wet–dry) anomaly for 200 hPa geopotential height (hPa, *contour*) and wind vector (ms^{-1} , *arrow*) for (a) Dec, (b) Jan, and (c) Feb. The hatched region corresponds to $\geq 95\%$. Similarly, only winds with 95% significance and above are shown

becomes an anomalous cyclonic circulation during February. It was observed that during January, the anomalous cyclonic circulation weakens over the Himalayas, in contrast to the situation observed during December and February. Corresponding significant wind data indicates that winds over the equatorial Indian Ocean, which are slower westerlies during December, are almost neutral during January and then become faster during February. In addition, northward propagation weakens during January. In the lower troposphere, at 850 hPa, stronger northwest wind propagation dominates during December and February, becoming almost neutral during January

(data not shown). This propagation at the surface, arising from moisture-flux transport from the equatorial Indian Ocean to the WH, strengthens the IWM during December and February more than during January.

Corresponding air-temperature conditions associated with the IWM illustrates the upper tropospheric wet-minus-dry composite air temperature distribution (data not shown). It can be clearly observed that January is much warmer over the Himalayas than December and February during wet seasons. This anomalous warming during January may be due to the presence of anomalous anticyclonic circulation, which in the process reduces flux exchanges from northern winter currents. This anomalous warming during January may contribute to a weakening of cyclonic formation in the sub-seasonal phase. At the mid-tropospheric level (data not shown), January also exhibits an anomalous warming over the Himalayan region, greater than that during December and February. Similarly, in the lower troposphere, at 850 hPa (data not shown), significant cooling occurs over the head of the Arabian Sea and the entire Indian subcontinent during December and February, in contrast to the relative warming observed during January.

To analyse the associated convection on the global scale, Fig. 4.9 illustrates the anomalous OLR for wet-minus-dry-month composites. The resulting OLR distribution shows a negative OLR (strong convection) over the eastern equatorial Pacific Ocean, a positive OLR (weak convection) over the western equatorial Pacific Ocean, and a negative OLR (strong convection) over the Indian Ocean. This distribution of OLR is related to warming (cooling) of the eastern (western) equatorial Pacific Ocean linked with El Niño. During the positive phase of El Niño, enhanced warming is associated with strong convection and hence enhanced cloud cover over the eastern equatorial Pacific region, whereas suppressed convection occurs over the western equatorial Pacific region due to anomalous cooling. This suppressed convection over the western equatorial Pacific Ocean generates increased anomalous cyclonic circulation over the Himalayan region due to the Rossby response (Kawamura 1998; Dimri 2013a). Convection associated with attenuated Walker circulation over the eastern equatorial Pacific Ocean remains similar during all 3 months, but convection is suppressed over the western equatorial Pacific Ocean, and convection over the equatorial Indian Ocean weakens more during January than during December and February. The Indian Ocean exhibits higher convection during December and February, which does not occur during January. The increased convection over the Indian Ocean is mainly suppressed by low-level clouds during the IWM (Bony et al. 2000). This stronger heating during December and February compared with January (around $\sim 60\text{--}70^\circ\text{E}$) enhances the Hadley circulation during December and February compared to January (Tanaka et al. 2004), along with an attenuated Walker circulation (Kawamura 1998). This increased Hadley circulation provides a greater mass transport from the Southern to Northern Hemisphere during December and February when compared to January.

Corresponding monthly moisture fluxes (wet–dry) and divergence were analysed to establish the repercussion of the dynamics discussed above. It depicts the enhanced convergence over the WH associated with the IWM during December, which almost becomes neutral during January and then shows higher convergence

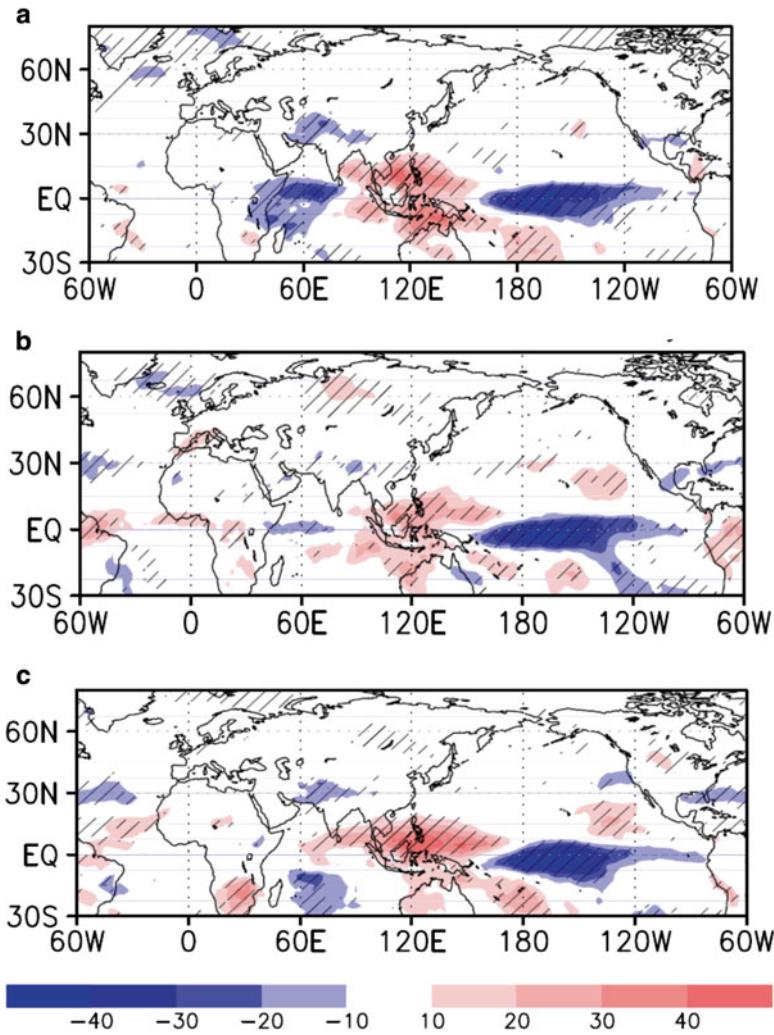


Fig. 4.9 Same as Fig. 4.8, but for outgoing longwave radiation (W/m^2 ; shaded)

during February. Stronger anomalous southwesterly moisture fluxes transport moisture from the equatorial Indian Ocean to the Himalayan region (Dimri 2007). During January, this flow weakens and becomes anomalously high over the Arabian Sea. To investigate this further, Fig. 4.10 illustrates the longitudinal–vertical cross-sectional distribution of anomalous meridional transport at $30^\circ N$ during wet (Fig. 4.10a, b, and c) and dry (Fig. 4.10d, e, and f) months. It can be clearly seen that wet conditions in December and February result in higher meridional moisture flux, which weakens during January particularly beyond $75^\circ E$ and in the lower troposphere. During dry composites, the opposite is seen.

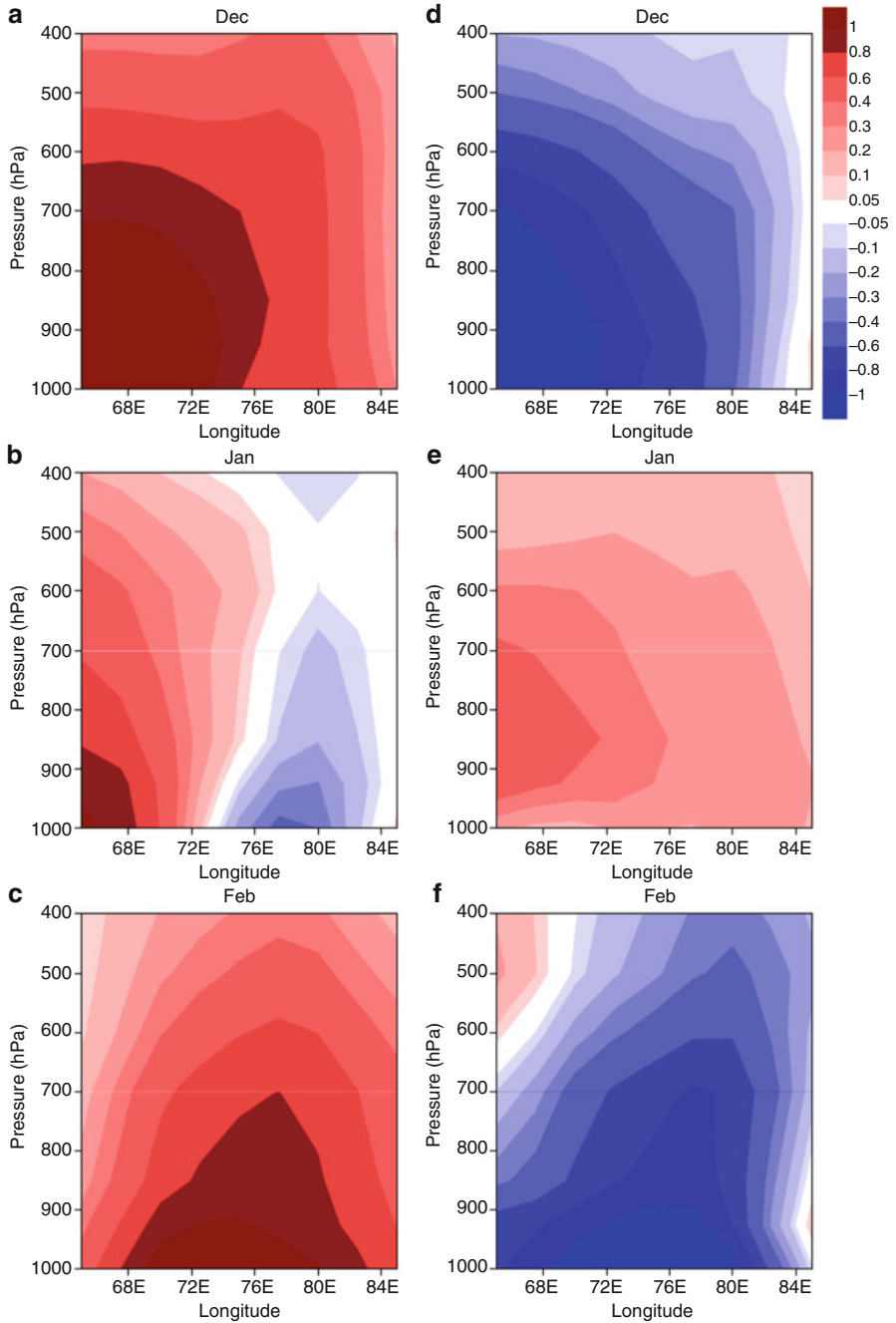


Fig. 4.10 Longitude–pressure vertical cross section at 30°N of the anomalous meridional moisture flux (kg/m/s) during wet ((a), (b), and (c)) and dry ((d), (e), and (f)) composites of Dec, Jan, and Feb, respectively

During an El-Niño phase, symmetric circulations over the equatorial Pacific Ocean, anticyclonic in the Northern Hemisphere and cyclonic in the Southern Hemisphere start building up in December and peak in February. The response from the IWM is similar throughout the winter. For the whole winter season (DJF), the IWM remains in phase with these when compared to January. The anomalous lower precipitation during January is influenced by sub-seasonal oscillations within the IWM. The discussion above suggests that warming/cooling of the Indian Ocean basin seems to be the dominant effect in defining sub-seasonal behavior during the IWM.

4.3.2 Large-Scale Global and Local Forcings

To determine large-scale global forcing, first the correlation of monthly winter precipitation over the WH with the concurrent and preceding months' sea-surface temperature (data not shown) for 28 years (1980–2007) was studied. The correlation of December and February monthly winter precipitation over the WH with the concurrent month's sea-surface temperature reveals similar patterns. Both were positively (negatively) correlated with the eastern (western) equatorial Pacific Ocean and the equatorial Indian Ocean sea-surface temperatures. This suggests that the eastern (western) equatorial Pacific Ocean warming (cooling) during December and February is in phase with the increased precipitation over the WH. For January, no significant correlation exists. Rather January precipitation is negatively correlated with the equatorial Indian Ocean sea-surface temperature for the preceding December, whereas February precipitation is strongly and positively correlated with equatorial Indian and western equatorial Pacific Ocean sea-surface temperatures for December and January. These results suggest that warming (cooling) over the eastern (western) equatorial Pacific Ocean influences December and February precipitation more than January precipitation. The Indian Ocean warming also influences December and February precipitation opposite to the influence found in January. A similar analysis using 2 m surface-air temperatures shows that January precipitation is influenced more by the preceding December surface-air temperature (data not shown). A correlation between January precipitation and December 2 m-surface temperature indicates that the preceding month's cooling over the equatorial Indian Ocean and the warming west of the WH provides conditions conducive to higher precipitation. December cooling over the north equatorial Pacific Ocean also corresponds to higher precipitation. A similar analysis using February precipitation and January temperature data produced opposite correlations. In this case, the equatorial Indian Ocean warming and the western (eastern) equatorial Pacific Ocean cooling (warming) were positively and strongly correlated. This may be attributed to the fact that, during the wet phase, January precipitation is controlled more strongly by the Indian Ocean temperature patterns, by local forcing over the WH region, or by both, and contrasts with conditions during December and February.

To further investigate the role of air temperature in controlling precipitation, anomalous air temperatures averaged over the WH region in wet and dry monthly composites are presented in Fig. 4.11a, b, respectively. During the wet phase, December and February temperatures show cooling (warming) in the middle (upper) troposphere. This is in contrast to January, when warming (cooling) takes place in the middle (upper) troposphere. January remains warmer (colder) in the middle (upper) troposphere than in December and February. Also, almost similar vertical temperature distributions from the surface to the mid-troposphere are seen during January. In the case of dry years, December and February remain warmer (colder) than January from the middle to upper (lower) troposphere. In wet and dry phases, both December and February show similar vertical distributions of air temperature compared with January. Such a distribution leads to the warmer mid-atmosphere during January. The WH area-averaged anomalous 2 m surface-air temperatures and anomalous precipitation for wet and dry years are shown in Fig. 4.11c, d. These data show that if the preceding month's surface temperature increases (decreases),

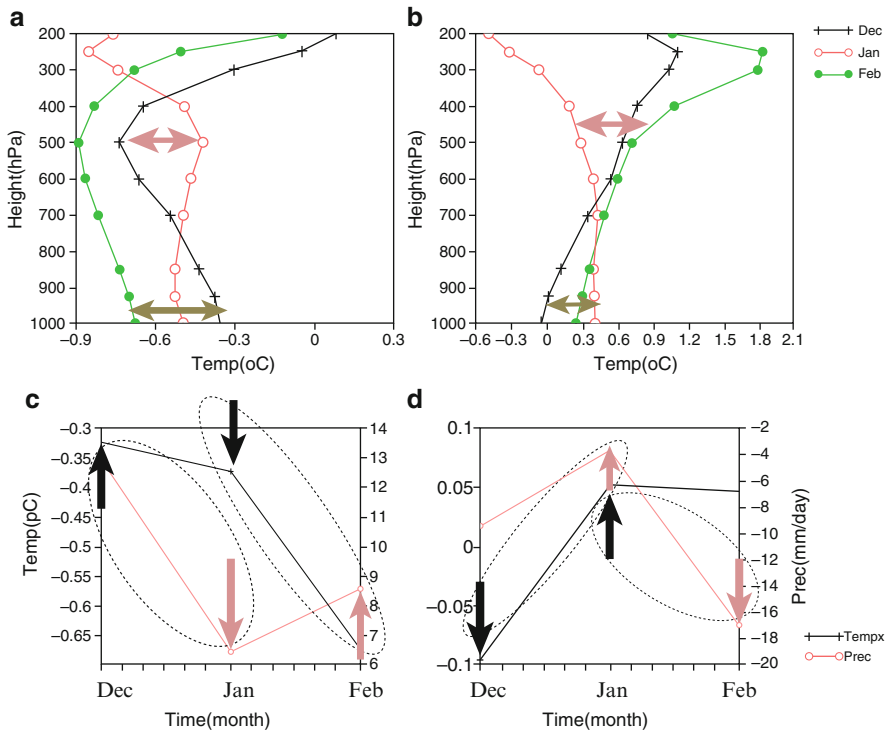


Fig. 4.11 Area-averaged (30°N 72°E to 37°N 82°E) vertical cross-sectional distribution of anomalous air temperature ($^{\circ}\text{C}$) in (a) wet and (b) dry composites for Dec (black line), Jan (red line), and Feb (green line) and area-averaged (30°N 72°E to 37°N 82°E) anomalous 2-m surface-air temperature (black line; $^{\circ}\text{C}$) and anomalous precipitation (mm/day) during (c) wet and (d) dry year composites of Dec, Jan, and Feb

the succeeding month's precipitation decreases (increases). Based on such an observation, a hypothesis is proposed that the preceding month's surface forcing also affects the succeeding month's precipitation. This hypothesis still needs to be studied in detail; however it is clear that sub-seasonal oscillations are observed in the IWM.

4.4 Intraseasonal Oscillation Associated with the Indian Winter Monsoon

Here robust features of the ISOs of the IWM and associated atmospheric circulation patterns are discussed. 28 years The WH daily precipitation (hereafter WHDP) (see bar), corresponding pentad climatology (see black curve with open circles) and 7–25-day filtered precipitation (see red curve with open circles) are shown in Fig. 4.12a. The ISO on sub-monthly timescales with active and break peaks is seen. Defined active (break) peak phases are considered which exceeded above (below) the 28-winter climatological 0.5 standard deviation in the 7–25-day WHDP anomalies. On doing so, 140 active and 119 break peak phases are identified. To investigate the temporal relationship of WHDP variability, circulation fields, OLR composites and daily time-lag composites were used.

Using the fast Fourier transform (FFT), the dominant mode of the ISO in the WHDP during the 28 winters was seen. WHDP (the first three harmonics of the annual cycle were removed) is detrended and masked from 15 November to 15 March (120 days) (Dimri 2013a, b). Figure 4.12b, c shows the FFT spectrum for the WHDP for 28 winters. A pronounced periodic ~16-day peak with a 95 % statistical significance appears (Fig. 4.12b). The corresponding Fig. 4.12c presents 28 years' power spectrum of IAV of the WHDP showing approximately a 16-day period scale in each year. This corresponds closely with the ensemble spectrum (Fig. 4.12b) at a sub-monthly-scale. Hence analysis of ISO mode of ~7–25 days-periodicity in the WHDP is proposed.

The sub-monthly scale pace-time structure of atmospheric circulation and convection in composites of active and break phases is investigated. Total 140 active- and 119 break-peak phases are chosen out of 28 years of climatology. A daily-lag composite of vertically integrated moisture flux and divergence from day –8 to day +8, based on the 7–25-day precipitation variation over the WH, is presented in Fig. 4.13. Day 0 corresponds to active precipitation-peak phases and day –8 and day +8 corresponds to break-peak phases. This cycle corresponds to a composite variation of 16 days. A peak-break phase is characterized by divergence over the WH with moisture exiting out of the region. On day –6, convergence builds up over the Arabian Sea near the Gujarat coast with fluxes still exiting out from the WH. On subsequent day –4, subtle changes in flux direction with shift in convergence zone towards the Himalayas is observed. Crucial flow transfer starts by this time with two breakaway streams. First one flows into the WH as the second move farther out

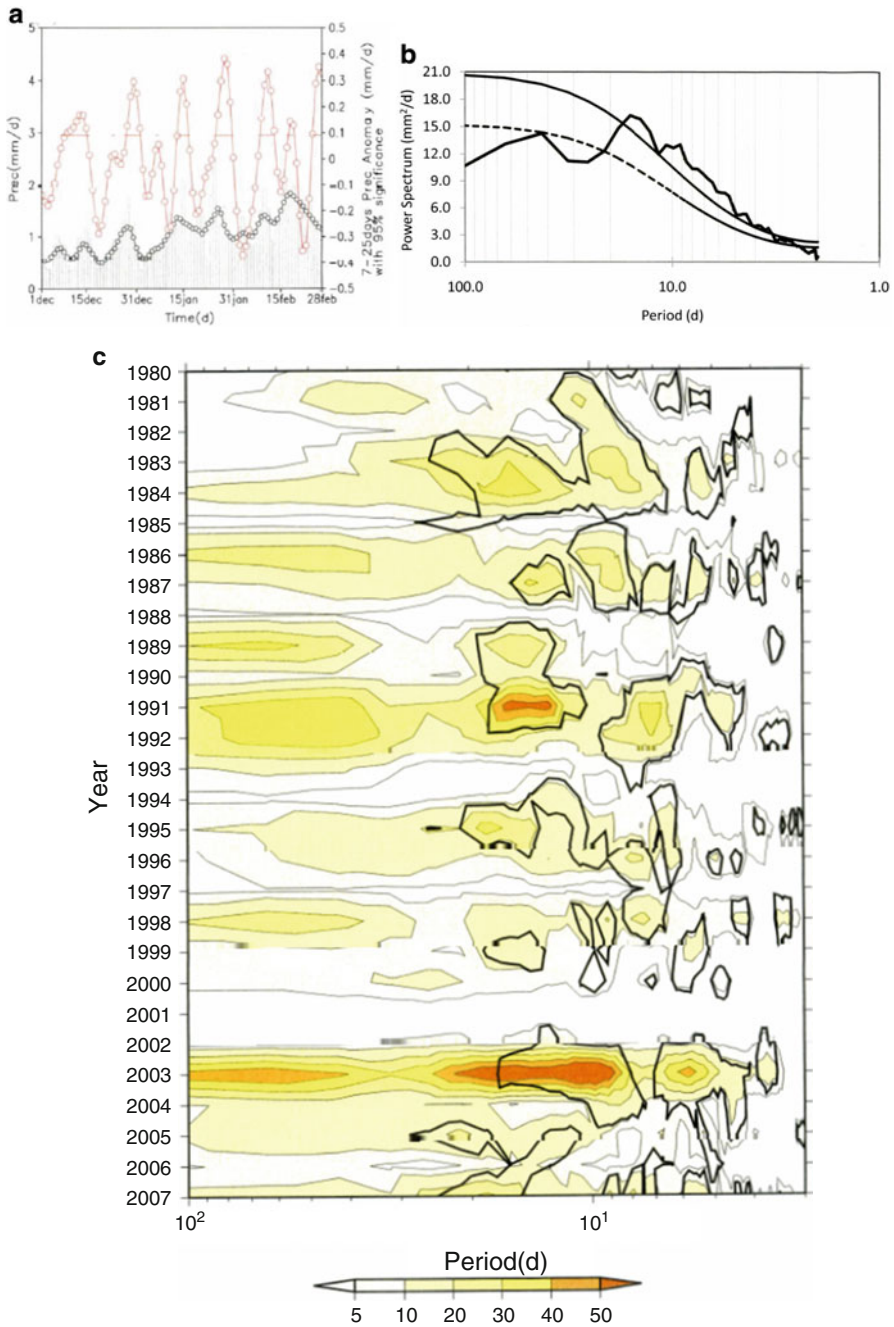


Fig. 4.12 (a) Based on 28 years (Dec 1979, Jan, Feb 1980 to Dec 2006, Jan, Feb 2007) of data, time-series of WHDP climatology (*bar; left axis*), pentad precipitation climatology (*black line with open circles; left axis*), and 7–25-day filtered precipitation anomaly (*red line with open circles; right axis*). The line of 95 % significance is also shown and the period above this corresponds to climatological active phases. (b) The 28-winter (DJF) ensemble spectrum of the WHDP time series from 15 Nov. to 15 Mar. (120 days). A red noise spectrum (*dashed curve*) and its 95 % level of significance (*solid curve*) are also shown. (c) Interannual variation in the WHDP spectrum from 1980–2007. The thick *black solid line* shows the 95 % level of significance

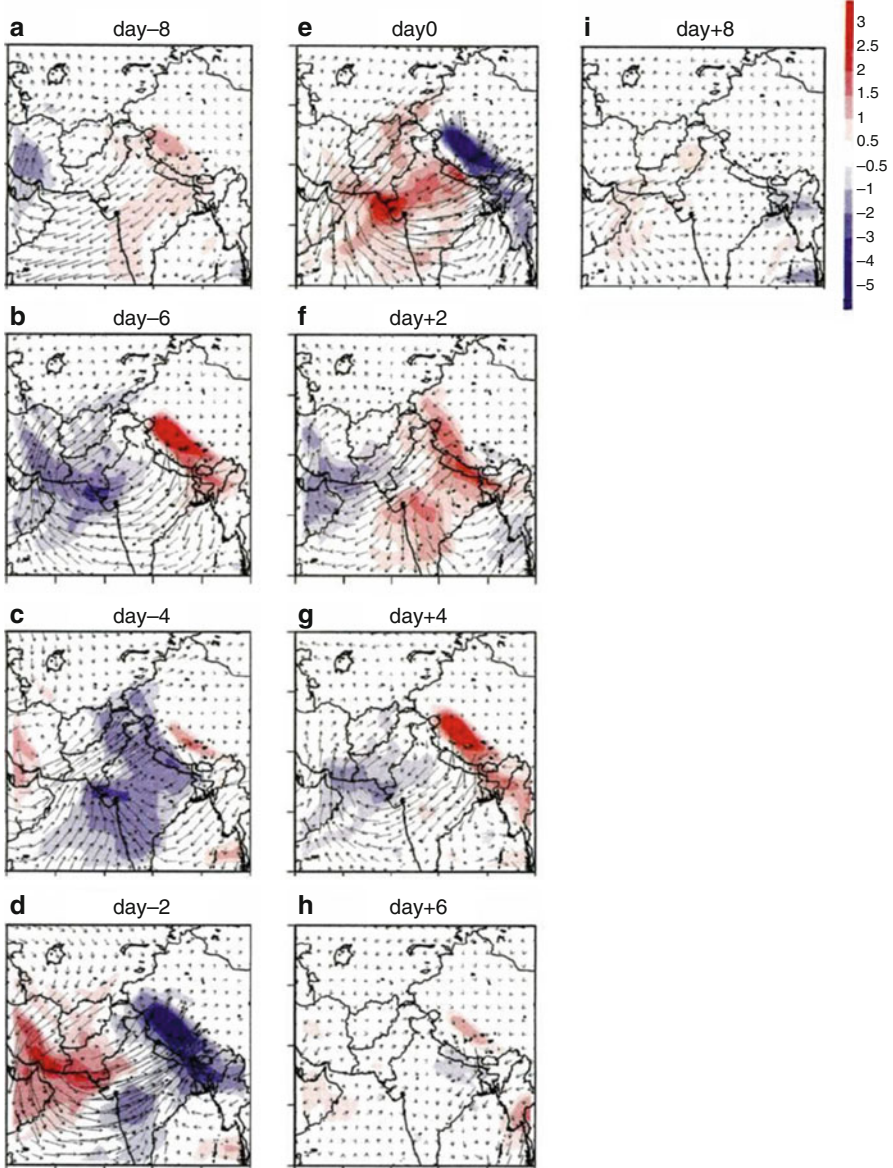


Fig. 4.13 Composite of vertical integrated moisture flux (vector; 40 kg/m/s) and divergence (*shaded*; $\times 10^5/s$) based on 7–25-day filtered values of specific humidity and wind anomalous fields from day –8 to day +8 based on WHDP. Day 0 corresponds to the active peak of 7–25-day WHDP variation. Values above 95 % statistically significant are plotted with *shade*

from the eastern Himalayas. During the precipitation peak in the active phase, well-defined moisture influx with a well-defined convergence zone over the Himalayas sets in. This characteristic weakens on day +2 with increased outflow and divergence over the Himalayas. Such a situation dominates and strengthens in the following days.

Daily-lag composites of 500 hPa stream function and wind from day -8 to day +8 based for 7–25-day precipitation variation over the WH are investigated to establish the character of dynamical atmosphere (Fig. 4.14). An anomalous higher stream function, corresponding to anticyclonic circulation, builds up over the western part of the WH on day -8. This moves eastwards on subsequent days. With this, on day -4, anomalous cyclonic circulation characterized by lower stream-function values develops over Saudi Arabia. Significant winds succeeding (preceding) the anomalous anticyclonic (cyclonic) circulation are seen. This situation of anomalous cyclonic circulation intensified and moved eastward over the Afghanistan and Pakistan region by day -2. Such a situation is as well associated with strong winds. On peak phase, day 0, intense wind located over the WH and adjoining Pakistan region dominate. It is interesting to note that the center of anomalous cyclonic circulation over and near the WH persists for at least 4 days, from day -2 to day +2. Such positioning provides a situation conducive to southwesterly moisture influx from the Arabian Sea during active peak phases. This dominance in association with the WDs' life cycle defines the rationale for higher precipitation in active phases. The Himalayan topography as well weakens, stagnates and/or changes the direction of the southwesterly flow and the significant winds. In the upper troposphere (200 hPa – data not shown), similar structure of the mid-troposphere dominates except that, at this level, a larger and more elongated significant area with significant southwesterly winds preceding the system persists. This vertical distribution of deep cyclonic circulation extends from the mid- to upper-troposphere during the peak active phase. The cascading of anomalous anticyclones and anomalous cyclones persist in the upper troposphere which on subsequent days decay and so on. The upper tropospheric anomalous cyclonic circulation persists longer than that found in the mid-troposphere.

Further OLR distribution from day -8 to day +8 based on the 7–25-day precipitation along with a similar distribution of 500 hPa stream-function and wind as shown in Fig. 4.14 (for better assessment) is illustrated in Fig. 4.15. Increased and faster advancement of the anomalous cyclonic circulation due to suppressed convection dominates over the Himalayan region. This deepens by day -4 and further build up of convection leads to more localized precipitation over the WH. Increased (suppressed) convection ahead (rear) of the anomalous cyclonic circulation is seen. The active peak displays strongest convection ahead of anomalous cyclonic circulation on day 0. Here as well, such a situation is seen occurring in a cascading manner which corresponds to a chain of anomalous cyclonic circulations, followed by another anomalous anticyclonic circulation, and so on.

To understand the periodic occurrences of alternating anomalous anticyclonic and cyclonic circulations and its association with associated precipitation, Fig. 4.16 presents time-lag composites based on 7–25-day active peak phases. It shows evolution

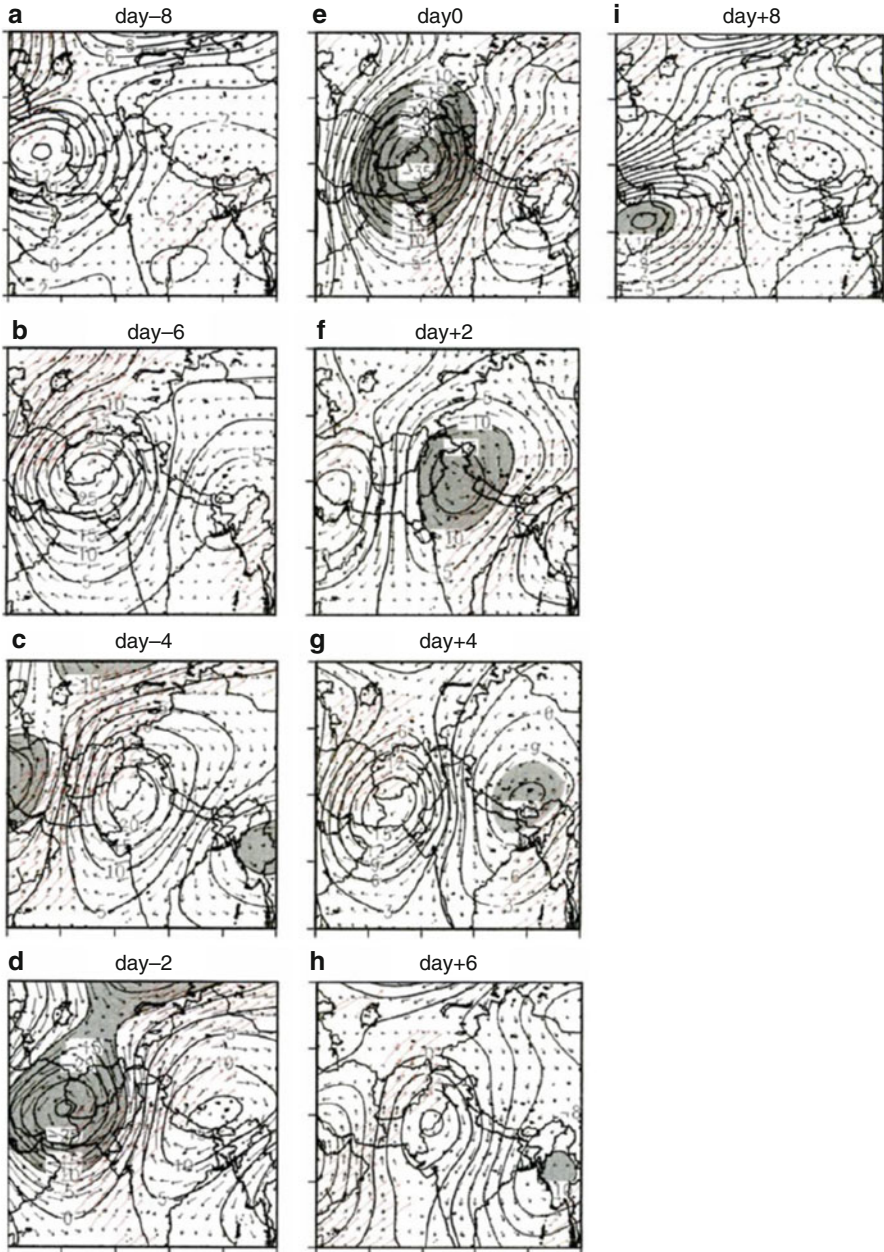


Fig. 4.14 Composite of 7–25-day filtered 500 hPa streamfunction ($\times 10^{-6} \text{ m}^2/\text{s}$) and wind (m/s) anomalies from day –8 to day +8 based on WHDP. Day 0 corresponds to the active peak of 7–25-day WHDP variation. The contour interval for streamfunction is $5 \times 10^{-6} \text{ m}^2/\text{s}$, and the 95 % statistically significant streamfunction is shaded. The strength of the wind vector is 15 m/s, and the 95 % statistically significant wind is plotted with red color

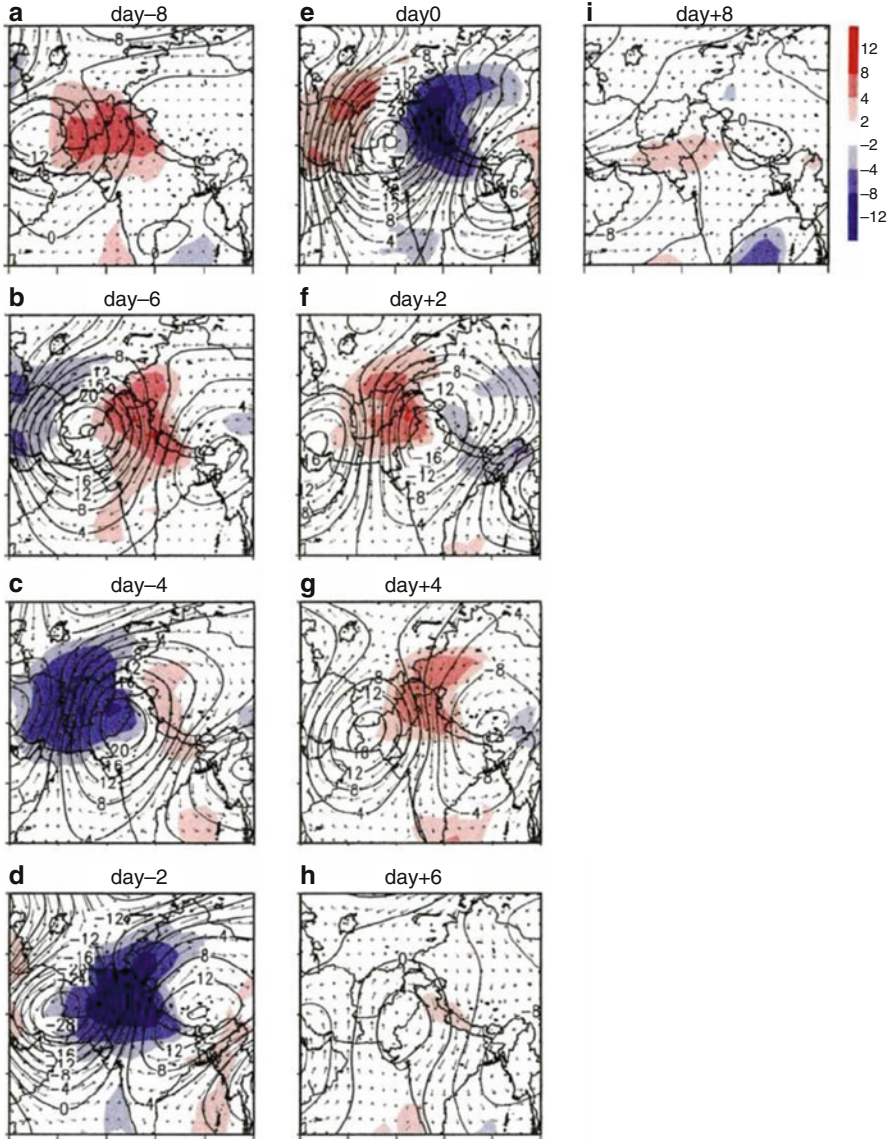


Fig. 4.15 Composite of 7–25-day filtered OLR (W/m^2 ; *shade*), 500 hPa streamfunction ($\times 10^{-6} m^2/s$), and wind (m/s) anomalies from day -8 to day +8 based on WHDP. Day 0 corresponds to the active peak of 7–25-day WHDP variation. The contour interval for streamfunction is $4 \times 10^{-6} m^2/s$. The strength of the wind vector is 5 m/s

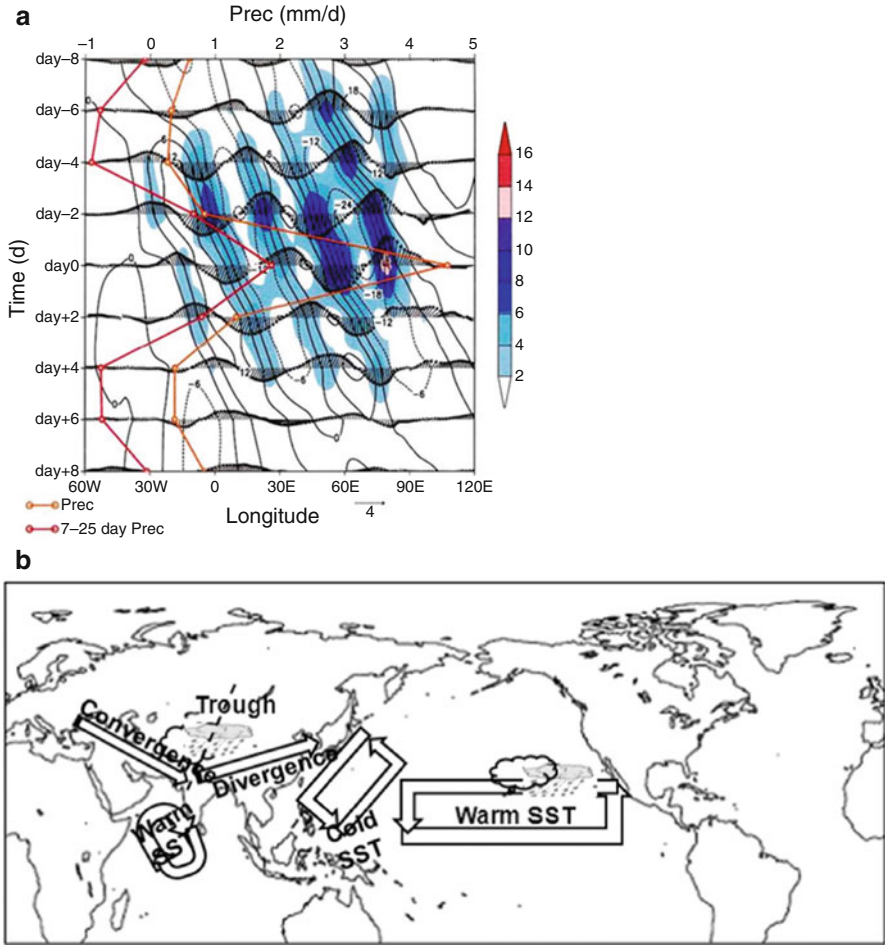


Fig. 4.16 Time-longitude cross-sectional distribution at 35°N of composites for 7–25-day filtered OLR (W/m^2 ; shade), 500 hPa height (hPa; contour), 500 hPa wind (m/s; arrow), and precipitation (mm/d; red curve; upper axis) anomalies from day –8 to day +8 based on WHDP. Day 0 corresponds to the active peak of 7–25-day WHDP variation. The yellow curve corresponds to anomalous precipitation (mm/d; yellow curve; upper axis) from day –8 to day +8 based on WHDP and (b) Schematic representation of physical mechanism associated with enhanced IWM during ENSO phases

of cyclonic systems which is in correspondence with the life cycle of the WDs. This conformity of WDs as a “family,” with one following the other in a symmetric wave which peaks at day 0, followed by subsequent decay, is associated with its precipitation distribution as well. Associated convection and corresponding 500 hPa height indicate the evolution of the storm by day –6 and/or day –4 with peaking by day 0. Wind distribution shows symmetrical in phase movement associated with each peaking cyclonic storm. Primarily WDs moves as a ‘family’ – a set of a number of evolu-

ing and decaying WDs - in periodic occurrences of alternating anomalous anticyclonic and cyclonic circulations. Such a traveling pattern forms a kind of wave structure. Figure 4.16a shows time-travel composites based on 28 years of data (1980–2008) for active WD peak phases. Here a very clear evolution of WD with time is seen. 'Family' structure – evolution and decay – in a phased manner in which one WD following the other in a symmetric wave followed by decay is seen. Such evolution associated with an outgoing long-wave corresponding to convection starts building up by day –6 and peaked on day 0. At 500 hPa, corresponding anomalous geopotential height depicts WD intensification starts by day –6 and/or day –4 which peak by day 0. Here as well, we see symmetrical phase movement associated with each WD at 500 hPa wind. Every WD peaked in a similar phase of wind. Associated precipitation is highest on day 0, and this shows the corroborative correspondence of its distribution as per the WD evolution and decay. This baroclinic structure is a dominant mechanism for storm intensification during storms evolution (Dimri 2013b).

To analyse the significant coupling with the SWJ during winter conditions and explicitly during enhance ENSO, warming over equatorial central/eastern Pacific and Indian Ocean provides attenuated Walker circulation. This warm episode over equatorial Pacific corresponding to the attenuated Walker circulation creates conditions for the SWJ to move southwards (Kawamura 1998; Dimri 2013a, b). In addition, significant cooling with an extension over eastern Pacific Ocean provides north–south gradient (Webster et al. 1998) provide a physical mechanism for an intense IWM over the WH (Fig. 4.16b). Such response produces anomalous WD evolution in the west of the WH. This significant cooling and convective heating over the equator results in the Rossby type of response. These two processes of increased convection over tropical Indian Ocean and anomalous WDs establish a strengthening Hadley circulation. In such provisioning, large scale meridional transport due to ascending atmospheric motion over the tropical Indian Ocean and descending motion over the west of Himalayan region become established. This coupling provides more moisture intake from the southern latitudes and which substantially adds moisture to the anomalous WDs and hence increases associated precipitation. Thus vertical baroclinic response over the Himalayan region provides more suitable condition for genesis/intensification of cyclonic storms (Fig. 4.16a) during wet conditions (Kawamura 1998). Therefore, such baroclinic response assists intensification of WDs and hence increases associated precipitation during wet years. This physical mechanism as well shows significant southward shifting of the SWJ over south Asian regions associated with deepening of northwesterly flow immediately west of northern India. Such situations are conducive to enhanced cold surges. As discussed, attenuated Walker circulation associated with El-Niño conditions and strengthened Hadley circulation due to asymmetric meridional upper tropospheric flow from the Southern Hemisphere to the Northern Hemisphere with strengthening of Hadley circulation work in tandem to push the SWJ southwards and help in providing moisture to evolved WDs. Such stationary wave-phase formation in the mid-troposphere provides suitable conditions for genesis/intensification of WDs/troughs. Also, vertical structure from the lower to the upper troposphere strengthens the formation of such synoptic weather resulting in higher precipitation over the WH.

A physical mechanism of interannual variability associated with the IWM during wet years shows significant southward shift of the SWJ over south Asian regions. It manifests in a deepening of the northwesterly incoming flow over the northern Indian region. This situation is favorable for enhanced cold surges associated with WDs. Increased convection over the central equatorial Pacific region corresponds to higher convection and hence attenuated Walker circulation. In tandem with it, a strengthened Hadley Cell causing asymmetric meridional upper tropospheric flow from the Southern to Northern Hemisphere forms a stationary wave in the mid-troposphere. This situation supports genesis/intensification of WDs/troughs consisting of more frontal systems. Such a situation corresponds to higher precipitation over the WH. Although the interannual variability of individual months is in phase with seasonal interannual variability, the interannual variability of individual months is not in phase with other months. A positive ENSO phase corresponds to a southward positioning/shifting of the 200 hPa SWJ. The reduction in January precipitation is influenced by the equatorial Indian-Ocean surface temperature due to the weakening of the Hadley response during January compared to December and/or February. Additionally, comparatively greater middle-tropospheric warming during January enhances the middle tropospheric anticyclone with an increased northerly wind to the east compared to December and February. Such sub-seasonal/bi-monthly oscillations in the IWM correspond to higher precipitation during December and February relative to January. ISO characteristics associated with the WHDP show an average life cycle of approximately 10–12 days of evolution and decay. Dominance of ~16-day periodicity is associated with the WHDP. Correspondingly, a cascading wave train of peaking and decaying of cyclonic storm is observed. In the active peak phase, convective activities in association with westerly to southwesterly enhanced moisture flux dominates and provides higher precipitation. Convection in association with the storm seems to always precede anomalous cyclonic circulation. A succession of cyclonic–anticyclonic–cyclonic, and so on, circulation dominates in the SWJ.

References

- Adler RF, Huffman GJ, Chang A, Ferraro R, Xie P, Januaryowiak J, Rudolf B, Schneider U, Curtis S, Bolvin J, Gruber A, Susskind J, Arkin P (2003) The version 2 global precipitation climatology project (GPCP) monthly precipitation analysis (1979–present). *J Hydrometeorol* 4:1147–1167
- Annamalai H, Hamilton K, Sperber KR (2007) The south Asian summer monsoon and its relationship with ENSO in IPCC AR4 simulations. *J Clim* 20:1071–1092
- Bony S, Collins WD, Fillmore DW (2000) Indian ocean low clouds during the winter monsoon. *J Clim* 13:2028–2043
- Dai J (1990) Climate in the Qinghai-Xizang Plateau (in Chinese). China Meteorol Press, Beijing
- Das S, Singh SV, Rajagopal EN, Gall R (2003) Mesoscale modeling for mountain weather forecasting over the Himalayas. *Bull Am Meteorol Soc* 84:1237–1244
- Dimri AP (2004) Impact of horizontal model resolution and orography on the simulation of a western disturbance and its associated precipitation. *Meteorol Appl* 11:115–127

- Dimri AP (2006) Surface and upper air fields during extreme winter precipitation over the western Himalayas. *Pure Appl Geophys* 163:1679–1698
- Dimri AP (2007) The transport of momentum, sensible heat, potential energy and moisture over the western Himalayas during the winter season. *Theor Appl Climatol* 90(1–2):49–63
- Dimri AP (2012) Relationship between ENSO phases with northwest India winter precipitation. *Int J Climatol* 33(8):1917–1923. doi:[10.1002/joc.3559](https://doi.org/10.1002/joc.3559)
- Dimri AP (2013a) Interannual variability of Indian winter monsoon over the western Himalaya. *Glob Planet Chang* 106:39–50
- Dimri AP (2013b) Intraseasonal oscillation associated with the Indian winter monsoon. *J Geophys Res* 118:1–10
- Dimri AP (2014) Sub-seasonal interannual variability associated with the excess and deficit Indian winter monsoon over the western Himalayas. *Clim Dyn* 42(7–8):1793–1805
- Dimri AP, Mohanty UC (2009) Simulation of mesoscale features associated with intense western disturbances over western Himalayas. *Meteorol Appl* 16:289–308
- Dimri AP, Niyogi D (2012) Regional climate model application at subgrid scale on Indian winter monsoon over the western Himalayas. *Int J Climatol* 33(9):2185–2205
- Dimri AP, Yasunari T, Wiltshire A, Kumar P, Mathison C, Ridley J, Jacob D (2013) Application of regional climate models to the Indian winter monsoon over the western Himalayas. *Sci Total Environ*. <http://dx.doi.org/10.1016/j.scitotenv.2013.01.040>
- Duchon CE (1979) Lanczos filtering in one and two dimensions. *J Appl Meteorol* 18:1016–1022
- Goswami BN, Mohan RSA (2001) Intraseasonal oscillations and interannual variability of the Indian summer monsoon. *J Clim* 14:1180–1198
- Hadley Centre (2006) HadiSST 1.1 global sea-ice coverage and SST (1870-present). British atmospheric Data Centre. <http://badc.nerc.ac.uk/data/hadisst>
- Hartmann DL, Michelsen ML (1989) Intraseasonal periodicities in Indian rainfall. *J Atmos Sci* 46:2838–2862
- Hoyos CD, Webster PJ (2007) The role of intraseasonal variability in the nature of Asian monsoon precipitation. *J Clim* 20:4402–4424
- Kanamitsu M, Ebisuzaki W, Woollen J, Yang S–K, Hnilo JJ, Fiorino M, Potter GL (2002) NCEP–DEO AMIP-II reanalysis (R-2). *Bull Am Meteorol Soc* 83(11):1631–1643
- Kawamura R (1998) A possible mechanism of the Asian summer monsoon–ENSO coupling. *J Meteorol Soc Jpn* 76:1009–1027
- Kripalani RH, Kumar P (2004) Northeast monsoon rainfall variability over south peninsular India vis-à-vis Indian ocean dipole mode. *Int J Climatol* 24:1267–1282
- KrishnaKumar K, Rajagopalan B, Cane MA (1999) On the weakening relationship between the Indian monsoon and ENSO. *Science* 284(5423):2156–2159
- KrishnaKumar K, Rajagopalan B, Hoerling M, Bates G, Cane MA (2006) Unraveling the mystery of Indian monsoon failure during El Niño. *Science* 314(5796):115–119
- Kumar P, Rupakumar K, Rajeevan M, Sahai AK (2007) On the recent strengthening of the relationship between ENSO and northeast monsoon rainfall over South Asia. *Clim Dyn* 28:649–660
- Laat ATJ, Lelieveld J (2002) Interannual variability of the Indian winter monsoon circulation and consequences for pollution levels. *J Geophys Res* 107(D24):4739. doi:[10.1029/2001JD001483](https://doi.org/10.1029/2001JD001483)
- Lang TJ, Barros AP (2004) Winter storms in central Himalayas. *J Meteorol Soc Jpn* 82(3):829–844
- Liebmann B, Smith CA (1996) Description of complete (interpolated) outgoing longwave radiation dataset. *Bull Am Meteorol Soc* 77:1275–1277
- Mitas CM, Clement A (2005) Has the Hadley cell been strengthening in recent decades? *Geophys Res Lett* 32. doi:[10.1029/2004GL021765](https://doi.org/10.1029/2004GL021765)
- New MG, Hulme M, Jones PD (2000) Representing twentieth century space time climate variability, part II: development of a 1901–96 monthly grids of terrestrial surface climate. *J Clim* 13:2217–2238
- Oort AH, Yienger JJ (1996) Observed interannual variability in the Hadley circulation and its connection to ENSO. *J Clim* 9(11):2751–2767

- Raman CRV, Maliekal JA (1985) A northern oscillation relating northern hemispheric pressure anomalies and the Indian summer monsoon? *Nature* 314:430–432
- Rudolf B, Beck C, Grieser J, Schneider U (2005) Global precipitation analysis products. Global Precipitation Climatology Centre (GPCC), DWD, Internet publication, pp 1–8
- Saha SK, Halder S, KrishnaKumar K, Goswami BN (2011) Pre-onset land surface processes and ‘internal’ interannual variabilities of the Indian summer monsoon. *Clim Dyn* 36:2077–2089
- Sato T, Kimura F (2007) How does Tibetan Plateau affect transition of Indian monsoon rainfall? *Mon Weather Rev* 135:2006–2015
- Tanaka HL, Ishizaki N, Kitoh A (2004) Trend and interannual variability of Walker, monsoon and Hadley circulations defined by velocity potential in the upper troposphere. *Tellus* 56A:250–269
- Turner AG, Inness PM, Slingo JM (2007) The effect of double CO₂ and model basic state biases on the monsoon ENSO system. I: mean response and interannual variability. *Q J Roy Meteorol Soc* 133:1143–1157
- Webster PJ, Magana VO, Palmer TN, Shukla J, Tomas RA, Yanai M, Yasunari T (1998) Monsoons: processes, predictability, and the prospects for prediction. *J Geophys Res* 103:14451–14510
- Wu TW, Qian ZA (2003) The relation between the Tibetan winter snow and the Asian summer monsoon and rainfall: an observational investigation. *J Clim* 16(12):2038–2051
- Yadav RK (2012) Why is ENSO influencing India north-east monsoon in the recent decades? *Int J Climatol* 32(14):2163–2180. doi:[10.1002/joc.2430](https://doi.org/10.1002/joc.2430)
- Yadav RK, Yoo JH, Kucharski F, Abid MA (2010) Why is ENSO influencing northwest India winter precipitation in recent decades? *J Clim* 23:1979–1993. doi:[10.1175/2009JCLI3202.1](https://doi.org/10.1175/2009JCLI3202.1)
- Yadav RK, Ramu DA, Dimri AP (2013) On the relationship between ENSO patterns and winter precipitation over North and Central India. *Global Planet Change* 107:50–58. doi:[10.1016/j.gloplacha.2013.04.006](https://doi.org/10.1016/j.gloplacha.2013.04.006)
- Yasunari T, Kitoh A, Tokioka T (1991) Local and remote responses to excessive snow mass over Eurasia appearing in the northern spring and summer climate. *J Meteorol Soc Jpn* 69:473–487
- Yatagai A, Kamiguchi K, Arakawa O, Hamada A, Yasutomi N, Kitoh A (2012) APHRODITE: constructing a long term daily gridded precipitation dataset for Asia based on a dense network of rain gauges. *Bull Am Meteorol Soc*. doi:[10.1175/BAMS-D-11-00122.1](https://doi.org/10.1175/BAMS-D-11-00122.1)

Chapter 5

Western Disturbances – Impacts and Climate Change

Abstract The significance of a weather system is usually measured on the basis its impacts. Impacts related to the western disturbances (WDs) have been mentioned briefly in a preceding chapter. Without detailing the impacts of the WDs, one cannot justify the significance of studying the topic. In this chapter, we will discuss in detail the various positive (on the cryosphere and hydrology of the region) and negative (severe weather and natural hazards) impacts of the WDs and how these influence India as a whole. Discussion of the evolution of WDs in the changing climate is also included in the chapter, along with speculation on how a warming climate might affect changes in the direct and indirect impacts of WDs.

Impacts related to the WDs have been mentioned briefly before in a preceding chapter. In this chapter we detail the importance and justify the significance of WDs as measured in form of their impact. This book is focused on the WDs in an Indian parlance as WDs have significant impact on India. Various positive and negative impacts will be discussed in the sub-sections below. Discussion of the evolution of WDs in the changing climate is also included in the chapter, along with speculation on how a warming climate might affect the changes in the direct and indirect impacts of WDs.

5.1 Winter Precipitation and Its Impacts

The winter precipitation is one of the major impacts of the WDs, and the Indian winter monsoon has been discussed in great detail in the previous chapter. So in this chapter dealing with the impacts of WDs, we will not be repeating this impacts of the weather system. Rather we discuss the effects of the winter precipitation due to WDs. Winter season WDs contribute up to 15 % of the precipitation over the north-western region. This precipitation reduces in frequency and intensity southwards and eastwards (Yadav et al. 2012). As mentioned in the first chapter, precipitation can be a resource for life in moderation or be disastrous in extreme cases. In this section, we discuss both the positive as well as the negative consequences related to the WD-related winter precipitation.

Precipitation over a region has a high ecological and environmental impact. These rainfall events render ecological services and help in the maintenance of the regional flora and fauna. Natural ecology is acclimatized to this climatological feature and requires the winter precipitation for its preservation. The economic equivalent of the environmental services performed by the precipitation is unquantifiable. This is not only important in the catchment area but also along the downstream flow. Precipitation is also very important for the agriculture sector. This is especially so in a country like India where the irrigation network is not well developed and the farmers are dependent on natural sources for irrigating their fields. Even in the case of the current irrigational infrastructure, the precipitation always supplements the irrigational requirements. Winter precipitation as rainfall is important for 'rabi' crops or winter crops. In Arabic the term rabi refers to spring, which is when the rabi crop is harvested, but it actually grows in the winter season. Examples of rabi crops are wheat, barley, peas, gram and mustard, which are sown in November and harvested in April (Yadav et al. 2012). The WD-related winter precipitation and the cold and dry winds from the northern side at the rear of WDs maintain the moisture and low -temperature conditions required for the development of these crops, specifically wheat. For the sustenance of the region with high food requirements for the growing population, the winter precipitation is very important for the high yield of these staple crops. Winter rainfall also supplements the land-based water bodies, i.e. the lakes, aquifers and rivers of the region. Thus the precipitation is of utmost important for the ecological health and socio-economic requirements of the Himalayan and Gangetic regions.

Winter precipitation over the region might also occur in the form of snow. The snowfall during winters due to WDs is the source for glacier growth over the mountainous regions of the northern India (Benn and Owen 1998). This snowfall is also significant for the ecology of the region. But mainly the glacier mass-balance maintenance is a very important effect of winter snowfall. The snow line of the western Himalayas is as low as 1500 m and for the eastern Himalayas is 3000 m during the winters (Barry 2008). The glaciers are storehouses of fresh water on land, which feeds the watershed hydrology of the region (Thayyen and Gergan 2010). The summer melt of these glaciers (the ablation period) and surface run-off originates and supplements all the major rivers and lakes of the region (Archer and Fowler 2004). So even in cases of summer drought conditions when monsoons might fail, there is a constant source of fresh water over the region. Other than agriculture and power generation, this water supply is essential for domestic, developmental and industrial usage. According to Barros et al. (2006), the storm precipitation over the Himalayas (which also includes winter precipitation) may lead to erosion processes over the mountain range. Also, as already discussed, the snow cover generated during winters has much larger impact than just on the winter-time climate, and impacts the regional climate and large-scale flow patterns.

Glaciological and hydrological impacts of the WDs are very significant. On the other hand, extreme precipitating events during the winter time may lead to hazards and are dangerous in nature (Dimri and Chevuturi 2014). During winter, the Himalayan region is prone to severe weather due to large amounts of precipitation

produced by WDs. According to Dimri (2006), out of six – seven WDs occurrences per month, two – three WDs can cause severe weather conditions. These events may be realized in the form of heavy rainfall events (Zafar and Rasul 2009). These may be in the form of severe thunderstorms which, if not disastrous, most certainly can disrupt life and damage property. There may be cases of heavy snow storms precipitating high amounts of snow over the north-western Himalayan region during winters (Dimri and Mohanty 1999; De et al. 2005; Dimri 2006). Such blizzards are hazardous for road, rail or air transport, cause agricultural losses, and negatively impact the day-to-day lives of the people. Though uncommon in winters, sometimes hail precipitation also occurs over the northern Indian region under the influences of WDs (Chevuturi et al. 2014). Hailstorms can cause destruction of crops, infrastructure, property and, in extreme cases, may cause injuries to humans (De et al. 2005). Also due to the perception that hailstorms occur only in summer, hailstorms are not expected in the winter months. This may lead to unpreparedness which may increase the devastating consequences.

Extreme precipitating events are quite hazardous in nature, but sometimes these events lead to secondary natural disasters that are even worse. These secondary natural disasters can occur in the form of avalanches, landslides, glacial-lake outburst floods, landslides and flashfloods. The Himalayan region, with pockets of high population density and a migrating tourist population, is very susceptible to natural hazards causing devastating impacts. Also, the precipitating events which are considered as moderate over the plains might have hazardous impacts over the region. On the other hand, heavy precipitation events might not culminate in disasters if the geophysical features of that particular location are not conducive to disasters. For example, heavy precipitation due to WD and MT interaction occurred over the entire Uttarakhand state, but the natural disaster in the form of flashflood struck only the city of Kedarnath.

Avalanches are caused by structural collapse of the snow cover in the mountains. This can be either in the form of loose snow collapsing or a slab of snow and ice falling down the slope of the mountain. Moreover, avalanches can be caused by the internal factors of snow metamorphosis. In this chapter, we focus on the avalanches due to external factors that cause excessive snow loading to the existing snow cover (Srinivasan et al. 2005). For the northern Indian regions, the external factor is snow precipitation during winters caused by WDs. The north-western Himalayan region is under constant threat of avalanches during winter snow storms, as the avalanches in this region are quite frequent. These avalanche incidences can be widespread under the influence of a very intense WD (Rangachary and Bandyopadhyay 1987). These are very hazardous because they sometimes bury whole regions under a huge mass of snow and ice. Tragic human fatalities are a major concern during avalanches and infrastructure destruction is quite high (Ganju and Dimri 2004). Unusually heavy snowfall from 1 to 3 January 1991 triggered a severe avalanche which led to the tragic demise of many mountain climbers at the base camp (Hara et al. 2004). Landslides are another possible impact of heavy precipitation events during winter or even during summer glacier-melt flow over the Himalayan range (Lang and Barros 2004). The vulnerable geomorphological region of the Himalayan moun-

tains is susceptible to landslides in heavy waterflow conditions. With severe anthropogenic changes to the land use and land cover due to rapid and unplanned developmental activities, the region becomes even more vulnerable. Similar to avalanches, the landslides displace large swaths of land surface down the slope of the mountains. These also have similar devastating impacts on life, property and infrastructure (De et al. 2005).

Glacial lakes are naturally-dammed or moraine-dammed lakes within or at the margin of glaciers which may be left behind when the glaciers retreats. Snow and rain lead to formation of glaciers and supplement the glacial lakes. Sometimes the heavy winter precipitation overwhelms the glacial lakes. Then in summer, when further stress is added from meltwater, there is a possibility of natural moraine breaking. This causes the outburst of water from the glacial lake in the form of the glacial-lake outburst floods (Bajracharya et al. 2007). The structural integrity of the geomorphological features and the drainage of the region changes without warning. Thus, these floods are sudden, showing no prior indication, and thus are very dangerous. Himalayan region is highly prone to the risk of these glacial-lake outburst floods.

The ultimate impact of the winter precipitation events discussed here are the flashfloods. Extreme precipitation or even moderate rainfall events over the Himalayas may collect through multi-channel flow in the catchment area and the natural drainage systems to form flood water (Kala 2014). Due to the steep hill slopes of the region, this collected mass of water gains large momentum and rushes as a flood over a region. An example of flashflood was the Kedarnath disaster of 16 and 17 June 2013. This was the flashflood caused by the heavy precipitation resulting from the interaction of a WD with the MT (Chevuturi and Dimri in review). The flood water dragged along with it eroded surface debris along the steep slope, leading to further devastation throughout the city. Flashfloods in general cause severe damage to the region by causing erosion, destruction to transport and communication lines, and harm to life.

5.2 Severe Weather

A major impact of WDs over the Indian region is the associated precipitation that occurs. Cases of heavy precipitation events leading to natural disasters have been discussed above in detail. But WDs also might lead to other meteorological impacts or weather events which also fall under the category of severe weather conditions. Out of six – seven WDs impacting India during winters, two – three WDs might lead to severe weather conditions (Dimri 2006). There are two types of severe weather that form due to the occurrence of WDs. First is the possibility of severe fog conditions where the visibility over the region drops considerably. And the second severe weather event are the cold waves which reduce the temperature of the region. These two weather events have significant consequences and will be described in this section in detail.

During the winter period, fog is a severe weather hazard impacting the northern Indian region. Though fog is a localized phenomenon, during conditions favorable to its formation, the fog cover may extend over thousands of kilometers and persist for many days. The local occurrence and non-occurrence is dependent on local conditions (Rao and Srinivasan 1969). This blanket of fog usually covers a large area from west to east parallel and south to the Himalayan range over the Gangetic plains, from Pakistan to Bangladesh across the whole of north India (Syed et al. 2012). The formation of fog is usually limited to the lower layers of the atmosphere where the gases and aerosols are in higher concentrations. Fog is a precipitation type with droplets much smaller than rain drops (approximately 100 times smaller). Due to their small size and condensation method, they are suspended in the air and are more concentrated than rain drops (Ali et al. 2004). Fog over the northern Indian region occurs in rare cases during the post-monsoon season (October–November) and is usually seen in the winter season (December–February). The months with peak incidences of fog which is dense and persistent, are December and January.

Of the different types of fog types being formed over the northern India during winters, one is formed due to radiative cooling. A synthesis of the fog formation during winters by Syed et al. (2012) is provided in this paragraph. Radiation fog forms near the surface when an anticyclone occurs over a region of stable conditions. The cause of the radiation fog is, as the name suggests, radiative cooling of the surface and the near -surface cooling due to the loss of energy. Other reasons for the formation of the radiation fog can also be upward heat flux from the soil, dew deposition leading to warming and moisture loss from the atmosphere and turbulent mixing in the stable boundary layer. The capacity of the soil types to hold moisture and its thermal conductivity are important factors that influence the latent heat flux of the surface and determines the capacity of radiative cooling and surface inversions. Conditions of low wind speed, high humidity and low surface temperatures are conducive to the formation of radiation fog. Such conditions lead to the very stable conditions or even inversion conditions that form boundary trapping, since there is limited mixing of air within the troposphere. These conditions lead to condensation of the moisture available into the fog droplets. The presence of gases and particles such as aerosols influence the formation and the composition of the fog particles (Ali et al. 2004). Persistent fog form in regions of high air pollution due to the availability of additional nuclei to generate a larger frequency of smaller fog particles. The physico-chemical interactions between the pollutant gases and particles and the fog droplets allow the formation of the fog in sub-saturated conditions. Some occurrences of advection fog are also observed over this region during the winter season. The advection fog occurs when a warmer air mass moves over a colder surface. But such cases are more common over bodies of water and rare over this region.

These are the mechanisms of typical localized fog formation. The fog formation during winters covering large areas of northern Indian region is associated with the occurrence of the WDs (Rao and Srinivasan 1969). The precipitation related to the WDs causes an inundation of water vapor in the lower levels due to evaporation of the precipitation. And the WDs are the only source of precipitation during the win-

ter season. As discussed before, ahead of the migrating WD trough there is low-level warm air and moisture incursion from the Arabian Sea and the Bay of Bengal that is the source of the high humidity also required for the fog formation. As the WD passes through the region, the rear end of the trough contains a high-pressure (anti-cyclonic) system which develops stable atmospheric conditions. These synoptic conditions, along with low wind speeds, form surface-based inversions with the moisture availability triggers and promotes fog formation (Syed et al. 2012). But these conditions are generated just in the immediate rear vicinity of the WD and thus the fog conditions usually occur immediately after the passing of the WD over a region. Further, as this region is influenced by different aerosols and atmospheric particles in the lower atmosphere, solar radiation further heats up the region (Ali et al. 2004). In cases of large moisture influx, dense and persistent fog may last up to days. In the rare case of advection fog formation, the warm moist air flow in the front of the WD arrives over the cold surface. Another mechanism for advection fog formation is due to an easterly warm wind being drawn towards the region due to the presence of a WD. Such conditions where the fog is formed ahead of the WD by the first method can cause fog over the regions of Orissa and West Bengal. The second mechanism of advection fog formation causes fog occurrences over Bihar and Uttar Pradesh (Rao and Srinivasan 1969).

Changes in land-use and land-cover in the form of urbanization, industrialization, agriculture (leading to crop burning) and road development (increasing transport) lead to the massive increase in the air pollutant load of the region (Syed et al. 2012). Specifically the Gangetic plains are a hub of increased human activity with huge population density. With this region being the focus of the fog formation, there are reports suggesting that these pollutants and emissions are increasing the dense fog incidences over the region (De et al. 2005). On the other hand, the increase in urbanization has led to an urban heat island effect which is said to help disperse fog much more quickly. But still, according to Syed et al. (2012), the frequency of fog incidences have increased three times in three decades (1976–2010) over India. While the fog incidences over the whole region are a significant impact of the WDs, these fog occurrences have their own impact. One of the major consequences of concentrated fog is the human health hazard. Inhalation within a foggy environment may cause many health issues to humans, for example respiratory distress and disorders. The fog composition may be acidic or alkaline depending on the forming aerosols or emissions which determine the chemistry of the fog (Ali et al 2004). In extreme cases the chemical composition of fog might be a potential hazard to the humans, vegetation, wildlife, cattle and infrastructure due to its corrosiveness. Another impact of fog incidences is the severe reduction of visibility. This reduction in visibility causes obstruction of the transport system. The foggy conditions may lead to transport accidents which may be injurious or fatal to humans (De et al. 2005). These may also cause delays and various other inconveniences specifically in the railway and aviation sector. The fog is a major hazard for aviation which may lead to the necessity of diverting, delaying or grounding aircraft (Jenamani 2012a, b). In these regions of high urbanization and heavy air traffic, the fog occurrences are highly disadvantageous. With the guarantee of increased transport- network density

and frequency in the future, these increasing fog events become even more serious. According to De and Dandekar (2001), visibility over northern Indian airports show an increasing trend during winters for more very poor visibility days, due to fog, as compared to the southern airports. Due to all these negative impacts, major economic losses that are comparable to the natural disasters like hurricanes are attributed to the fog events (Syed et al. 2012).

The second severe weather events which are a consequence of WD during winters that we are discussing in this section are the cold waves or cold surges. Conditions in which the minimum temperatures of a region drops well below the normal minimum temperatures are designated as cold wave conditions. Only departures from normal minimum temperatures are used to define cold waves, and no set minimum temperature is set as it may vary for different regions (Bedekar et al. 1974). In such instances, associated reductions in maximum temperatures as well as lowering of moisture conditions are also observed. Strong wind speeds during certain cases of cold waves may add to the wind chill factor. Cold wave conditions are sometimes also associated with ground frost. Ground frost is caused due to the direct deposition of frozen water vapor onto the surface due to freezing temperatures. The cold waves impact mostly northern India during winters, but may also extend their influence southwards and eastwards during severe cases. The frequency of the cold waves reduces drastically southwards and eastwards even within the northern region. This can be explained due to the warming of the cold stream as it descends and moves along the orography. The intensity of the cold waves are generally said to decrease east of 80°E and south of 20°N. These events usually last up to 4–5 days and in extreme cases 7–10 days (Rao and Srinivasan 1969). Due to the migration of the WDs, the cold wave events appear along the track of the WDs.

Cold and dry air from the north is a characteristic feature associated with the rear of the WD. As the WD migrates past a region, cold and dry air from the higher latitudes sweeps over the same region (Yadav et al. 2012). This region is mostly the northern India region as discussed above. Cold waves may form due to active (precipitating) as well as weak (non-precipitating) WD occurrences. In the wake of an active WD, there is a sudden drop in the minimum temperatures due to stronger circulation patterns which draw in cold air quickly from the north. Whereas, if there are already low minimum temperatures associated with weak WD instances, then there is a gradual further fall in minimum temperatures. In certain cases, a low or a disturbance north of India may also generate cold waves from the high at the rear of the disturbance, where the high extends towards the Indian region. From the discussion it can be concluded that cold waves usually are northerly or north-westerly and flow towards southern and eastern directions (Rao and Srinivasan 1969). As the pressure gradient at the back of the WDs can be strong, winds with high speeds might develop along with the cold waves. These winds can be associated with the term wind chill factor which increases the cold impact during such an event and strong wind will also cause the spread of the cold waves over a large spatial extent. Fog conditions may also enhance cold waves as dense fog conditions mute the solar radiation by inhibiting the heating of the ground and causing further cooling (Bedekar et al. 1974). Mooley (1957) stated that to maintain cold wave conditions

there should be no successive WD after the first one. This maintains the northerly cold air flow without interruption. A second WD right after the first causes an influx of warm air in the front of the second WD. This warm flow disrupts the cold wave conditions. Thus cold wave conditions are maintained if a intense WD is not followed by another WD or even develop a disturbance in the north of India or an induced low in the south. In fact, continuous and successive WDs over the northern India leads to unusually warm conditions during otherwise colder winter season.

Physiologically, people are acclimatized to a temperature range specifically associated with the region of their long-stay residence. The cold wave events are damaging to the humans due to their sensitivity to extreme lowering of temperatures beyond their acclimatized temperature range (Bedekar et al. 1974). Thus, cold wave events may cause health hazards like frost bite or even claim fatalities in the human population (De et al. 2005). Extremely cold conditions are also not favorable for winter or rabi crops or even wildlife and natural vegetation (Yadav et al. 2012). Frosting conditions are even more harmful for the agriculture sector.

5.3 Western Disturbances in the Changing Climate

Climate change is the most debated scientific topic of the twenty first century. India, with its large expanse and heterogeneous geography, already has a wide variety of climatic sub-divisions, and any change in the climate has a large temporal and spatial impact. Specifically over India, issues of vulnerability, prevention, mitigation and adaptation are usually associated with climate change. But as it is not in the scope of this book, we will not be getting into this debate of the truth about the climate change over India. Instead this section focuses on the question if there is an impact of climate change on the WDs or even vice versa. And in addition, as there might be very few studies relating the climate change and WDs directly, hence we will also focus on the relation between changing climate and the impacts of WDs (winter precipitation, cold waves or low temperature conditions etc.) that have been discussed previously in this chapter. According to Dash et al. (2007), the general perception is that there has been an increase in the frequency of the extreme events like cold waves, natural disasters etc. But as they suggested, such a perception should be supported by scientifically sound facts. Thus this section provides a review of the different scientific studies on WDs or their impacts on changing climate.

The global hydrological cycle is expected to accelerate with increased CO₂ as the warmer atmosphere can hold more water (Zahn and Allan 2013). Thus regions where the precipitation is strongly dependent on ocean moisture uptake will experience stronger precipitation events (Gimeno et al. 2013). The variability of mid-latitude winter weather is strongly governed by extratropical cyclones, although there is very little evidence that the frequency or wind speed of these cyclones will increase. However, more intense precipitation from the cyclones associated with WDs will have socioeconomic impacts over the western Himalayas. This remains an open question for social scientists to investigate further in line of existing scien-

tific knowledge and understanding. So far there are no observation-based studies concerning the changing nature of WDs with increased CO₂ concentrations. Based on Coupled Model Intercomparison Project Phase 3 (CMIP3) experiments, Meehl et al. (2007) revealed possible increased future storm activity; however, the more recent CMIP5 simulations show a decline in Northern Hemisphere storm activity (Chang et al. 2012). Therefore, extensive investigations in line with various model projections are needed to establish how exactly the trend of these storms will be in future. It is important to note that accurately simulating snow/rain differentiation in models are likely to be significantly limited in their ability to capture this. Of the climate drivers presented within the model environment, snowfall amounts are likely to be more uncertain, as well as how good the regional topography is represented in the coarse resolution global CMIP series of models. In addition, since polar amplification means that the higher latitudes will warm faster than the Northern Hemisphere as a whole, the temperature gradient will decrease (Hall 2004). It can be expected that the total winter snowfall from WDs will increase, but the frequency of such events will remain largely unchanged.

According to Dash et al. (2007) there has been a slight increase in the precipitation during winter over the northern Indian region. This study also reported a warming trend, and an increasing trend in the maximum temperature and fluctuating minimum temperatures during winters in northern India in the recent decades. This warming trend has become more pronounced after 1960s (Bhutiyan et al. 2007). Winter rainfall over the hilly region shows a decreasing trend for moderate rainfall days and increasing trends for heavy rainfall days (Dash et al. 2009). Also the short burst events of precipitation interspersed with longer dry spells show significant increasing trends. Due to the increasing temperatures, the melting of the winter snow cover during summer period has been enhanced (Kripalani et al. 2003). Dash et al. (2009) specifically mentioned that the increase in the short but heavy precipitating events are an indication of increasing frequency of intensified WDs which leads to strong localized storms. Syed et al. (2009) also reported an increase of winter precipitation over central and southwest Asia during the period 1951–2000 which is possibly due to intensification of eastward moving synoptic disturbances from the Mediterranean. According to Fowler and Archer (2006) and Dimri and Dash (2012), there is a warming trend over the western Himalayas during the winter, thus indicating the lowering of the frequency of the cold waves events. Though the trends in the winter precipitation are inconsistent, still the study showed a decreasing trend in the winter precipitation over the western Himalayas (Dimri and Dash 2012). There is a decrease in the heavy precipitation events. The inconsistency is due to the variable orography which leads to highly variable precipitation events over such terrain which might not be detected on the sparse observational station network. On the other hand, variability within the winter precipitation over the north of India shows an increase in the recent decades (Yadav et al. 2012). And the future trend of the precipitation patterns and surface air temperatures show an increase over northwestern India during winters at the end of the twenty-first century (Yadav et al. 2010). Shekhar et al. (2010) also showed a decreasing trend in the winter seasonal snowfall and frequency of snowfall days. As previously discussed, there is a

possible teleconnection between the snow cover over the north and the ISM. But after 1970s there has been weakening of this teleconnection which is attributed to the warming trends observed during winters and post-winters which is causing the rapid melt of the snow cover post-winters (Bhutiyani et al. 2007). In fact the study of Kripalani et al. (2003) suggests that the earlier negative correlation between this winter snow cover and ISM in recent decades has turned positive in certain cases as there is higher impact of snow melt on the monsoon circulation. Such rapid melting of snow in the warming climate has also lead to flood situations over the region.

In the scenario of the changing climate, we need to understand the alterations in the frequency, intensity and tracks of the WDs. Studies have found a decreasing trend (Das et al. 2002) or no consistent significant trends (Shekhar et al. 2010) in the WD occurrences in the recent decades. Shekhar et al. (2010) suggest that there is decreasing amount of snowfall in winter, but WDs are not reducing in frequency. Though they are suggesting no correlation between WDs and winter snowfall, it can mean that intensity of the WDs is reducing and thus leading to lower precipitation. Observations suggest recent decreasing trends in cyclonic activity over the western Mediterranean, whereas no significant change over the central and eastern Mediterranean (Syed et al. 2006). With specific reference to the frequency of WDs, Ridley et al. (2013) have provided a comprehensive overview of the increase in WD frequencies up to 2100, and associated snowfall is also predicted to increase over the region. Ridley et al. (2013) explained this by changes in circulations using the regional climate model (HadCM3) which simulated increased occurrence of WDs and an associated overall 37 % increase in winter snowfall. In view of this model, the environment produces higher circulation corresponding to the evolution of the WDs and hence higher precipitation. But one of the regional climate models (HadRM3-E) used in the study did not show any significant changes in the frequency of the WDs or the snow precipitation. Madhura et al. (2014) also indicate an increase in the frequency of the WDs due to the mid-tropospheric warming trends in recent decade over the west-central Asia. Such warming enhances the meridional temperature gradient which will in turn increase the baroclinic instability of the mean westerly wind. These changes favor increased variability of the WDs and higher propensity of the associated precipitation. Another important finding for such increase is based on elevation dependency of the climatic signals over the Tibetan Plateau and Himalayan region, which introduces zonally asymmetric changes in the winter circulation through mid- and upper tropospheric temperatures over the Eurasian region.

There exists still no in-depth study on the trends of the intensities of WDs in the changing climate or even future predictions, let alone on the track changes of the WDs. But studies on the typical extra-tropical cyclones in the northern hemisphere show a decreasing trend in the frequency of the extra-tropical cyclones with increasing temperatures (Catto et al. 2011; Mizuta et al. 2011; IPCC 2012). A warming environment is also suggested to increase the intensity of the extreme extra-tropical cyclones (Mizuta et al. 2011) due to changes in the temperature gradients required for the development of these cyclones. Such cases of sporadic but extreme weather events are predicted to produce higher episodic losses increasing the risk of such

events even in the face of decreasing frequency of the events (Air Worldwide 2012). Increase in such disasters due to extreme WDs are also possible in the future warming climate. But there is another school of thought that suggests that the warming environment may cause a decrease in the temperature gradient between latitudes and so will reduce the intensity and frequency of these disturbances. Additionally, studies also predict a poleward migration of the tracks of the extra-tropical cyclones in a warming climate (Catto et al. 2011; IPCC 2012). These changes predicted for the typical extra-tropical cyclones might be reflected in the changes in the WDs. Thus, this might even mean a poleward shift of WDs which would result in reduction in the winter precipitation over India. As already discussed, the winter precipitation is a very important part of the Indian ecology and economy and loss of this part of Indian climatology would be disastrous. Thus, there is possibility of a change in WDs in the changing climate, and these changes will have significant direct or indirect impacts on the Indian subcontinent. There is a need to list and quantify these changes in the different scenarios so as to develop mitigation and adaptation strategies.

Regional model studies suggest an increase in mean annual temperature, averaged over the Ganges basin, in the range of 1–4 °C for the period from 2000 to 2050 (Moors et al. 2011). Projections of precipitation indicate that natural variability dominates the climate change signal, and there is considerable uncertainty concerning changes in regional annual mean precipitation by 2050. Glaciers in headwater tributary basins of the Ganges appear to continue to decline (Bolch et al. 2012), but it is not clear whether meltwater runoff would continue to increase in the future since this depends on the snow accumulation regime. Future changes of monsoon intensity will have an important effect on Himalayan glaciers, but current climate projections do not agree even on the sign of change, thus introducing further uncertainties (Moors et al. 2011). Nevertheless, all models project glacial mass losses in the coming decades that are substantial for most parts of the Himalayas, but consistently fall well short of complete region-wide glacier disappearance even by 2100. Water availability is subject to decadal variability, with much uncertainty in the contribution from climate change (Moors et al. 2011). Meltwater is extremely important in the Indus basin and important for the Brahmaputra basin, but plays only a modest role for the Ganges (Immerzeel et al. 2010). Interannual variability of the monsoon onset alone can have a strong influence on monsoon rainfall totals (20–30 %) and the patterns of accumulation (Lang and Barros 2004; Barros and Lang 2003), which are difficult to predict. The predicted changes in precipitation and temperature will probably not lead to a significant increase in water availability by 2050, but the timing of runoff from snowmelt will likely shift to earlier in the spring and summer.

Although global socioeconomic scenarios show trends to urbanization, locally these trends are less evident and in some districts rural population is increasing. Falling ground-water levels in the Ganges plain may prevent expansion of irrigated areas for food supply (Rodell et al. 2009). Changes in socioeconomic development in combination with projected changes in the timing of runoff outside the monsoon period may increase flash floods associated with more extreme rainfall (Thayyen

et al. 2012), and will make choices difficult for water managers. Because of the uncertainty in future water availability trends, decreasing vulnerability by augmenting resilience is the preferred way to adapt to climate change. Adaptive policies are required to increase society's capacity to adapt to both anticipated and unanticipated conditions.

This work on the role of the WDs during the present climate provides motivation to anticipate the impacts on various socio-economic issues particularly over the northern Indian region. Better understanding and an improved corresponding forecast will provide advantages in cases of adaptation and vulnerability within a changing global context.

5.4 Western Disturbances and Future Research

Despite the all the information reviewed and synthesized in this book about the WDs, there are still gaps in our knowledge on these complex systems, the WDs. With ongoing research, future studies need to be planned for the different focus areas related to WDs. From our understanding, we can classify the some areas of focus for improvements as follows:

1. Dynamical studies

- These should include more exhaustive research on the origin and tracks of the WDs before they reach the Indian sub-continent.
- More studies to quantify the impact of surface variability on the WDs in light of urbanization and other increasing anthropogenic activities.
- Directed studies on the influence of WDs during the non-winter season and the WD linkages with global teleconnections.

2. Impact studies

- Performing correlation studies to define the various significant impacts of the WDs over the Indian subcontinent.
- Inter-disciplinary studies to understand the hydrological and geomorphological impacts of the WDs
- Quantification of the socio-economic losses associated with the disasters linked with the WDs.

3. Climate change studies

- Understanding the changes in the WDs' intensity, track and frequency due to the changing environment.
- Listing the possible impacts due to the changes in the WDs and developing possible mitigation and adaptation strategies.
- Understanding possible impacts of WDs on the regional climate and how these might influence the changing climate.

References

- AIR Worldwide (2012) The impact of climate change on extratropical cyclones: a review of the current scientific literature. <http://www.air-worldwide.com/Publications/White-Papers/documents/The-Impact-of-Climate-Change-on-Extratropical-Cyclones---A-Review-of-the-Literature/>. Accessed on 24 Jan 2013
- Ali K, Momin GA, Tiwari S, Safai PD, Chate DM, Rao PSP (2004) Fog and precipitation chemistry at Delhi, North India. *Atmos Environ* 38(25):4215–4222
- Archer DR, Fowler HJ (2004) Spatial and temporal variations in precipitation in the Upper Indus Basin, global teleconnections and hydrological implications. *Hydrol Earth Syst Sci* 8(1):47–61
- Bajracharya SR, Mool PK, Shrestha B (2007) Impact of climate change on Himalayan glaciers and glacial lakes: case studies on GLOF and associated hazards in Nepal and Bhutan. Kathmandu, International Centre for Integrated Mountain Development and United Nations Environment Programme Regional Office, Asia and the Pacific. ICIMOD Publication 169
- Barros AP, Lang TJ (2003) Monitoring the monsoon in the Himalayas: observations in central Nepal, June 2001. *Mon Weather Rev* 131(7):1408–1427
- Barros AP, Chiao S, Lang TJ, Burbank D, Putkonen J (2006) From weather to climate – seasonal and interannual variability of storms and implications for erosion processes in the Himalaya. In: Willett SD, Hovius N, Brandon MT, Fisher DM (eds) *Tectonics, climate, and landscape evolution: geological society of America special paper 398*. Penrose Conference Series, pp 17–28
- Barry RG (2008) *Mountain weather and climate*. Cambridge University Press, New York
- Bedekar VC, Dekate MV, Banerjee AK (1974) Heat and cold waves in India. Indian Meteorological Department: Forecasting Manual Part IV
- Benn DI, Owen LA (1998) The role of the Indian summer monsoon and the mid-latitude westerlies in Himalayan glaciation: review and speculative discussion. *J Geol Soc Lond* 155:353–363
- Bhutiyani MR, Kale VS, Pawar NJ (2007) Long term trends in maximum, minimum and mean annual temperatures across the northwestern Himalaya during the twentieth century. *Clim Chang* 85:159–177
- Bolch T, Kulkarni A, Kääb A, Huggel C, Paul F, Cogley JG, Frey H, Kargel JS, Fujita K, Scheel M, Bajracharya S, Stoffel M (2012) The state and fate of Himalayan glaciers. *Science* 336(6079):310–314
- Catto JL, Shaffrey LC, Hodges KI (2011) Northern Hemisphere extratropical cyclones in a warming climate in the HiGEM high-resolution climate model. *J Clim* 24(20):5336–5352
- Chang EKM, Guo Y, Xia X (2012) CMIP5 multimodel ensemble projection of storm track change under global warming. *J Geophys Res* 117:D23118. doi:10.1029/2012JD018578
- Chevuturi A, Dimri AP (in review) Investigation of Uttarakhand (India) disaster- 2013 using Weather Research and Forecasting model
- Chevuturi A, Dimri AP, Gunturu UB (2014) Numerical simulation of a rare winter hailstorm event over Delhi, India on 17 January 2013. *Nat Hazards Earth Syst Sci* 14(12):3331–3344
- Das MR, Mukhopadhyay SR, Dandekar MM, Kshirsagar SR (2002) Pre-monsoon western disturbances in relation to monsoon rainfall, its advancement over NW India and their trends. *Curr Sci* 82(11):1320–1321
- Dash SK, Jenamani RK, Kalsi SR, Panda SK (2007) Some evidence of climate change in twentieth-century India. *Clim Chang* 85(3–4):299–321
- Dash SK, Kulkarni MA, Mohanty UC, Prasad K (2009) Changes in the characteristics of rain events in India. *J Geophys Res* 114(D10109):1–12
- De US, Dandekar MM (2001) Natural disasters in urban areas. *Deccan Geogr* 39(2):1–12
- De US, Dube RK, Rao GP (2005) Extreme weather events over India in the last 100 years. *J Indian Geophys Union* 9(3):173–187
- Dimri AP (2006) Surface and upper air fields during extreme winter precipitation over the Western Himalayas. *Pure Appl Geophys* 163:1679–1698

- Dimri AP, Chevuturi A (2014) Model sensitivity analysis study for western disturbances over the Himalayas. *Meteorol Atmos Phys* 123(3–4):155–180
- Dimri AP, Dash SK (2012) Wintertime climatic trends in the Western Himalayas. *Clim Chang* 111(3–4):775–800
- Dimri AP, Mohanty UC (1999) Snowfall statistics of some SASE field stations in J&K. *Def Sci J* 49(5):437–445
- Fowler HJ, Archer DR (2006) Conflicting signals of climatic change in the Upper Indus Basin. *J Clim* 19(17):4276–4293
- Ganju A, Dimri AP (2004) Prevention and mitigation of avalanche disasters in Western Himalayan region. *Nat Hazards* 31:357–371
- Gimeno LR, Nieto A, Drumond R, Castillo R, Trigo R (2013) Influence of the intensification of the major oceanic moisture sources on continental precipitation. *Geophys Res Lett* 40:1443–1450. doi:[10.1002/grl.50338](https://doi.org/10.1002/grl.50338)
- Hall A (2004) The role of surface albedo feedback in climate. *J Clim* 17(7):1550–1568
- Hara M, Kimura F, Yasunari T (2004) The generating mechanism of western disturbances over the Himalayas. In: 6th international GAME conference
- Immerzeel WW, van Beek LP, Bierkens MF (2010) Climate change will affect the Asian water towers. *Science* 328(5984):1382–1385
- IPCC (2012) Summary for Policymakers. In: Field CB, Barros V, Stocker TF, Qin D, Dokken DJ, Ebi KL, Mastrandrea MD, Mach KJ, Plattner G-K, Allen SK, Tignor M, Midgley PM (eds) *Managing the risks of extreme events and disasters to advance climate change adaptation. A special report of working groups I and II of the intergovernmental panel on climate change*. Cambridge University Press, Cambridge/New York, pp 1–19
- Jenamani RK (2012a) Micro-climatic study and trend analysis of fog characteristics at IGI airport New Delhi using hourly data (1981–2005). *Mausam* 63(2):203–218
- Jenamani RK (2012b) Development of intensity based fog climatological information system (daily and hourly) at IGI airport, New Delhi for use in fog forecasting and aviation. *Mausam* 63(1):89–112
- Kala CP (2014) Deluge, disaster and development in Uttarakhand Himalayan region of India: challenges and lessons for disaster management. *Int J Disaster Risk Reduct* 8:143–152
- Kripalani RH, Kulkarni A, Sabade SS (2003) Western Himalayan snow cover and Indian monsoon rainfall: a re-examination with INSAT and NCEP/NCAR data. *Theor Appl Climatol* 74(1–2):1–18
- Lang TJ, Barros AP (2004) Winter storms in central Himalayas. *J Meteorol Soc Jpn* 82(3):829–844
- Madhura RK, Krishnan R, Revadekar JV, Majumdar M, Goswami BN (2014) Changes in western disturbances over the western Himalayas in a warming environment. *Clim Dyn*. doi:[10.1007/s00382-014-2166-9](https://doi.org/10.1007/s00382-014-2166-9)
- Meehl G, Covey C, Delworth T, Latif M, McAvaney B, Mitchell J, Stouffer R, Taylor K (2007) The WCRP CMIP3 multi-model dataset: a new era in climate change research. *Bull Am Meteorol Soc* 88:1383–1394
- Mizuta R, Matsueda M, Endo H, Yukimoto S (2011) Future change in extratropical cyclones associated with change in the upper troposphere. *J Clim* 24(24):6456–6470
- Mooley DA (1957) The role of western disturbances in the production of weather over India during different seasons. *Indian J Meteorol Geophys* 8(3):253–260
- Moors EJ, Biemans H, Groot A, TerwisschvanScheltinga C, Siderius C, Stoffel M, Huggelb C, Wiltshire A, Mathison C, Ridley J, Jacob D, Kumar P, Bhadwal S, Gosain A, Collins DN (2011) Adaptation to changing water resources in the Ganges basin, Northern India. *Environ Sci Policy* 14(7). doi: <http://dx.doi.org/10.1016/j.envsci.2011.03.005>
- Rangachary N, Bandyopadhyay BK (1987) An analysis of the synoptic weather pattern associated with extensive avalanching in Western Himalaya. *Int Assoc Hydrol Sci Publ* 162:311–316

- Rao YP, Srinivasan V (1969) Discussion of typical synoptic weather situation: winter western disturbances and their associated features. Indian Meteorological Department: Forecasting Manual Part III
- Ridley J, Wiltshire A, Mathison C (2013) More frequent occurrence of westerly disturbances in Karakoram up to 2100. *Sci Total Environ*. doi:[10.1016/j.scitotenv.2013.03.074](https://doi.org/10.1016/j.scitotenv.2013.03.074)
- Rodell M, Velicogna I, Famiglietti JS (2009) Satellite-based estimates of groundwater depletion in India. *Nature* 460:999–1002. doi:[10.1038/nature08238](https://doi.org/10.1038/nature08238)
- Shekhar MS, Chand H, Kumar S, Srinivasan K, Ganju A (2010) Climate-change studies in the Western Himalaya. *Ann Glaciol* 51(54):105–112
- Srinivasan K, Ganju A, Sharma SS (2005) Usefulness of mesoscale weather forecast for avalanche forecasting. *Curr Sci* 88(6):921–926
- Syed FS, Giorgi F, Pal JS, King MP (2006) Effect of remote forcings on the winter precipitation of central southwest Asia part 1: observations. *Theor Appl Climatol* 86(1):147–160
- Syed FS, Giorgi F, Pal JS, Keay K (2009) Regional climate model simulation of winter climate over Central–Southwest Asia, with emphasis on NAO and ENSO effects. *Int J Climatol* 30(2):220–235
- Syed FS, Körnich H, Tjernström M (2012) On the fog variability over South Asia. *Clim Dyn* 39(12):993–3005
- Thayyen RJ, Gergan JT (2010) Role of glaciers in watershed hydrology: a preliminary study of a “Himalayan catchment”. *Cryosphere* 4:115–128
- Thayyen RJ, Dimri AP, Kumar P, Agnihotri G (2012) Study of cloudburst and flash floods around Leh, India during August 4–6, 2010. *Nat Hazards*. doi: [10.1007/s11069-012-0464-2](https://doi.org/10.1007/s11069-012-0464-2)
- Yadav RK, RupaKumar K, Rajeevan M (2010) Climate change scenarios for Northwest India winter season. *Quat Int* 213(1):12–19
- Yadav RK, RupaKumar K, Rajeevan M (2012) Characteristic features of winter precipitation and its variability over northwest India. *J Earth Syst Sci* 121(3):611–623
- Zafar Q, Rasul G (2009) Diagnosis and numerical simulation of a heavy rainfall event in winter over upper parts of Pakistan. *Pak J Meteorol* 5:81–96
- Zahn M, Allan RP (2013) Climate warming–related strengthening of the tropical hydrological cycle. *J Clim* 26:562–574. doi:<http://dx.doi.org/10.1175/JCLI-D-12-00222.1>

Index

A

Ablation, 114
Adiabatic, 29, 30, 52
Advanced microwave sounding unit (AMSU), 31
Advection, 30, 39, 70, 72, 74, 75, 117, 118
Aerosols, 117–118
Ageostrophic wind, 74
Albedo, 4, 21, 76, 77
Alto-clouds, 13
Angular momentum, 21
Anomaly, 15, 17, 19, 21, 42, 43, 52, 72, 73, 76, 86, 87, 95, 102
Arkin's methodology, 31
The Asian precipitation–highly resolved observational data integration towards evaluation of the water resources (APHRODITE), 49, 51, 52, 84–87, 92
Avalanche, 2, 4, 5, 13, 45, 61, 115

B

Baroclinic, 10, 13, 21, 32, 42–44, 68, 74, 75, 108, 122
Baroclinic instability, 32, 42, 44, 122
Baroclinicity, 10, 42, 68
Bjerknes cyclones, 11
Blanford-type, 76
Blizzard, 115
Boreal, 20, 89
Boundary condition, 32, 45, 52
Boundary layer, 32, 37, 117
Break monsoon, 62, 67–69, 72

C

Catchment, 47, 114, 116
Cirrus, 13
Climate research unit (CRU), 84, 86
Cloudburst, 4
Cloud surge, 31
CMIP5, 121
Cold wave, 2, 61, 64, 116, 119–121
Compression, 72, 74
Conditional instability, 30
Coniferous, 28
Convection, 9, 20, 21, 30, 32, 41, 67, 68, 71, 73, 89, 93, 96, 101, 104, 107–109
Convective available potential energy (CAPE), 19, 30, 41, 42, 44, 66
Convective energy, 43
Convective instability, 41, 76
Convergence, 12, 15, 20, 21, 30, 44, 52, 63, 65, 68–70, 78, 89, 96, 101, 104
Coriolis force, 62
Coupled model intercomparison project phase 3 (CMIP3), 121
Cryosphere, 113
Cumulus, 37
Cyclogenesis, 6, 10, 14, 77
Cyclone, 2, 5–7, 11–15, 29, 62, 63, 65, 68, 77, 78, 83, 89, 104, 120, 122, 123

D

Dew, 117
Diabatic, 55
Diurnal, 61

Divergence, 6, 14, 65, 66, 68, 71, 73, 78,
96, 101, 103, 104
Drainage, 47, 116
Drought, 2, 62, 68, 69, 114
Duststorms, 68

E

Ecology, 4, 114, 123
El Niño, 4, 20, 21, 99, 108
El-Niño southern oscillation (ENSO),
4, 19, 21, 84, 92, 107–109
Entropy, 55
Eurasian snow cover, 4, 19, 76
Extra tropical, 5–7, 11, 13–15, 27, 29, 31,
45, 67, 69, 70, 78, 83, 122, 123

F

Fast Fourier transform (FFT), 101
Fauna, 114
Flashflood, 2, 4, 115, 116
Flora, 114
Fog, 2, 5, 61, 116–119
Frontogenesis, 6, 14, 70, 74, 75
Frost, 119, 120
Frost bite, 120

G

Geopotential height, 15, 17, 39, 41, 43,
51–53, 72, 73, 84, 88, 95, 108
Geopotential height anomaly, 15, 17, 42,
43, 72, 73
Geopotential surface, 74
Geostrophic balance, 74
Geostrophic wind, 72, 74
Glaciation, 21
Global circulation model, 45
Global precipitation climatology centre
(GPCC), 84, 86
Global precipitation climatology project
(GPCP), 84, 86

H

Hadley cell, 21, 92, 109
Hadley circulation, 89, 96, 108
Hail, 43, 62, 66, 115
Hailstorm, 2, 4, 42, 43, 65, 66, 115
Heat low, 62, 68, 77
Heat wave, 2, 61, 65
Hydrometeor, 5, 66, 74
Hydrometeorological, 5
Hydrometeors, 66, 74

I

Indian summer monsoon (ISM), 4, 9, 10,
12, 19, 29, 55, 62, 68, 70–72, 76,
77, 83, 84, 122
Indian winter monsoon (IWM), 3, 19–21, 61,
62, 83–84, 86, 89, 92, 93, 96, 99, 101,
107, 109, 113
Initial condition, 32
Interactions between the tropics and
mid-latitudes (ITML), 67, 68, 70, 71
Interannual variations (IAVs),
84, 86, 101
Inter tropical convergence zone (ITCZ),
12, 63, 64, 71, 77
Inversion, 117
Isobars, 15
ITML. *See* Interactions between the tropics
and mid-latitudes (ITML)

K

Kalbaisakhi, 65
Kinetic energy, 19–21, 29, 30, 41,
44, 46, 75
Koppen-Geiger climatic classification, 1

L

Lanczos filter, 86
Land cover, 1, 27–29, 45–55, 116, 118
Landslide, 2, 4, 5, 29, 45, 62, 115, 116
Land use, 1, 27–29, 45–55, 84, 116, 118
La Niña, 69
Latent heat flux, 117
Latent instability, 66
Lower troposphere, 32, 49, 72, 95–97, 100
Low level jet (LLJ), 68, 70, 72, 76

M

Madden-Julian oscillation (MJO), 21
Mascarenes high, 62, 68
Meridional wind, 29, 49, 50, 72
Meso-alpha scale, 15
Mesoscale, 13, 35, 45, 47
Mid-latitude, 5, 9, 12, 14, 29, 31, 42, 67, 68,
74, 76, 78, 86, 89, 120
Mid troposphere, 14, 15, 49, 52, 70, 74, 89,
93, 100, 104, 108, 109
Modern era retrospective analysis
for research and applications
(MERRA), 40, 41
Monsoon index, 19
Monsoon trough, 12, 62, 63, 67, 68, 70
Moraine, 116

N

National center for environmental prediction–National center for atmospheric research reanalysis project (NCEP–NNRPII), 40, 41
 National center of environmental prediction/
 National center for atmospheric research (NCEP/NCAR), 84
 North east monsoon (NEM), 62, 77, 83
 Northern Atlantic oscillation (NAO), 21
 Nor' westers, 62, 65, 66
 Nucleation, 43
 Numerical modelling technique, 27, 32
 Numerical weather prediction, 31, 32, 42

O

Occluded discontinuity, 73–75
 Orography, 5, 10, 13, 14, 19, 28–31, 45–55, 64, 70, 72–74, 119, 121
 Outgoing longwave radiation (OLR), 84, 89, 96, 101, 104, 106, 107

P

Pacific decadal oscillation (PDO), 21
 Parameterization schemes, 33–37, 45
 Planetary boundary layer, 37
 Potential energy, 19, 29, 30, 41, 44, 66
 Potential instability, 71
 Precipitation, 1, 3–5, 7, 10, 12–14, 19–21, 28, 30, 32, 37, 40–43, 45–49, 51, 52, 55, 61–64, 67–72, 74–79, 83–87, 89, 91–94, 99–102, 104, 107–109, 113–117, 120–123
 Pulsatory extension of the monsoon (PEM), 67–70, 72, 73, 75

Q

Quasi-biennial, 19
 Quasi-periodicity, 6
 Quasi-permanent, 9
 Quasi-stationary, 13, 69

R

Rabi, 4, 114, 120
 Rarification, 72, 74
 Reflectivity, 74
 Regional climate model (RCM), 45, 52, 122
 Relative humidity, 52, 54
 Rossby-Gyre dynamics, 21

Rosby wave, 13

S

Sea surface temperature (SST), 19, 21, 84, 89, 91, 99
 Semi-permanent high, 78
 Sensible heat, 76
 Sensitivity, 45, 47, 120
 Somali jet, 62
 Specific humidity, 44, 49, 50, 52, 53, 103
 Spectral model, 32
 Steppe, 28
 Stream function, 84, 89, 90, 104
 Sub tropical westerly jet (SWJ), 4–6, 9–16, 19, 21, 30, 32, 44, 46, 63, 64, 67–72, 74, 75, 77, 86, 89, 108, 109
 Synoptic, 7, 9–15, 29–32, 35, 41, 55, 61, 63, 68, 69, 73, 74, 108, 118, 121

T

Teleconnection, 76, 122, 124
 Thermal insulation, 55
 Thunderstorm, 2, 4, 9, 61, 65, 115
 Tibetan high, 5, 68, 69, 83
 Topography, 5, 9, 12, 27, 28, 37, 39–41, 45–47, 49, 50, 52, 53, 54, 62, 74, 84–86, 104, 121
 Tornado, 65
 Transient cloud system (TCS), 31, 70, 73, 75
 Tropical easterly jet (TEJ), 9, 68, 71, 72
 Tropopause fold, 42

U

Upper troposphere, 10, 21, 65, 70–74, 89, 93, 100, 104, 108

V

Velocity potential, 89, 90
 Vortex, 17, 78
 Vorticity, 6, 11, 12, 20, 21, 47–49, 52, 54, 69

W

Walker circulation, 20, 92, 96, 108, 109
 Wind shear, 49, 71

Z

Zonal wind, 29, 32, 86